Approved for public release; distribution is unlimited

PERFORMANCE OF A FAST FREQUENCY-HOPPED NONCOHERENT MFSK RECEIVER OVER RICIAN FADING CHANNELS WITH EITHER PARTIAL -BAND INTERFERENCE OR MULTI-TONE INTERFERENCE

by

Joseph F. Sheltry
Lieutenant, U.S. Navy
B.S. Chemistry, University of Idaho, 1988

Submitted in partial fulfillment
of the requirements for the degree of

MASTER OF SCIENCE IN ELECTRICAL ENGINEERING

from the

NAVAL POSTGRADUATE SCHOOL
September 1994

REPORT DOCUMENTATION PAGE

Form Approved OMB No. 0704

1. AGENCY USE ONLY *(Leave blank)*	2. REPORT DATE	3. REPORT TYPE AND DATES COVERED
	September 1994	Master's Thesis

4. TITLE AND SUBTITLE : PERFORMANCE OF A FAST FREQUENCY-HOPPED NONCOHERENT MFSK RECEIVER OVER RICIAN FADING CHANNELS WITH EITHER PARTIAL -BAND INTERFERENCE OR MULTI-TONE INTERFERENCE (U)

5. FUNDING NUMBERS

6. AUTHOR(S) Joseph Francis Sheltry

7. PERFORMING ORGANIZATION NAME(S) AND ADDRESS(ES)
Naval Postgraduate School
Monterey CA 93943-5000

8. PERFORMING ORGANIZATION REPORT NUMBER

9. SPONSORING/MONITORING AGENCY NAME(S) AND ADDRESS(ES)

10. SPONSORING/MONITORING AGENCY REPORT NUMBER

11. SUPPLEMENTARY NOTES The views expressed in this thesis are those of the author and do not reflect the official policy or position of the Department of Defense or the U.S. Government.

12a. DISTRIBUTION/AVAILABILITY STATEMENT Approved for public release; distribution unlimited

12b. DISTRIBUTION CODE
A

13. ABSTRACT *(maximum 200 words)* An error probability analysis is performed for a conventional noncoherent M-ary orthogonal frequency-shift keying (MFSK) receiver employing fast frequency-hopped (FFH) spread spectrum waveforms transmitted over a frequency-nonselective, slowly fading Ricean channel with partial-band noise interference. Each diversity reception is assumed to fade independently. The partial-band interference is modeled as a Gaussian process. The effects of wideband thermal noise are also included. The energy per hop is held constant; thus, as diversity increases, energy per symbol increases. Previous analyses considered only constant energy per symbol systems, however, practical military systems are likely to employ fixed hop rates. There is some performance enhancement to be obtained from implementing diversity in a conventional FFH/MFSK system with fixed hop rates, but partial band interference still results in significant degradation.

Additionally, the performance of this FFH receiver is investigated over the same channel in the presence of partial-band tone jamming without diversity for the case of binary frequency-shift keying (BFSK) when both the signal and the jammer can fade independently. Performance when only a single jamming tone per hop slot is allowed is compared to that obtained when two jamming tones per hop slot are possible. When the jamming signal experiences Rayleigh fading there is very little degradation of the jammer's effectiveness as compared to when the jamming signal is not affected by fading.

14. SUBJECT TERMS Spread spectrum communications, fast frequency-hopping, partial-band interference, multi-tone interference, MFSK

15. NUMBER OF PAGES
102

16. PRICE CODE

17. SECURITY CLASSIFICATION OF REPORT	18. SECURITY CLASSIFICATION OF THIS PAGE	19. SECURITY CLASSIFICATION OF ABSTRACT	20. LIMITATION OF ABSTRACT
Unclassified	Unclassified	Unclassified	UL

ABSTRACT

An error probability analysis is performed for a conventional noncoherent M-ary orthogonal frequency-shift keying (MFSK) receiver employing fast frequency-hopped (FFH) spread spectrum waveforms transmitted over a frequency-nonselective, slowly fading Ricean channel with partial-band noise interference . Each diversity reception is assumed to fade independently. The partial-band interference is modeled as a Gaussian process. The effects of wideband thermal noise are also included. The energy per hop is held constant; thus, as diversity increases, energy per symbol increases. Previous analyses considered only constant energy per symbol systems, however, practical military systems are likely to employ fixed hop rates. There is some performance enhancement to be obtained from implementing diversity in a conventional FFH/MFSK system with fixed hop rates, but partial band interference still results in significant degradation.

Additionally, the performance of this FFH receiver is investigated over the same channel in the presence of partial-band tone jamming without diversity for the case of binary frequency-shift keying (BFSK) when both the signal and the jammer can fade independently. Performance when only a single jamming tone per hop slot is allowed is compared to that obtained when two jamming tones per hop slot are possible. When the jamming signal experiences Rayleigh fading there is very little degradation of the jammer's effectiveness as compared to when the jamming signal is not affected by fading.

TABLE OF CONTENTS

ACKNOWLEDGMENTS

I must first thank my patient mentor, Dr. R. Clark Robertson who helped me pull together two years worth of effort at the Naval Postgraduate School. I must also sincerely thank my wife, Lorraine, who supported me throughout my tour at NPS and endured a hot Summer in Hartford, CT, while I prepared this thesis. To my parents, thank-you for instilling in me a life long commitment to education and personal excellence. I must also thank the Lord who gave me the tools to get this job done.

I. INTRODUCTION

A fast frequency-hopping (FFH) communication system is a subset of spread spectrum communications that utilizes a bandwidth greatly exceeding that required for the information signal alone. Frequency-hopping spread spectrum is fundamentally different from direct sequence (DS) spread spectrum in the technique of signal generation and recovery. This thesis focuses on frequency-hopping spread spectrum systems because of their practical military importance. As spread spectrum systems grow more popular and occupy wider communications bandwidth, the likelihood of both hostile and non-hostile sources of narrowband interference also grows. It is important for mission planners to have a reliable estimate of the degradation that their communication systems will suffer under partial-band noise interference as well as tonal interference. Fast frequency-hopping spread spectrum techniques have evolved to counter the threat of intentional jamming [Ref. 1]. This thesis presents an error probability analysis of the conventional fast frequency-hopped orthogonal M-ary frequency-shift keying (FFH/MFSK) receiver with noncoherent detection for communications over channels with Ricean fading of the signal and partial-band noise interference. The influence of partial-band tonal interference on the binary orthogonal frequency-shift keying (FFH/BFSK) receiver without diversity where both the signal and jammer may fade independently is also considered.

A. FFH / MFSK

Frequency-shift keying is popular as a signaling scheme because it allows for noncoherent reception of the signal. A typical MFSK signal set can be expressed as

$$s_1(t) = \sqrt{2}\, A_c \cos(2\pi f_o t + \theta_1) \tag{1}$$

$$s_2(t) = \sqrt{2}\, A_c \cos\left[2\pi(f_o + \Delta f)t + \theta_2\right] \tag{2}$$

and so on to

$$s_M(t) = \sqrt{2}\, A_c \cos\left[2\pi(f_o + (M-1)\Delta f)t + \theta_M\right] \tag{3}$$

where f_o is the lowest signal tone, Δf is the tone spacing, and θ_m is the phase associated with each tone. This set is then modulated by a carrier that varies pseudorandomly in frequency for transmission as a frequency-hopped signal.

All communication signals suffer from interference and noise. One method to overcome this degradation is to transmit the signal more than once thus providing a form of diversity. Fast frequency-hopping employs this redundancy as well as deliberately spreading the bandwidth. Frequency-hopping systems in which several symbols are transmitted per hop are considered slow frequency-hopping, while those transmitting several hops per symbol are considered fast frequency-hopping. Our FFH/MFSK transmitter performs L hops per data symbol, which results in a diversity of L. At the receiver the dehopped signals are recovered noncoherently by two correlators in phase quadrature with the dehopped signal waveform. The correlator outputs are sampled every T_h seconds, where T_h is the hop period. The sampled output of each correlator pair is

squared and then these outputs are summed L times to obtain the decision statistic for each branch of the M-ary detector. The largest signal detected is selected as the transmitted symbol. A typical receiver structure is shown in Figure 1.

Proper reception and demodulation of the spread signal depend on the recovery of several pieces of timing information. Both the sender and receiver need the same pseudorandom sequence operating synchronously. Also required are the symbol period and the hop period. In practice these are estimated from the received waveforms. This thesis assumes that this information is recovered without error.

B. MULTI-PATH EFFECTS

The losses experienced by the signal during propagation is worthy of an entire study in itself. However, it is useful to make some general observations on the composition of the received signal. It is possible and even likely that the received signal arrives at the receiver after transiting a variety of different paths. Signals traveling a longer distance arrive delayed relative to the direct path signal. This leads to multi-path effects. The magnitude of the multi-path effects depends on the magnitude of the delayed signal strength versus the direct path signal strength. It is common to consider the sum of all delayed signals as the diffuse component of the received signal. [Ref. 2]

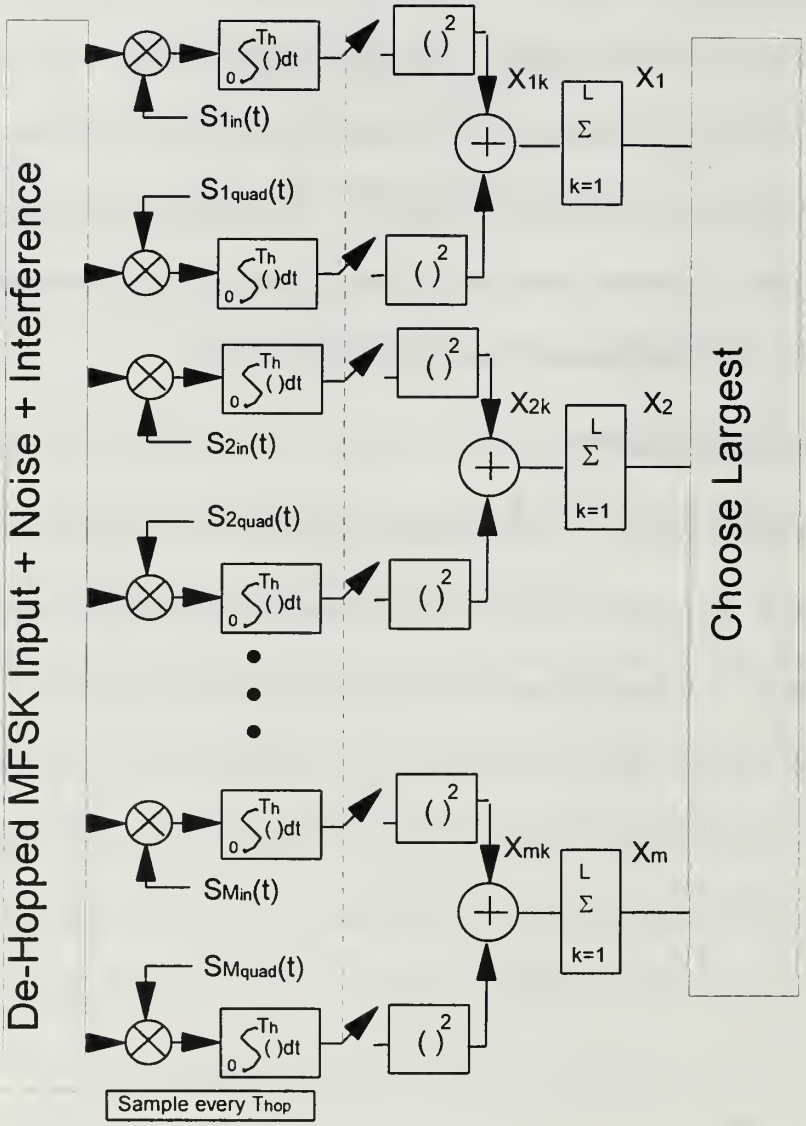

Figure 1. Typical MFSK Receiver Structure

The consequence of multi-path reception is to cause the signal to fade in a time varying fashion. We can broadly characterize the channel conditions by examining the magnitude of the direct signal power to the diffuse signal power. The Ricean channel is the general case. Channels that have nearly all the received signal energy in the direct component, i.e., direct-to-diffuse ratio greater than 100, have essentially no fading. In the limit, an infinite direct-to-diffuse ratio implies a Gaussian channel. Channels that have nearly all the received signal energy in the diffuse component, i.e., direct-to-diffuse ratio less than one, have strong fading. A direct-to-diffuse ratio of zero implies a Rayleigh channel. For direct-to-diffuse ratios between these extremes the channel experiences Ricean fading. This thesis examines the performance in each of these broad categories.

In addition to these broad categories, the time varying nature of the channel can be described as slow or fast. In this thesis the channel properties are assumed to be constant over the duration of a hop and, therefore, slowly varying. Further, the channel may introduce some signal distortion arising from the treatment of sinusoids comprising the signal set within a hop differently. This distortion is characteristic of frequency selective channels. However, it is reasonable to assume that the signal sinusoids experience the same multi-path effects. This is the case in frequency nonselective channels. One measure of this phenomenon is the coherence bandwidth of the signal. The coherence bandwidth is the frequency range over which the signal frequencies pass through without distortion. This can be summarized mathematically as

$$(\Delta f)_c = \frac{1}{T_m} \tag{4}$$

where $(\Delta f)_c$ is the coherence bandwidth and T_m is the multi-path spread of the channel. A frequency nonselective cannel displays a coherence bandwidth that is larger than the signal bandwidth. The rate of fading is related to

$$(\Delta t)_c = \frac{1}{B_d} \tag{5}$$

The coherence time is $(\Delta t)_c$ and B_d is the Doppler spread of the channel. Slowly fading channels display a large coherence time or, conversely, a small Doppler spread. These descriptors are discussed further in the system description.[Ref. 2] The use of diversity to mitigate the multi-path effects for conventional MFSK has been widely investigated [Refs. 2, 3, 4].

When analyzing performance it is important to distinguish between a constant energy per hop system and a constant energy per symbol system. As diversity increases, the total symbol energy in a constant energy per hop system increases, while the symbol rate decreases. However, in the constant energy per symbol system, increasing diversity, L, implies decreasing hop duration, T_h. Hence, a constant data rate is maintained, but the energy per hop is reduced. Since many practical military communication systems employ a fixed hop rate and a variable data rate, the constant energy per hop assumption is more logical [Ref. 5].

C. CONSTANT ENERGY PER HOP SYSTEMS

Previous work has examined the performance of the noncoherent MFSK receiver in a Ricean fading channel with partial-band noise interference and constant energy per

symbol [Ref. 3]. Additionally, the performance of the conventional BFSK receiver under partial-band noise jammin without the multi-path effect of fading is analyzed in [Ref. 6]. However, these investigations do not consider constant energy per hop signaling. The performance of several different types of diversity combining receivers, including the conventional receiver, utilizing constant energy per hop is simulated for Rayleigh fading channels in [Ref. 7].

Motivating this thesis is the uncertain degree of improved performance offered by more elaborate receiver designs, such as the noise normalized receiver, over the conventional receiver for variable data rate systems. [Refs. 3, 4] The expense and complexity of a more elaborate receiver may not be justified in some circumstances when utilizing a constant energy per hop system.

The constant energy per hop scheme is of practical value because it allows the potential for an adaptive signaling scheme in which the sender and receiver can optimize the data transmission rate. In poor environments, diversity can be increased at the expense of lowered data rate. In favorable environments, the level of diversity, L , can be lowered to accommodate a higher data rate. These adaptations will ideally not require any hardware modifications and will be transparent to a channel observer. With this adaptive scheme in mind , this thesis examines the improvement offered by varying the level of diversity possible when the jammer is sub-optimal.

D. TONE INTERFERENCE

Another type of narrowband interference is tone interference. This can consist of a single interfering or multiple interfering tones. In this thesis, a performance analysis for a FFH/BFSK receiver without diversity over fading channel conditions similar to those assumed for noise interference is considered. Since the interfering tone or tones are signal-like in nature, they too can suffer multi-path effects. This analysis considers the effects of fading on both the signal and jammer. In a FFH/BFSK system an intelligent jammer can potentially cause more degradation by splitting his available power over both the signal tones. The degree of communication impairment of the single tone interference per hop versus two interference tones per hop strategy is also considered. Clearly, the greatest performance degradation occurs when the interfering tones correspond exactly to the various frequency-hopped symbol tones. Tone jamming where the tones do not correspond exactly to the various frequency-hopped symbol tones are not considered in this thesis.

II. PARTIAL-BAND NOISE INTERFERENCE

A. SYSTEM DESCRIPTION

The partial-band noise interference, either intentional or unintentional, considered in this thesis is modeled as additive Gaussian noise and, when present, is assumed to be in all branches of the MFSK demodulator for any reception of the dehopped signal. Thermal noise and other wideband interferences which are also assumed to corrupt the signal are modeled as additive white Gaussian noise. Only the signal is assumed to be affected by channel fading. The smallest spacing between frequency hop slots is assumed larger than the coherence bandwidth of the channel, hence, each dehopped signal fades independently [Refs. 2,8]. As discussed in the Introduction, the signal bandwidth is assumed to be much smaller than the channel coherence bandwidth, and the channel coherence time is assumed to be much larger than the hop duration or, equivalently, the hop rate is assumed to be large compared to the Doppler spread of the channel. The first assumption implies that the channel is modeled as frequency-nonselective, while the second implies that the channel is slowly fading. The signal channel is modeled as a Ricean fading channel, hence, signal amplitude is a Ricean random variable [Refs. 2,8]. For Ricean fading, the total signal power consists of a direct signal component and a diffuse signal component, and the strength of the fading channel is characterized by the ratio of the direct signal component power to the diffuse signal component power.

The symbol rate is R_s. For MFSK with M order modulation, the corresponding bit rate is $\mathscr{R}_b = \log_2(\mathrm{M})$. For L hops per symbol, the hop rate is $R_h = LR_s$. The spread spectrum bandwidth, W, is considered very large compared to the hop rate.

B. PARTIAL-BAND NOISE JAMMING ANALYSIS

1. Problem Development

The partial-band noise interference when present is assumed to be in all branches of the MFSK demodulator and affects each chip of the dehopped signal with probability γ where γ is the fraction of the spread bandwidth being jammed. Hence, the fraction of the spread bandwidth not being jammed is $1-\gamma$. If the average power spectral density of the interference is $N_I/2$ over the entire spread bandwidth, then the power spectral density of the partial-band interference when present is $N_I/2\gamma$. The power spectral density of the thermal noise and other wideband interferences which are modeled as additive white Gaussian noise is $N_o/2$. Consequently, total noise power spectral density is $N_o/2$ in the absence of partial-band interference; otherwise,

$$\frac{N_T}{2} = \left(\frac{N_I}{2\gamma}\right) + \left(\frac{\mathrm{N_o}}{2}\right) \tag{6}$$

is the total noise power spectral density when narrowband interference is present.

If the equivalent noise bandwidth of each detector branch in the MFSK demodulator is B Hz, then the noise power received in a given hop is $\sigma_k^2 = \sigma_T^2 = \mathrm{N_o}B$ with probability $1-\gamma$ when no jamming is present. When jamming is present, the total noise power in a given hop k is $\sigma_k^2 = \sigma_I^2 + \sigma_T^2 = \left(\frac{N_I}{\gamma} + \mathrm{N_o}\right)B$ with a probability of γ.

We assume that each receiver hop slot has the same noise equivalent bandwidth. The noise equivalent bandwidth of the receiver investigated in this thesis is $B=R_h$.

2. Probability of Bit Error

When partial-band interference is present the probability of symbol error for a MFSK receiver is

$$P_s = \sum_{i=0}^{L} \binom{L}{i} \gamma^i (1-\gamma)^{L-i} P_s(i) \tag{7}$$

where $P_s(i)$ represents the conditional probability of a symbol error given that i of L hops of a symbol are jammed. Since each signal branch of the receiver is symmetric with the other branches, we can determine the probability of a symbol error , P_s , by considering the signal to be present only in branch one of the MFSK demodulator. The outputs of the other branches are assumed identical and independent (iid).

For orthogonal MFSK the probability of a bit error is related to the symbol error by

$$P_b = \frac{M}{2(M-1)} P_s \tag{8}$$

The energy per bit as a function of the symbol energy and the modulation order is

$$E_b = \frac{E_s}{\log_2(M)} \tag{9}$$

3. Probability of Symbol Error Under Partial-band Noise Interference

Assuming the signal is present in branch one of the MFSK demodulator allows us to write the probability of a symbol error based on the conditional probability density functions that i of L hops are jammed.The conditional probability density function for the output of the branch containing the signalis $f_{X_1}(x_1 | i)$ where X_1 is the random variable that represents the output of the signal branch. The conditional probability density functions for the non-signal branches are $f_{X_m}(x_m | i), m = 2, 3, 4..., M$ where the X_m's are the identically distributed random variables that represent the output of the branches that do not contain the signal. [Ref. 3] The conditional probability of symbol error is

$$P_s(i) = 1 - \int_0^\infty f_{X_1}(x_1 | i) \left[\int_0^{x_1} f_{X_m}(x_1 | i) dx_m \right]^{M-1} dx_1 \qquad (10)$$

for all $m \neq 1$.

Since the partial band interference may or may not be present in a hop, we must be able to differentiate between the two possibilities. Let the subscript n= 1, 2 denote that hop k of a symbol has interference and has no interference, respectively. The diversity summer acts to add together all L independent hops in its branch. Of those hops i of them are jammed; hence, we can express the random variable at the output of the diversity summer (10) as

$$X_m = \sum_{k=1}^{L} X_{mk_n} = \sum_{k=1}^{i} X_{mk_1} + \sum_{k=L-i}^{L} X_{mk_2} \qquad m = 1, 2, 3..., M \qquad (11)$$

a. *Probability Density Function for the Decision Variable X_m*

The probability density function of the independent, identically distributed (iid) random variables X_{mk} , m= 2,3,...,M that represent the demodulator branch outputs not containing the signal for hop k of a symbol is

$$f_{X_{mk}}(x_{mk}) = \frac{1}{2\sigma_k^2} \exp\left(\frac{-x_{mk}}{2\sigma_k^2}\right) u(x_{mk}) \qquad m = 2,3,...,M \tag{12}$$

where $u(\bullet)$ is the unit step function. [Ref. 9]

The Laplace transform of (12) is

$$F_{X_{mk}}(s) = \frac{1}{2\sigma_k^2 s + 1} \tag{13}$$

Since each hop is independent, from (11), we can express the Laplace transform of the conditional density function, $f_{X_m}(x_m|i)$, as

$$F_{X_m}(s|i) = \left[F_{X_{mk_1}}(s|i)\right]^i \times \left[F_{X_{mk_2}}(s|i)\right]^{L-i} \tag{14}$$

Direct inversion of (14) leads to an infinite series of confluent hypergeometric functions, but this proved difficult to program and slow to execute. To evaluate (34) we first invert the individual portions consisting of either all hops jammed or all hops not jammed. The conditional density function for the decision variable is then obtained by convolution.

The Laplace transform pairs are

$$\left[F_{X_{mk_1}}(s|i)\right]^i \Leftrightarrow \left(\frac{1}{2\sigma_{k1}^2}\right)^i \frac{x^{i-1}}{(i-1)!} \exp\left(\frac{-x}{2\sigma_{k1}^2}\right) u(x) \tag{15}$$

and

$$\left[F_{X_{mk_2}}(s|i)\right]^{L-i} \Leftrightarrow \left(\frac{1}{2\sigma_{k2}^2}\right)^{L-i} \frac{x^{L-i-1}}{(L-i-1)!} \exp\left(\frac{-x}{2\sigma_{k2}^2}\right) u(x) \tag{16}$$

where $\sigma_{k1}{}^2$ and $\sigma_{k2}{}^2$ represent the noise power in a hop experiencing interference and a hop experiencing only thermal noise, respectively. To recover $f_{X_m}(x_m)$, the two m-Erlang random variables above are convolved . Hence, the inverse Laplace transform of (14) is obtained from a convolution of the individual right hand sides (RHS) of (15) and (16) as

$$f_{X_m}(x_m|i) = \int_0^{x_m} \left(\frac{1}{2\sigma_{k1}^2}\right)^{i} \left(\frac{1}{2\sigma_{k2}^2}\right)^{L-i} \frac{t^{i-1}}{(i-1)!} \exp\left(\frac{-t}{2\sigma_{k1}^2}\right) \frac{(x_m-t)^{L-i-1}}{(L-i-1)!} \exp\left(\frac{-(x_m-t)}{2\sigma_{k2}^2}\right) dt \tag{17}$$

Applying the binomial theorem to the integrand of (17) and defining

$$\lambda = \left(\frac{1}{2\sigma_{k1}^2}\right)^{i} \left(\frac{1}{2\sigma_{k2}^2}\right)^{L-i} \frac{1}{(L-i-1)!(i-1)!} \tag{18}$$

we can express (17) as

$$f_{X_m}(x_m|i) = \lambda \int_0^{x_m} \sum_{k=0}^{L-i-1} \binom{L-i-1}{k} x_m^k (-t)^{L-i-1-k} \exp\left(\frac{-t}{\frac{1}{2\sigma_{k1}^2} - \frac{1}{2\sigma_{k2}^2}}\right) dt \tag{19}$$

Interchanging the order of integration and summation and integrating term by term, we get [Ref. 10, equation 3.351.1]

$$f_{X_m}(x_m|i) = \lambda \sum_{k=0}^{L-i-1} \binom{L-i-1}{k} (-1)^k x_m^{L-i-1-k} \exp\left(\frac{-x_m}{\alpha-\beta}\right) \sum_{l=0}^{k+i-1} \frac{(-1)(k+i-1)! x_m^{k+i-1-l}}{(k+i-1-l)!(\alpha-\beta)^{l+1}} \tag{20}$$

where for brevity

$$\alpha = \frac{1}{2\sigma_{k1}^2} \tag{21}$$

and

$$\beta = \frac{1}{2\sigma_{k2}^2} \tag{22}$$

The special cases of all hops jammed (i=L) and no hops jammed (i=0) are obtained directly from (15) and (16) respectively, since the analysis leading to (20) is not valid in theses cases. The remaining task is to evaluate the cumulative distribution function of $f_{X_m}(x_m|i)$ that is required for computing the probability of symbol error, (10). The computation required for the non-signal branch contribution to the probability of symbol error is $\int_0^{x_m} f_{X_m}(x_m)$. There are two avenues to compute this, the first based on direct integration or, equivalently, the second based on an inverse Laplace transform of $F_{X_m}(s|i)/s$.

Directly integrating (20), valid when $0 < i < L$, we have

$$\int_0^{x_m} f_{X_m}(x_m|i)dx_m = \frac{(\alpha^i)\beta^{L-i}}{(i-1)!(L-i-1)!} \sum_{k=0}^{L-i-1} (-1)^k \binom{L-i-1}{k}$$

$$\times(k+i-1)!\left[\frac{(L-i-1-k)!}{(\alpha-\beta)^{k+i}}\left\{\frac{1}{\beta^{L-i-1}} - \exp(-\beta x_m)\sum_{p=0}^{L-i-1-k}\frac{x_m^{L-1-1-k-p}}{(L-i-1-n-p)!\beta^{p+1}}\right\}\right.$$

$$\left. - \sum_{l=0}^{k+i-1}\frac{(L-i-1)!}{(k+i-1-l)(\alpha-\beta)^{l+1}}\left\{\frac{1}{\alpha^{L-1-l}} - \exp(-\alpha x_m)\sum_{q=0}^{L-2-m}\frac{x_m^{L-2-l-q}}{(L-2-l-q)!\alpha^{q+1}}\right\}\right] \tag{23}$$

This equation is simplified by expanding the binomial coefficient and canceling like terms to obtain

$$\int_0^{x_m} f_{X_m}(x_m|i)dx_m = \frac{1}{(i-1)!}\sum_{k=0}^{L-i-1}\frac{(k+i-1)!}{k!}\left\{\frac{\alpha^i\beta^k}{(-1)^i(\beta-\alpha)^{n+i}}\right.$$

$$\left[1-\exp(-\beta x_m)\sum_{p=0}^{L-i-1-k}\frac{(\beta x_m)^p}{p!}\right]-\frac{\beta^{L-i}}{(L-i-1-k)!}\sum_{l=0}^{k+i-1}\frac{(L-2-l)!(-1)^{k-l-1}}{(k+i-1-l)!(\beta-\alpha)^{m+1}\alpha^{L-i-1-l}}$$

$$\left.\left[1-\exp(-\alpha x_m)\sum_{q=0}^{L-2-l}\frac{(\alpha x_m)^q}{p!}\right]\right\} \tag{24}$$

when $0 < i < L$. For the case of all hops jammed, $i = L$, the cumulative density function is

$$\int_0^{x_m} f_{X_m}(x)dx = \int_0^{x_m}\left(\frac{1}{2\sigma_{k1}^2}\right)^L\frac{x^{L-1}}{(L-1)!}\exp\left\{\frac{x}{2\sigma_{k1}^2}\right\}dx$$

$$= 1-\exp\left\{\frac{x}{2\sigma_{k1}^2}\right\}\sum_{k=0}^{L-1}\frac{1}{k!}\left(\frac{x}{2\sigma_{k1}^2}\right)^k \tag{25}$$

and for the case of no hops jammed, $i = 0$, it is

$$\int_0^{x_m} f_{X_m}(x)dx = \int_0^{x_m}\left(\frac{1}{2\sigma_{k2}^2}\right)^L\frac{x^{L-1}}{(L-1)!}\exp\left\{\frac{x}{2\sigma_{k2}^2}\right\}dx$$

$$= 1-\exp\left\{\frac{x}{2\sigma_{k2}^2}\right\}\sum_{k=0}^{L-1}\frac{1}{k!}\left(\frac{x}{2\sigma_{k2}^2}\right)^k \tag{26}$$

A final useful form is obtained by making the linear transformation of the random variable X_m. Recognizing that $\alpha = \frac{1}{2\sigma_1^2}$ and $\beta = \frac{1}{2\sigma_2^2}$, then

$$\frac{\alpha}{\beta} = \frac{\frac{1}{2\sigma_1^2}}{\frac{1}{2\sigma_2^2}} = \frac{\sigma_2^2}{\sigma_1^2} = \frac{N_o}{N_T} \tag{27}$$

Then making the change of variables $y = \beta x_m$ in (24) we get

$$F_Y(y|i) = \frac{1}{(i-1)!}\sum_{k=0}^{L-i-1}\frac{(k+i-1)!}{n!}\left\{\frac{(N_T)^k}{(-1)^i(N_T-1)^{k+i}}\right.$$

$$\left[1-\exp(-y)\sum_{p=0}^{L-i-1-k}\frac{y^p}{p!}\right]-\frac{(N_T)^{L-i}}{(L-i)!}\sum_{l=0}^{k+i-1}\frac{(L-2-l)!(-1)^{k-l-1}}{(k+i-1-l)!(N_T-1)^{l+1}}$$

$$\left.\left[1-\exp\left(-\frac{y}{N_T}\right)\sum_{q=0}^{L-2-l}\frac{\left(\frac{y}{N_T}\right)^q}{q!}\right]\right\} \tag{28}$$

which is useful for numerical integration purposes. Applying the same substitution in (25) and (26), we get

$$F_Y(y|L) = 1-\exp\{-y\}\sum_{k=0}^{L-1}\frac{1}{k!}(y)^k \tag{29}$$

and

$$F_Y(y|0) = 1-\exp\left\{\frac{y}{N_T}\right\}\sum_{k=0}^{L-1}\frac{1}{k!}\left(\frac{y}{N_T}\right)^k \tag{30}$$

for the case of all hops jammed and no hops jammed, respectively.

Previous efforts to determine the cumulative distribution for the non-signal branches, the second technique, is based on a numerical inverse Laplace transform of the function $\frac{1}{s}\times F_{X_m}(s|i)$ [Refs. 3, 4]. Despite the finite sums of exponential-like terms in (28), this second method proved more accurate for large values of L.

b. Probability Density Function for the Decision Variable X_1

Continuing with the assumption that the signal is present in branch one of the MFSK demodulator accompanied by Gaussian noise , the random variable X_1 is described

by the conditional density function $f_{X_1}(x_1|i)$. Given a signal amplitude of $\sqrt{2}\,a_k$ and before diversity combining, the probability density function of X_{1k} is

$$f_{X_{1_k}}(x_{1_k}|a_k) = \frac{1}{2\sigma_k^2}\exp\left(\frac{-\left(x_{1k}+2a_k^2\right)}{2\sigma_k^2}\right) I_0\left(\frac{a_k\sqrt{2x_{1k}}}{\sigma_k^2}\right) u(x_{1k}) \tag{31}$$

where $I_0(\bullet)$ is the modified Bessel function of the first kind and order zero. The channel is assumed to have Ricean fading; therefore, a_k is a Ricean random variable with a probability density function given by

$$f_{A_k}(a_k) = \frac{a_k}{\sigma^2}\exp\left(\frac{-\left(a_k^2+\alpha^2\right)}{2\sigma^2}\right) I_0\left(\frac{a_k\alpha}{\sigma^2}\right) u(a_k) \tag{32}$$

where α^2 is the average power of the direct signal component and $2\sigma^2$ is the average power of the diffuse signal component [Refs. 2, 11]. The total average signal power of a hop k of a symbol is $\alpha^2+2\sigma^2$ and is assumed to remain constant from hop to hop.

The random variable X_{1k} when hop k of a symbol has interference and no interference is denoted by X_{1k_1} and X_{1k_2} respectively. The conditioning is removed by integrating the product of (31) and (32) with respect to a_k from zero to infinity with the result

$$f_{X_{1k_n}}(x_{1k_n}) = \frac{1}{2\left(\sigma_{k_n}^2+2\sigma^2\right)}\exp\left[\frac{-1}{2}\left(\frac{x_{1k_n}+2\alpha^2}{\sigma_{k_n}^2+2\sigma^2}\right)\right] I_0\left(\frac{\sqrt{2x_{1k_n}\alpha^2}}{\sigma_{k_n}^2+2\sigma^2}\right) \tag{33}$$

for $x_{1k_n} \geq 0$ where σ_{k1}^2 implies a jammed hop and σ_{k2}^2 implies no jamming. Since each hop is independent, from (11) we see that the Laplace transform of the conditional density function for the signal branch, $f_{X_1}(x_1|i)$, is

$$F_{X_1}(s|i) = [F_{X_1}(s|i)]^i \bullet [F_{X_1}(s|i)]^{L-i} \tag{34}$$

The Laplace transform of the density function describing a single hop, $f_{X_{1k}}(x_{1k})$, is

$$F_{X_{1k_n}}(s) = \frac{(\beta_{k_n})}{(s+\beta_{k_n})} \exp\left(\frac{-2\alpha^2\beta_{k_n}s}{s+\beta_{k_n}}\right) \tag{35}$$

where

$$\beta_{k_n} = \frac{1}{2\left(2\sigma^2 + \sigma_{k_n}^2\right)} \tag{36}$$

When(35) to the c_n power and the inverse Laplace transform is taken. the result is equivalent to taking the c_n fold convolution, denoted by $\otimes c_n$. Letting $c_1 = i$ and $c_2 = L - i$, so that elements subscripted with a 1 correspond to jammed hops while elements subscripted with a 2 correspond to hops experiencing only thermal noise, then

$$\left[f_{X_{1k_n}}(x_{1k_n})\right]^{\otimes c_n} = \frac{\beta_{k_n} x_{1k_n}^{(c_n-1)/2}}{(2c_n\alpha^2)^{(c_n-1)/2}}$$

$$\times \exp\left[-\beta_{k_n}(x_{1k_n} + 2c_n\alpha^2)\right] \times I_{c_n-1}\left(2\beta_{k_n}\sqrt{2c_n\alpha^2 x_{1k_n}}\right) u(x_{1k_n}) \tag{37}$$

where I_{c_n-1} represents the modified Bessel function of integer order c_n-1. [Refs. 3, 11]

Unlike the case of the non-signal branch analysis, no analytic solution for the final

convolution for the decision variable X_1 has been found. Symbolically, the probability density function for X_1 at the output of the diversity summer is described by

$$f_{X_1}(x_1|i) = \left[f_{X_{1k_1}}(x_{1k_1}|i)\right]^{\otimes i} \otimes \left[f_{X_{1k_2}}(x_{1k_2}|i)\right]^{\otimes(L-i)} \tag{38}$$

C. NUMERICAL EVALUATION OF PARTIAL-BAND NOISE JAMMING

For levels of diversity up to $L = 20$, the conditional probability of symbol error is first computed based on the signal energy-to-thermal noise power spectral density ratio, signal-to-jammer power spectral density ratio, signal fading direct-to-diffuse ratio, and fraction of spread spectrum bandwidth jammed. These input parameters form the basis for the probability of symbol error which is converted to probability of bit error using (8). To summarize

$$\zeta_k = \frac{\alpha_k^2}{\sigma_k^2} = \frac{\text{direct signal power/hop}}{\text{noise power/hop}} \tag{39}$$

$$\xi_k = \frac{2\sigma^2}{\sigma_{k^2}} = \frac{\text{diffuse signal power/hop}}{\text{noise power/hop}} \tag{40}$$

$$\frac{E_b}{N_o} = \frac{\text{average energy per bit}}{\text{thermal noise power spectral density}} \tag{41}$$

$$\frac{E_h}{N_J} = \frac{\text{average energy per hop}}{\text{interference power spectral density}} \tag{42}$$

$$R_b = \left(\frac{\zeta_k}{\xi_k}\right) = \left(\frac{\alpha_k^2}{2\sigma^2}\right) \tag{43}$$

and $0.0 < \gamma \leq 1.0$.

The computation of the probability of symbol error is achieved for each L by weighting and summing the probabilities of symbol error conditioned on i of L hops jammed. A numeric integration is performed over the product of the signal path contribution and the non-signal path contribution (10).

1. Non-Signal Path Contribution

The cumulative distribution function is computed using the analytic expression of finite summations given by (28) for $0 < i < L$ for small L. However, it is computationally faster and results in less round off error for large values of L if a numerical inverse Laplace transform is performed on $\frac{1}{s} \times F_{X_m}(s|i)$. The special cases of all hops jammed (i=L) or no hops jammed (i=0) can be computed directly from (25) or (26), respectively. The convergence of the inverse Laplace transform is accelerated by the Euler transformation [Ref. 12] usually taking about 60 terms to reach relative errors on the order of 10^{-9}. However, certain combinations of input parameters results in slower convergence. The inverse Laplace transform algorithm is limited to not more than 1000 iterations.

2. Signal Path Contribution

For the special cases either of all hops jammed or no hops jammed, the required probability function $f_{x_1}(x_1|i)$ is given by (37). In the case of all hops jammed n=1, $c_1 = L$, and $c_2 = 0$, and in the case of no hops jammed n=2, $c_1 = 0$, and $c_2 = L$. In both of these cases, (10) can be solved analytically, but the results are so complex that numerical evaluation is easier and more straightforward. When $i \neq 0$ and $i \neq L$,(38) is evaluated by

the numerical inversion of (34) after which the probability of symbol error, (10), is evaluated numerically.

The partial-band jamming fraction that yields the worst-case performance for the conventional receiver is obtained experimentally by computing the probability of bit error as a function of γ for fixed values of $\frac{E_h}{N_o}$ and $\frac{E_h}{N_J}$. To cover the broad range of channel fading severity, results are obtained for several values of the direct-to-diffuse ratio. For weakly fading channels, exhibiting a strong direct signal component, a direct-to-diffuse ratio of 100 is used. This is essentially a Gaussian channel. For strongly fading channels, considered as nearly Rayleigh channels, a direct-to-diffuse ratio of one is used. Typical of a moderate Ricean fading channel, a direct-to-diffuse ratio of ten is used .

D. PARTIAL-BAND NOISE JAMMING RESULTS

To determine the worst case partial-band jamming performance of the FFH/MFSK receiver the probability of bit error is computed as a function of γ. The process is repeated for levels of diversity up to twenty, which represents the upper end for practical systems in today's technology. Figure 2 through Figure 9 display the probability of bit error for various levels of signal-to-noise ratio, total jammer power, and modulation order. The figures are calculated with the assumption that the signal direct-to-diffuse ratio (R_b) is constant during a hop duration. Figure 2 demonstrates the performance for moderate signal-to-noise ratio with a near Gaussian channel. The signal-to-thermal noise ratio, E_h/N_o, is the signal energy contained in one hop for a conventional BFSK receiver. The table below summarizes the cases displayed in Figure 2 through Figure 9.

TABLE 1. PARAMETERS FOR WORST CASE ANALYSIS

FIGURE	E_h/N_o dB	E_h/N_J dB	R_b / Ricean Fading
Figure 2	13.35	3	100 / Very Weak
Figure 3	13.35	3	10 / Moderate
Figure 4	13.35	10	100 / Very Weak
Figure 5	13.35	10	10 / Moderate
Figure 6	16	3	10 / Moderate
Figure 7	16	10	10 / Moderate
Figure 8	20	3	1 / Strong
Figure 9	10	0	1 / Strong

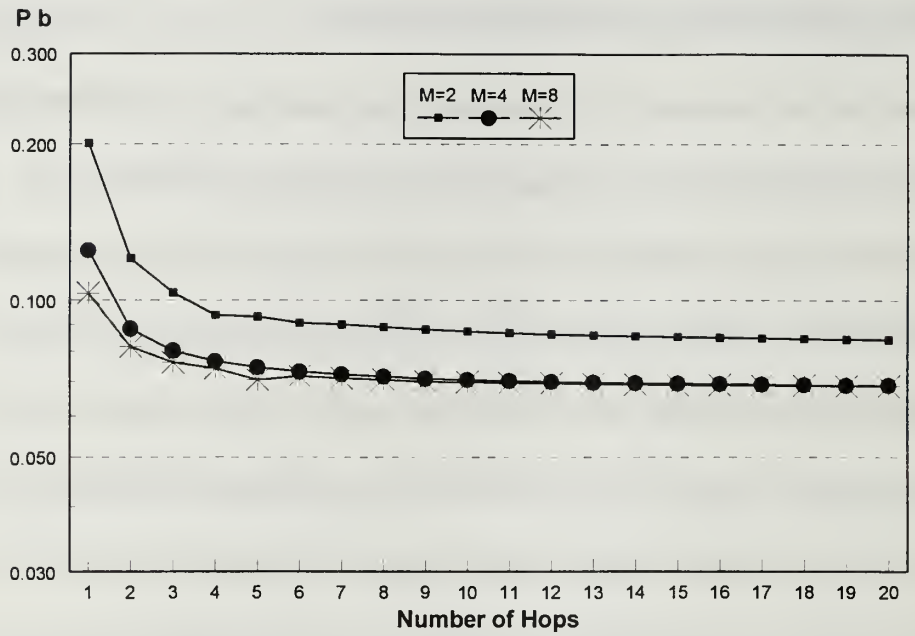

Figure 2. Worst Case Partial-band Jamming
E_h/N_o=13.35dB, E_h/N_J=3dB, R_b=100

The surprising result is that despite increased levels of diversity, the performance does not greatly improve. There will be more to say about this later, but the same trend is observed in Figure 3 where there is Ricean fading of the signal .

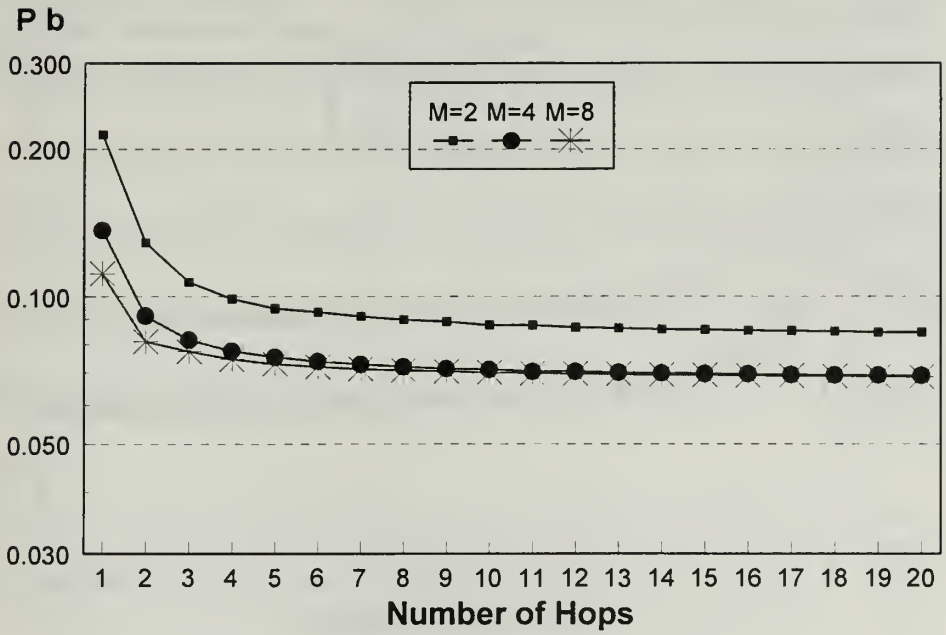

Figure 3. Worst Case Partial-band Jamming
E_h/N_o=13.35dB, E_h/N_J=3dB, R_b=10

Another, surprising result is that increasing the modulation order to four or eight does not provide much improvement. Figure 2 and Figure 3 display pessimistic performance from the communicator's viewpoint. However, they assume a high level of jammer power. We next investigate the performance when the jammer power is just one tenth of the communicator's power when L=1 (Figure 4 and Figure 5) . Since we are assuming 1000 hop slots, this is equivalent to assuming a signal-to-jammer power ratio of -20dB for BFSK with no frequency-hopping

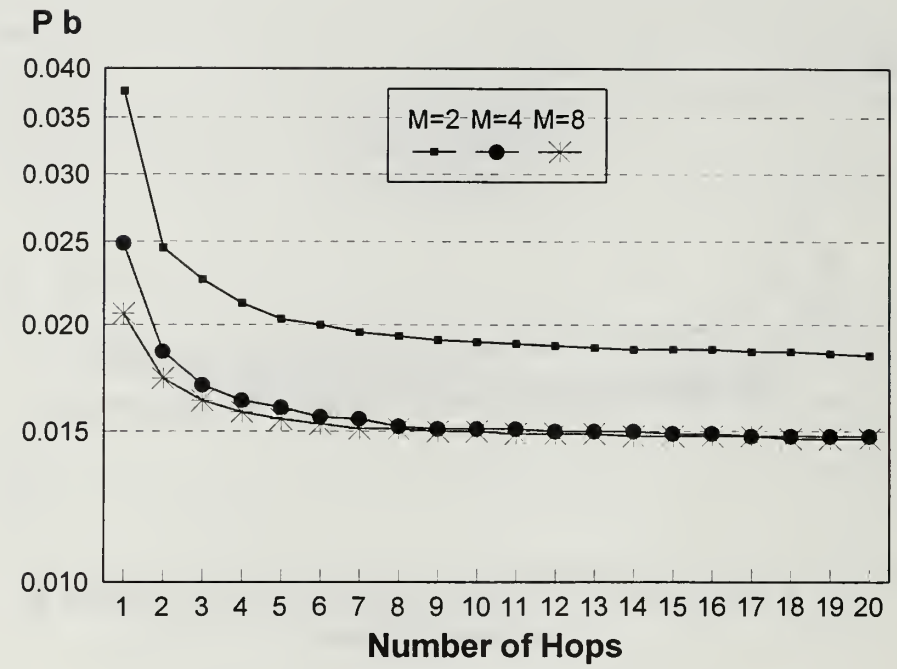

Figure 4. Worst Case Partial-band Jamming
E_h/N_o=13.35dB, E_h/N_J=10dB, R_b=100

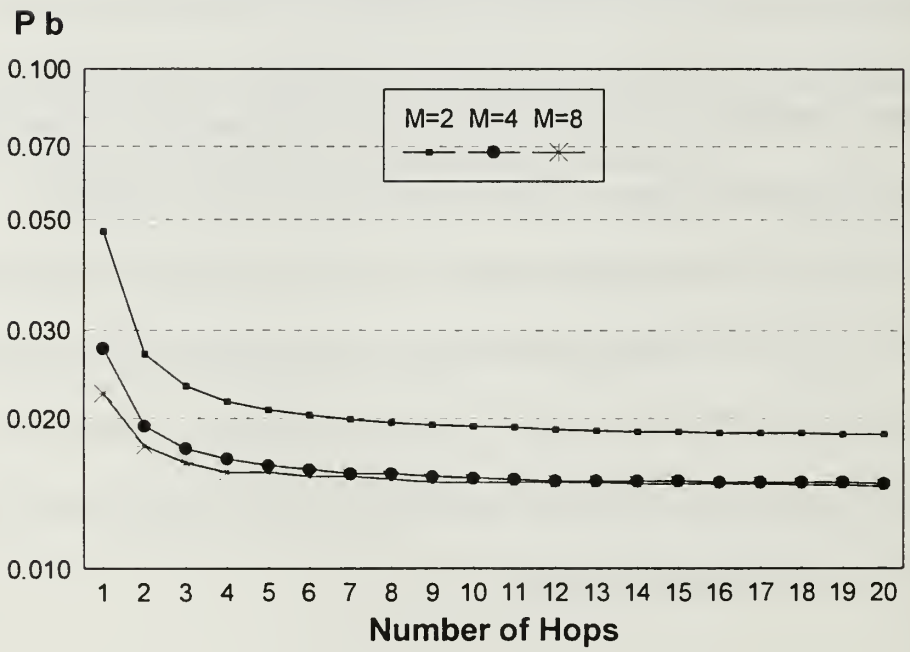

Figure 5. Worst Case Partial-band Jamming
E_h/N_o=13.35dB, E_h/N_J=10dB, R_b=10

A comparison of Figure 4 with Figure 5 illustrate the influences of Ricean fading on the probability of bit error when the communicator enjoys a significant power advantage over the jammer. Next we consider a situation where the communicator has a larger initial signal-to-thermal noise ratio, i.e. 16dB, to see if at higher levels the jammer could mitigate the effects of diversity with partial-band noise jamming. Figure 6 and Figure 7 display these results.

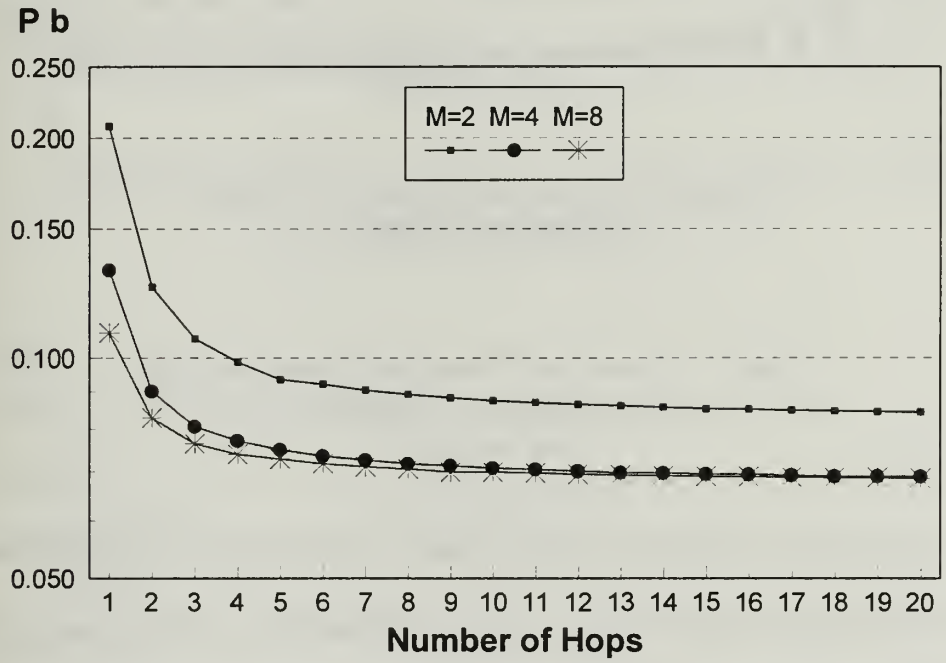

Figure 6. Worst Case Partial-band Jamming
E_h/N_o=16dB, E_h/N_J=3dB, R_b=10

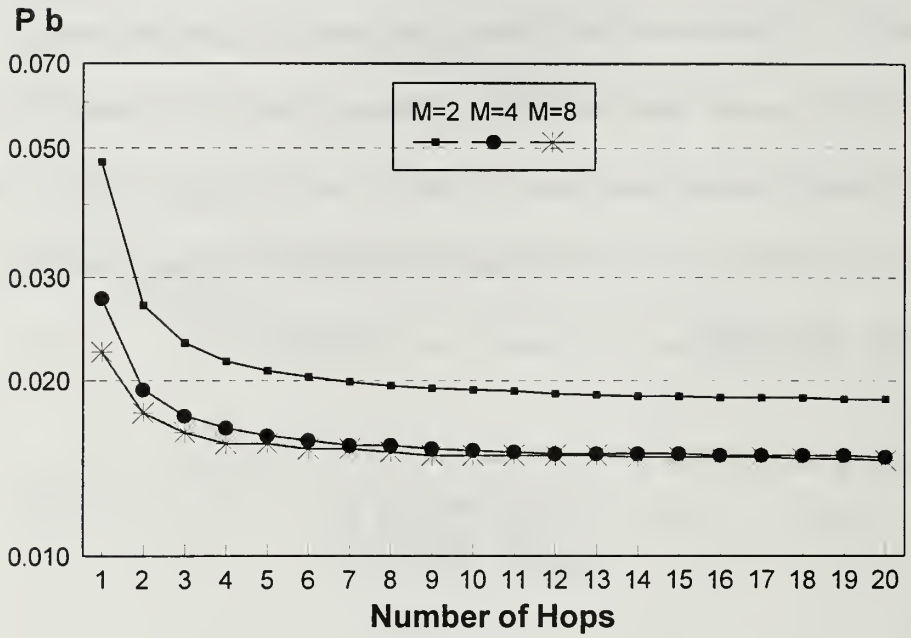

Figure 7. Worst Case Partial-band Noise Jamming
E_h/N_o=16dB, E_h/N_J=10dB, R_b=10

To examine the extremes of channel fading on the received signal, the case of near Rayleigh fading is examined with a direct-to-diffuse ratio of one. Since fading is severe, we would expect poor performance even without jamming, but with some improvement added by the increased diversity. The signal energy per hop is examined at 20 dB (Figure 8) and at 10dB (Figure 9).

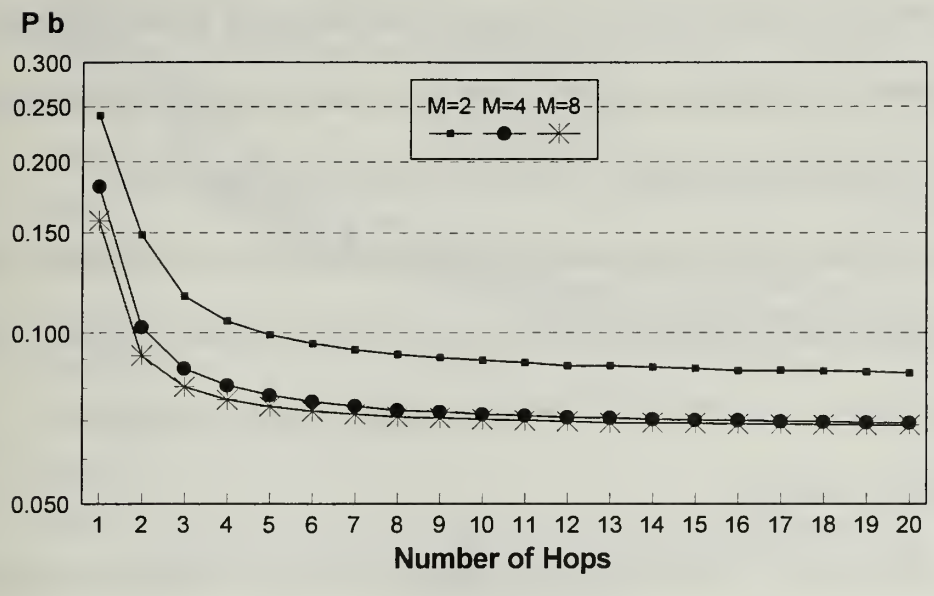

Figure 8. Worst Case Partial-band Jamming
E_h/N_o=20dB, E_h/N_J=3dB, R_b=1

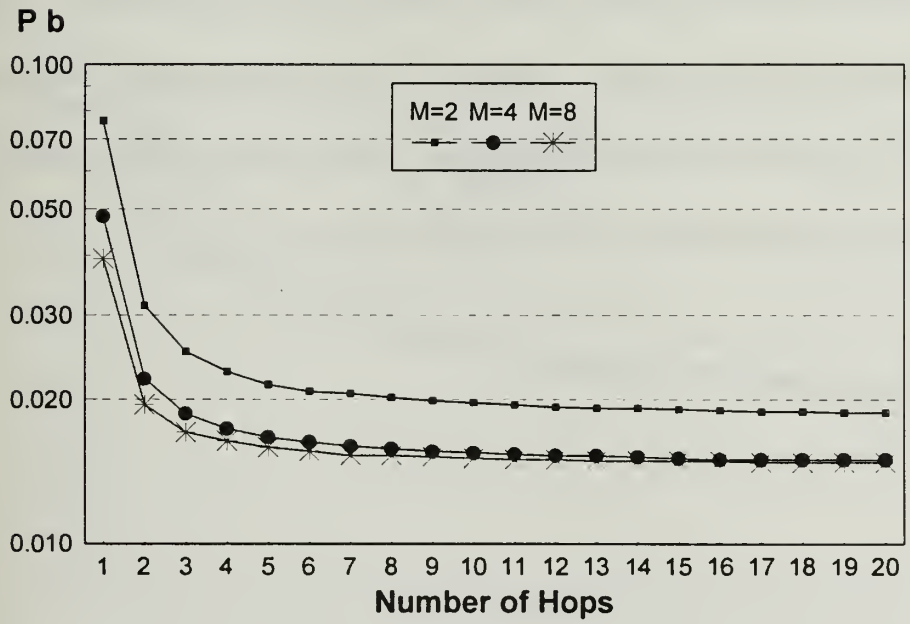

Figure 9. Worst Case Partial-band Jamming
E_h/N_o=10dB, E_h/N_J=0dB, R_b=1

In both Figure 8 and Figure 9 the improvement offered by diversity initially lowers the probability of bit error, but not to the extent that it can overcome the errors introduced by partial-band jamming. It should be noted also that the high signal-to-thermal noise ratio is received after passing through the near Rayleigh channel. Therefore, it has a diffuse signal component equal to the direct signal component. This represents a very poor channel for the communicator that is further degraded by partial-band noise jamming.

The conclusion to be drawn from the preceding series of performance plots is that for a wide range of signal-to-thermal noise level, jammer power, and channel conditions, the increase in diversity in the FFH/MFSK receiver alone is not enough to overcome the effects of partial-band noise jamming acting in concert with multipath effects. The critical parameter then is the fraction of the spread spectrum bandwidth, γ, over which the jammer power is spread. The Figures 10 through 17 demonstrate the fraction of jammed bandwidth that provides the worst case probability of bit error.

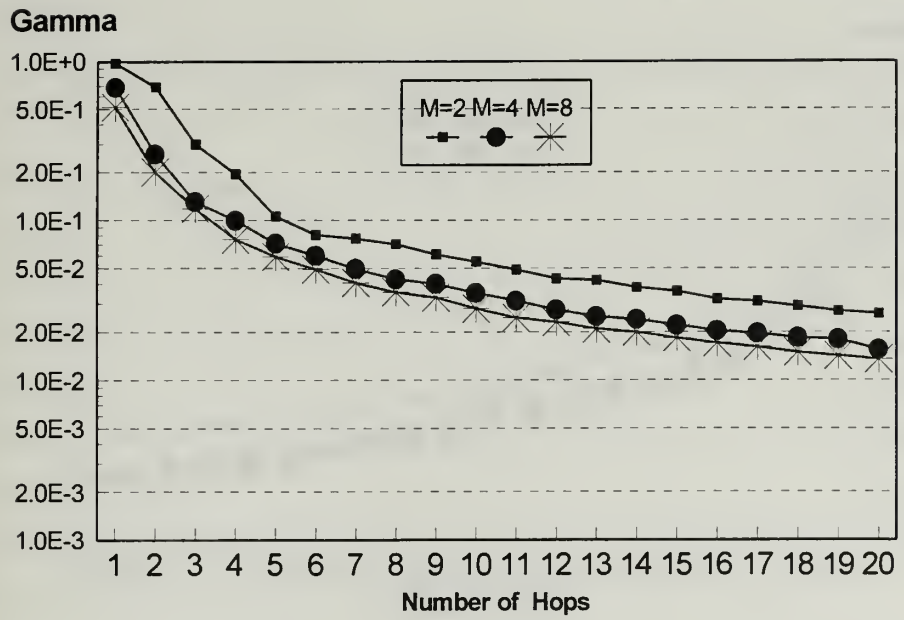

Figure 10. Fraction of Jammed Bandwidth
E_h/N_o=13.35dB, E_h/N_J=3dB, R_b=100

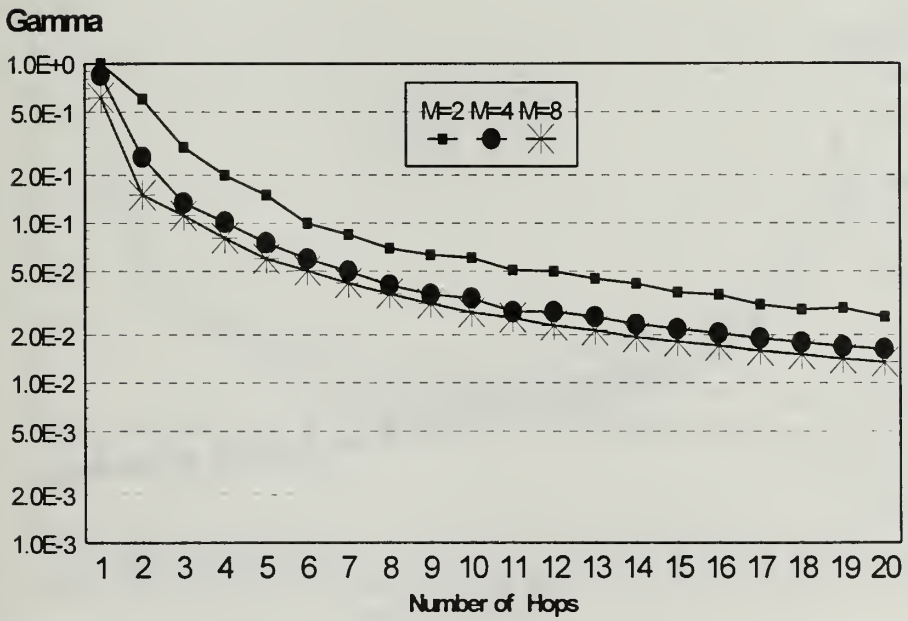

Figure 11. Fraction of Bandwidth Jammed
E_h/N_o=13.35dB, E_h/N_J=3dB, R_b=10

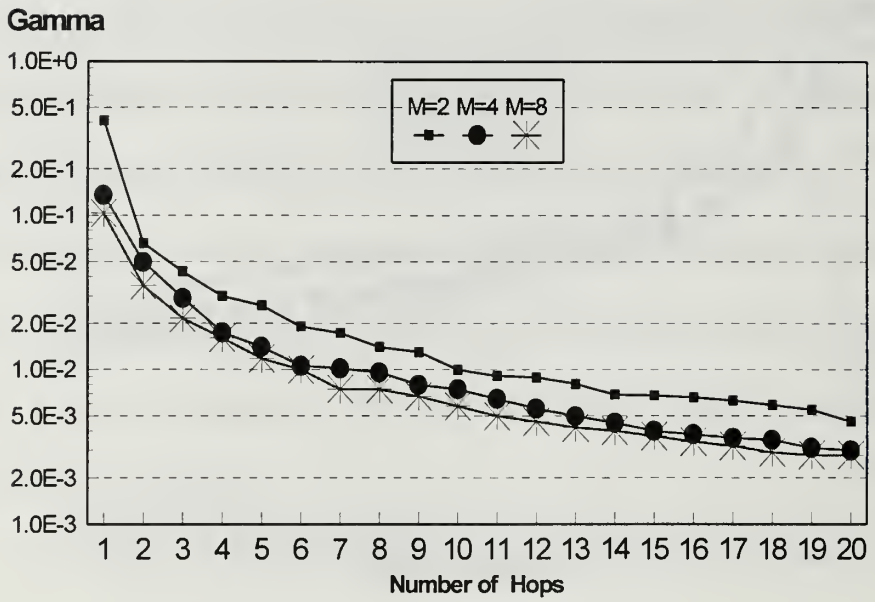

Figure 12. Fraction of Bandwidth Jammed
E_h/N_o=13.35dB, E_h/N_J=10dB, R_b=100

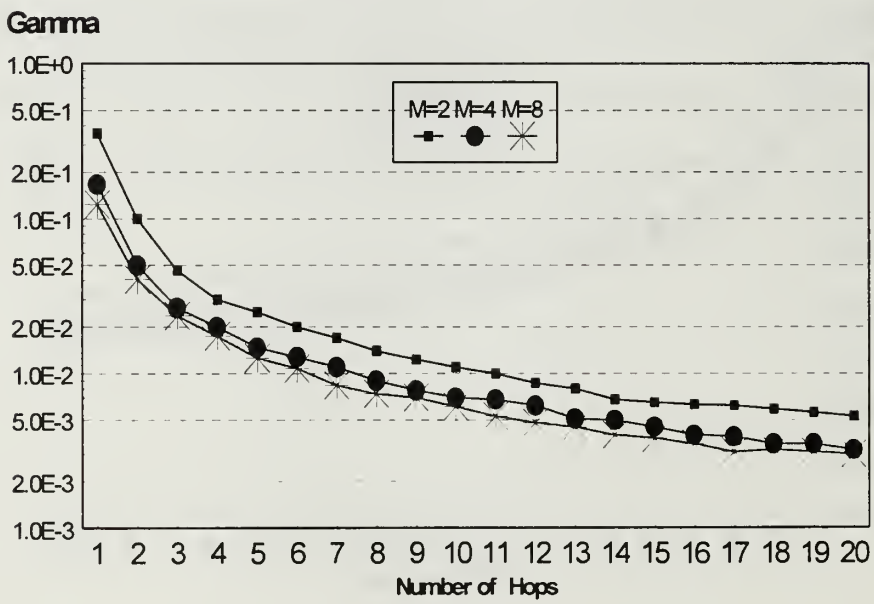

Figure 13. Fraction of Bandwidth Jammed
E_h/N_o=13.35dB, E_h/N_J=10dB, R_b=10

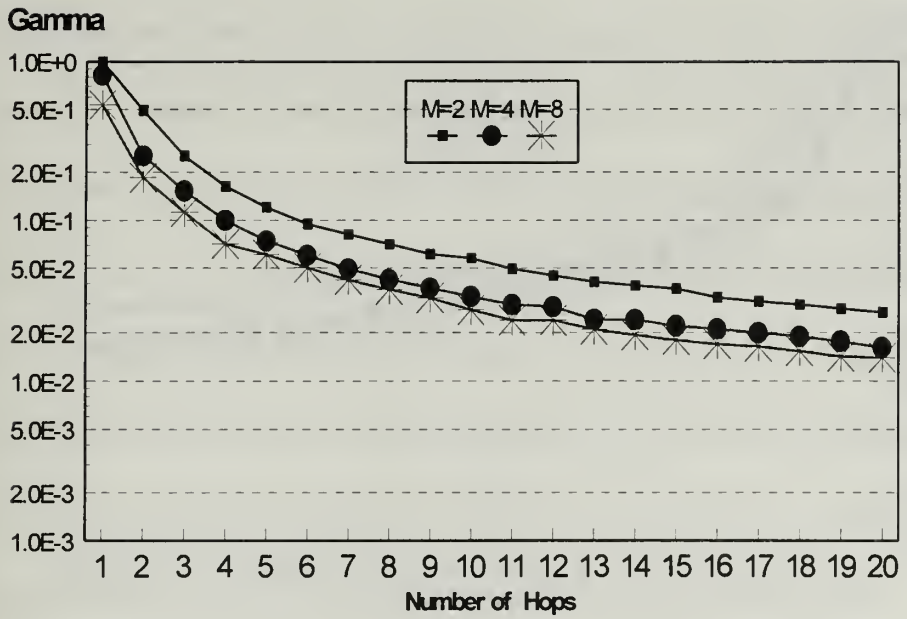

Figure 14. Fraction of Bandwidth Jammed
E_h/N_o=16dB, E_h/N_J=3dB, R_b=10

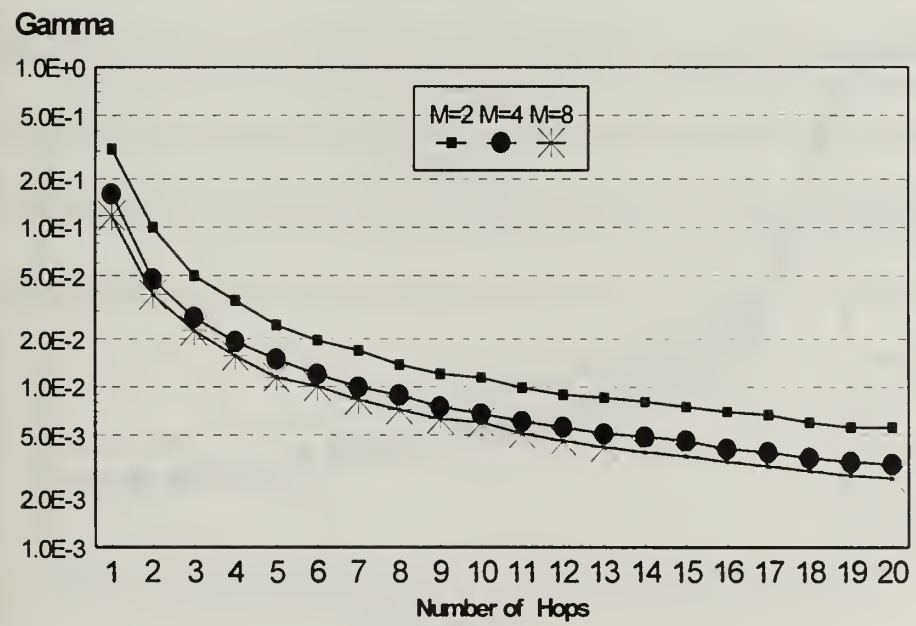

Figure 15. Fraction of Bandwidth Jammed
E_h/N_o=16dB, E_h/N_J=3dB, R_b=10

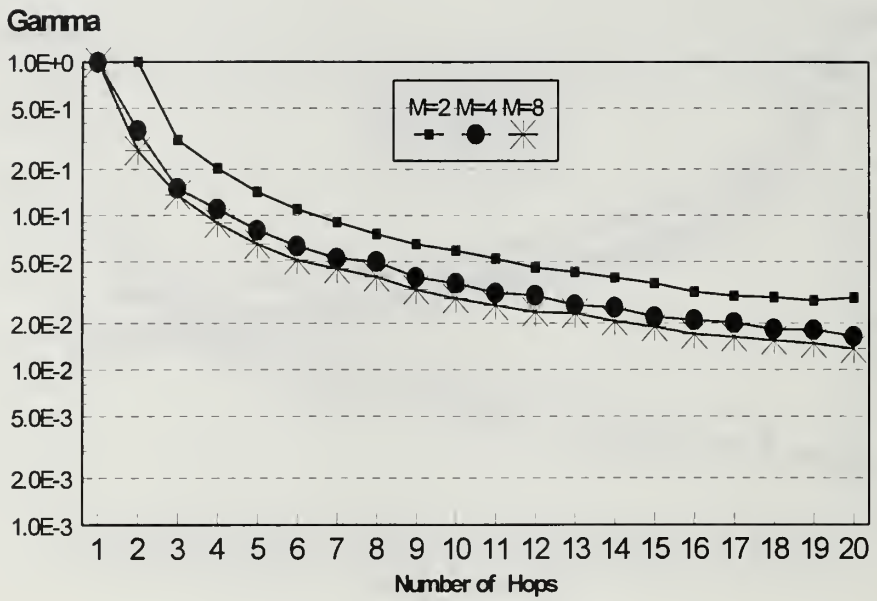

Figure 16. Fraction of Bandwidth Jammed
E_h/N_o=20dB, E_h/N_J=3dB, R_b=1

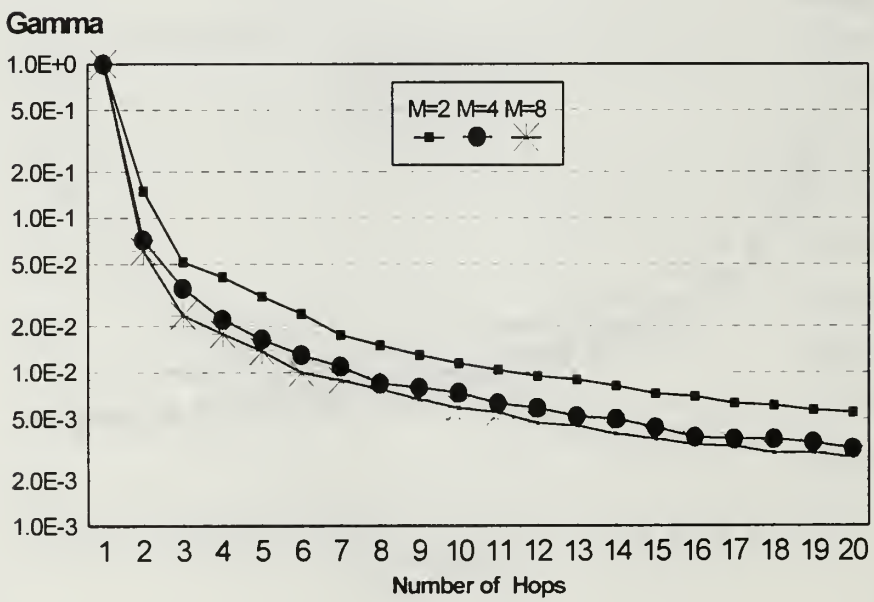

Figure 17. Fraction of Bandwidth Jammed
E_h/N_o=10dB, E_h/N_J=0dB, R_b=1

The worst case values γ are determined by computing the probability of bit error as a function of γ. Figure 10 through Figure 17 show that , in general γ, depends on the hop energy-to-thermal noise ratio (E_h/N_o), the hop energy-to-jammer power spectral density (E_h/N_J), the level of diversity (L), the modulation order (M), and the channel fading direct-to-diffuse ratio. Further, the shape of the worst case γ is generally the same, showing an initial drop as L increases with a gradually lowering slope. It is important to note that the lowest levels of γ are still above 10^{-3} which represent only one jammed hop slot when there are 1000 hops in the frequency-hopping system.

That the increase in diversity is unable to mitigate the partial band jamming is also indicated by looking at the trend of performance for fixed values of γ. Figure 10 through Figure 17 show that performance improves linearly as diversity increases. This is not unexpected since the constant energy per hop system increases the total energy per bit as diversity increases, however, the change in slope of the performance curves is indicative of the effect contributing to the worst case analysis. Figure 18 through Figure 23 display the performance for fixed values of γ.

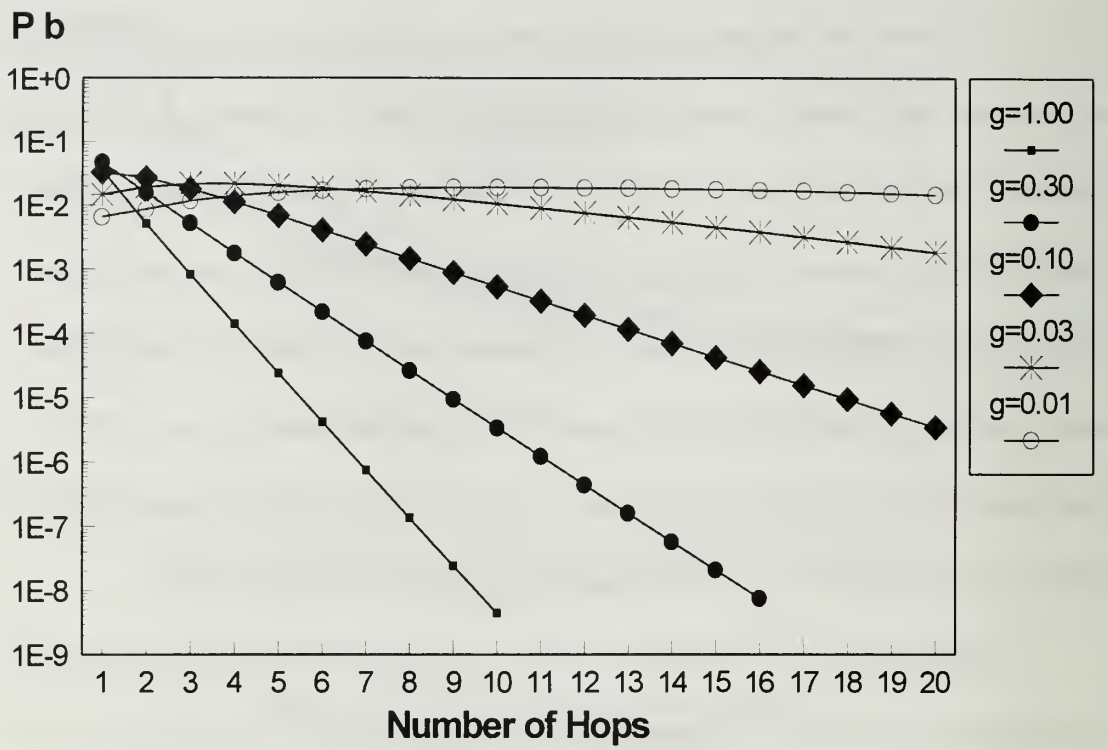

Figure 18. Performance for fixed values of gamma
E_h/N_o=13.35dB, E_h/N_J=10dB, R_b=10

Figure 18 displays the performance in a moderate Ricean fading channel where communicator enjoys a fair signal-to-jammer power advantage. The performance improves linearly as diversity increases. However, the slope of the performance curve is significantly reduced for decreasing values of γ. Further, we can see that for a given L there corresponds a worst case value for γ which becomes less sensitive as diversity increases. Figure 19 displays the performance when the signal enjoys less power advantage relative to the jammer. The trend is that for lower signal-to-jammer power ratio performance improves more slowly.

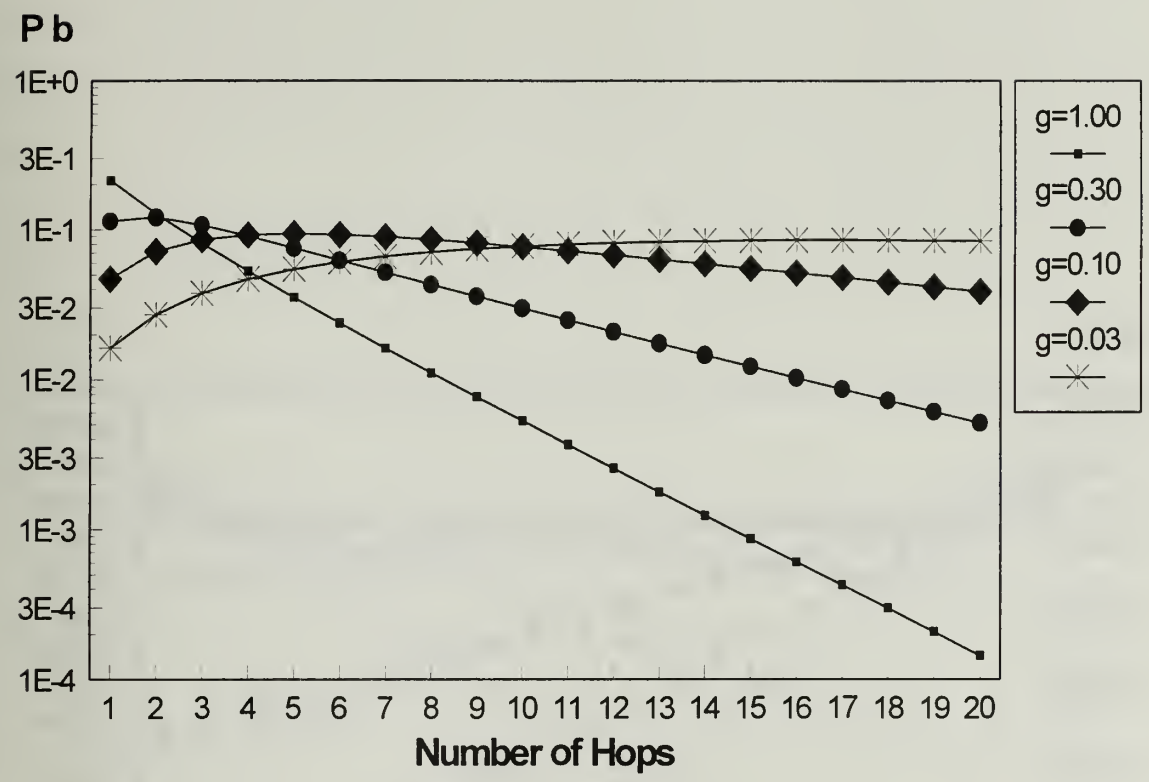

Figure 19. Performance for fixed values of gamma
E_h/N_o=13.35dB, E_h/N_J=3dB, R_b=10

The worst case fraction of bandwidth jammed is influenced by channel fading (Figure 10 through Figure 17). Likewise, the slope of the performance curves is influenced by channel fading . As the fading becomes more severe, i.e., near Rayleigh, the performance improves more slowly as demonstrated in Figure 21 through Figure 23.

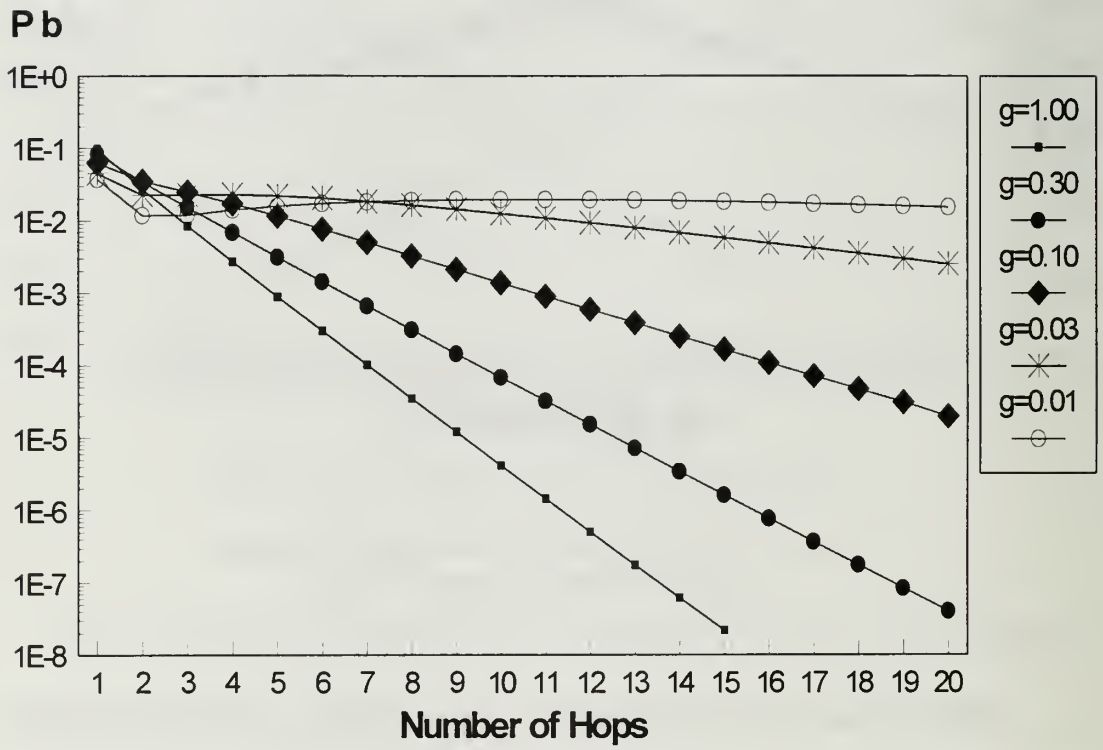

Figure 20. Performance for fixed values of gamma
E_h/N_o=13.35dB, E_h/N_J=10dB, R_b=1

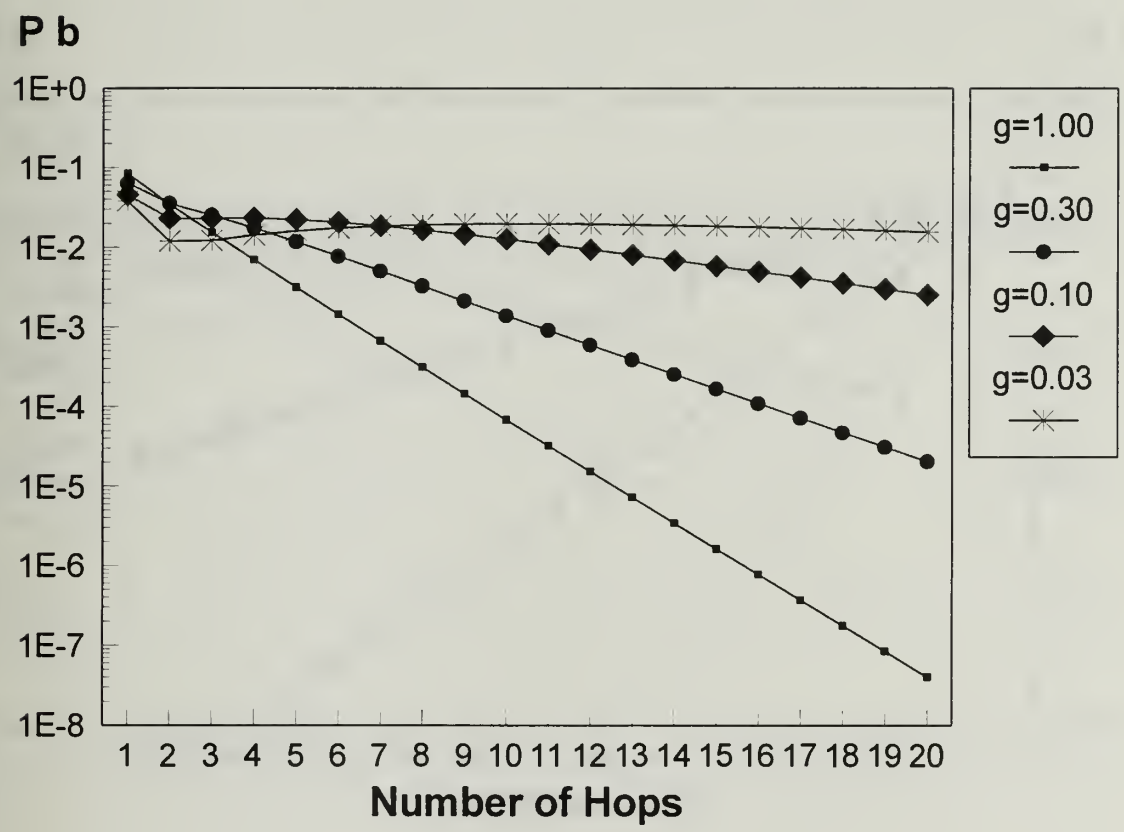

Figure 21. Performance for fixed values of gamma
E_h/N_o=13.35dB, E_h/N_J=3dB, R_b=1

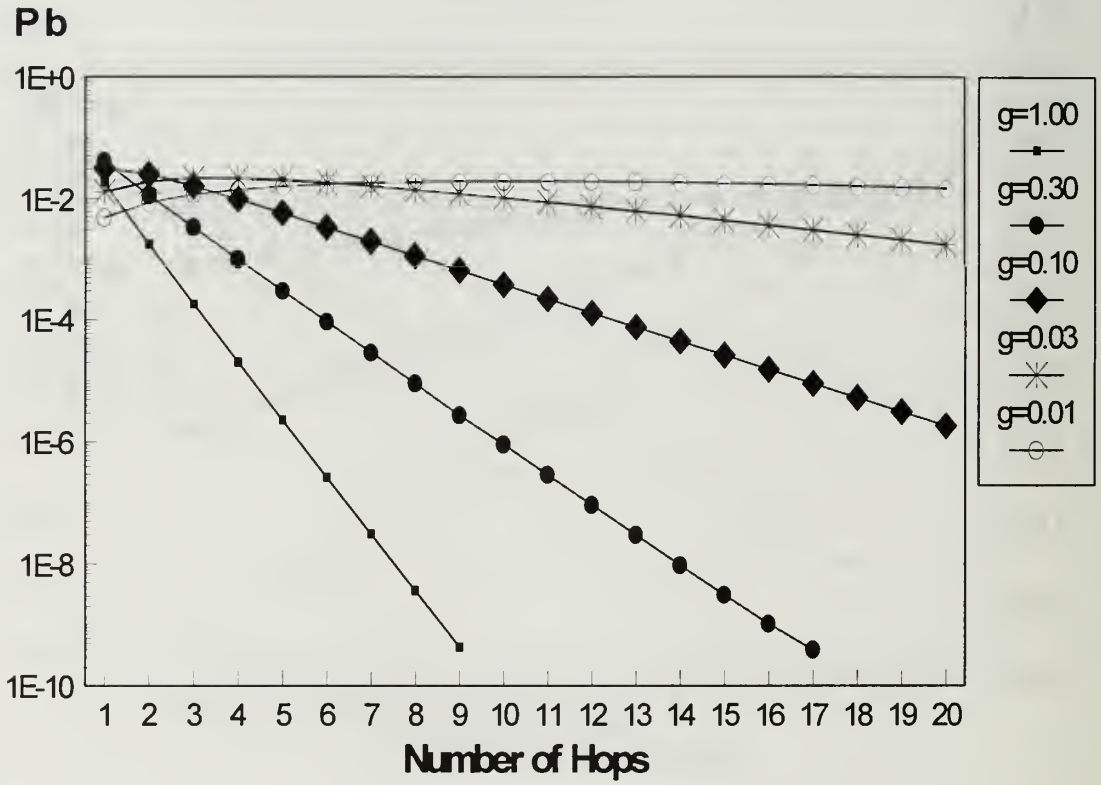

Figure 22. Performance for fixed values of gamma
E_h/N_o=13.35dB, E_h/N_J=10dB, R_b=100

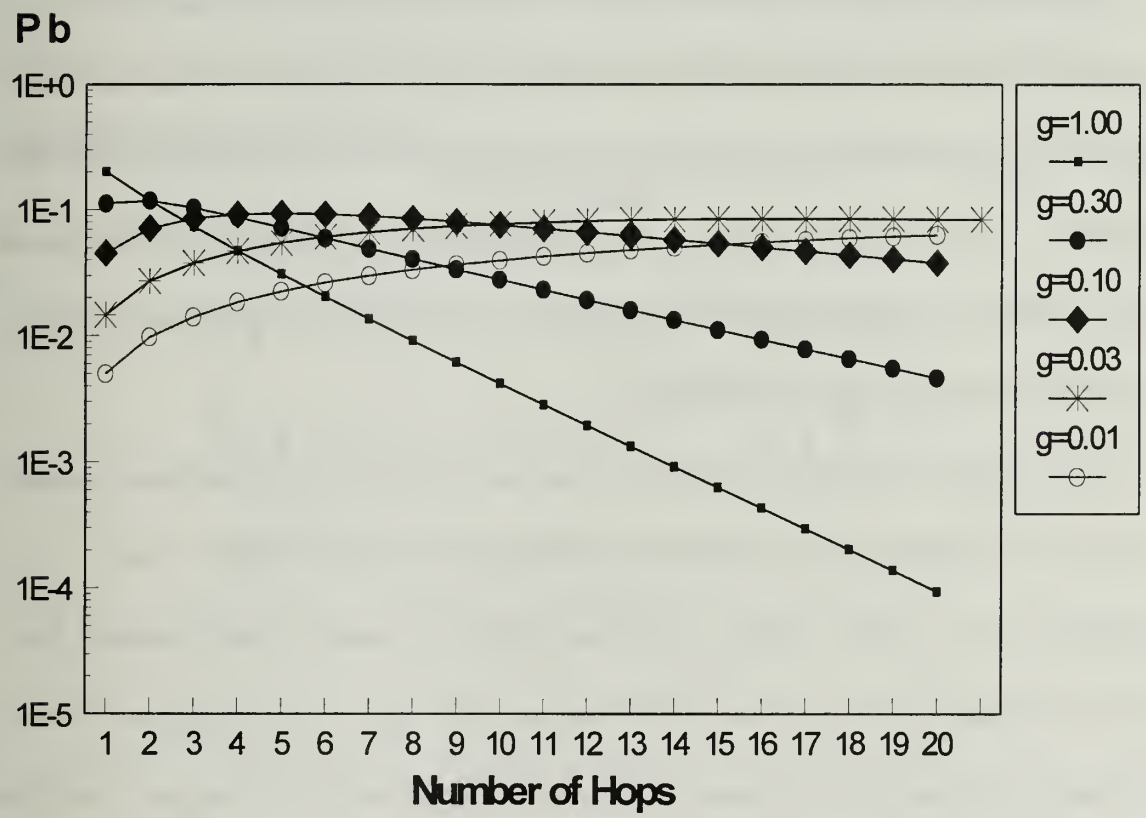

Figure 23. Performance for fixed values of gamma
E_h/N_o=13.35dB, E_h/N_J=3dB, R_b=100

III. MULTI-TONE INTERFERENCE

A. SYSTEM DESCRIPTION

In addition to partial-band noise jamming, spread spectrum communications can experience tonal or narrowband interference in one or more hop slots. We can similarly expect that as spread spectrum bandwidth grows the likelihood of tonal interference will also grow. This interference may arise from hostile sources as well as non-hostile ground communications, satellite transponders, and radars. The multi-tone interference problem is similar to the partial-band noise problem.

This chapter analyzes the probability of bit error arising from an "intelligent jammer" who knows the spread spectrum bandwidth, W, and the modulation order. This intelligent jammer is able to place a single interfering tone in one or more hop slots, but has no knowledge of the pseudonoise (PN) sequence driving the hopping pattern. This represents a very intelligent jammer. We then relax this situation and compare it with the performance of the jammer who places an interfering tone in none, one, or both of the symbol tone locations in a particular hop slot.

It is likely that the interfering tones may experience multi-path effects in a manner similar to the signal tone. However, since the interfering tones and signal tone can arrive from different paths, the interfering tones will in general arrive at the receiver with a different direct-to-diffuse power ratio from that of the signal. In this thesis, the performance when both the signal and the jammer experience fading is evaluated.

B. MULTI-TONE INTERFERENCE ANALYSIS

1. Problem Development

First we consider the case where the jammer places at most one tone in each fast frequency-hop slot. Only the worst case situation where the jamming tones exactly coincide with frequency-hopped symbol tones is considered. The situation may be visualized with the aid Figure 24.

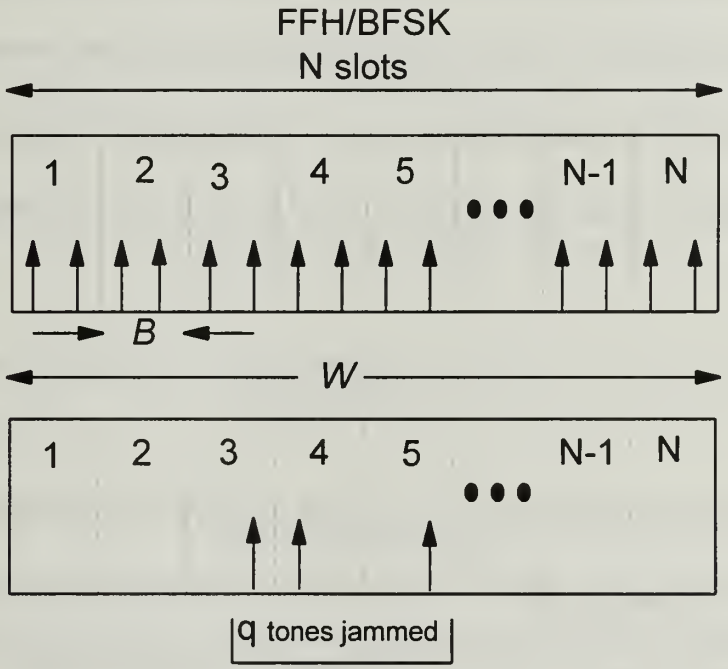

Figure 24. Multi-tone interference in FFH/BFSK

The FFH/BFSK receiver is a special case of the FFH/MFSK receiver described earlier. The orthogonal design is selected such that $\mathcal{R}_b$ is the system bit rate and each signal tone is placed $\mathcal{R}_b$ apart. In Figure 24 the bandwidth of a single hop, B, is $2\mathcal{R}_b$. The spread spectrum encompasses W Hz and is divided into N hop slots. Although numbered consecutively for illustration, the pseudonoise modulation will create a

random-like sequence to the hopping pattern. In this thesis, N=1000 is choosen as a representative number of hop slots. Further, the number of interfering tones, q, must be an integer

$$1 \leq q \leq N \tag{44}$$

Since the jammer spreads his available power, J, equally among q tones, each interfering tone has a power of $J_q = J/q$. Earlier work focuses on the simplifying case of no thermal noise [Ref. 13]. In the no thermal noise case an error can only occur if the hop is jammed and the the interfering tone power is larger than the signal power. In this instance the jammer can make most efficient use of his power by choosing the number of tones to jam as

$$q = \text{INTG}\left[\frac{J}{P_c}\right] \tag{45}$$

where P_c is the carrier power of the desired symbol and INTG[ ] represents the greatest integer less than the argument. [Ref. 13, pp.596-598] In this thesis, the probability of bit error is obtained using fixed values of q to determine a worst case scenario which includes the effects of both signal and jammer fading as well as thermal noise. The approach to this problem is to first detemine the probability of bit error for a conventional BFSK system without frequency-hopping and then generalize those results to the FFH/BFSK system.

2. BFSK Analysis with Single Tone Interference

For the binary case we begin with the familiar expression for the probability of bit error for the noncoherent FSK receiver

$$P_b = P_{s_1} \times P_r[R_2 > R_1 | s_1] + P_{s_2} \times P_r[R_1 > R_2 | s_2] \tag{46}$$

where R_1 and R_2 represent the demodulator outputs of the branch detecting signal s_1 and s_2, respectively. Making the assumption of equally likely signaling, we have

$$P_{s_1} = P_{s_2} = \frac{1}{2} \tag{47}$$

and

$$P_b = \frac{1}{2}[P_r(R_2 > R_1) + P_r(R_1 > R_2)] \tag{48}$$

The received energy consists of signal energy, thermal noise, and, if jammed, the interference signal

$$r(t) = s_i(t) + n(t) + s_J(t), \tag{49}$$

where s_i is the ith signal tone, s_J is the interference tone, and n(t) is additive white Gaussian noise with power spectral density $N_o / 2$. Since the receiver structure is symmetric, we can simplify the analysis problem by considering the case where branch two is jammed.

First we examine the case where the signal and interference occupy different frequencies. Then

$$P_r(error | s_1) = P_r(R_2 > R_1 | s1) \tag{50}$$

We express the received waveform as

$$r(t) = \sqrt{2}\, a_c \cos(\omega_1 t + \theta) + \sqrt{2}\, a_J \cos(\omega_2 t + \theta_J) + n(t) \tag{51}$$

where a_c and a_J are modeled as Ricean random variables. As previously discussed the received amplitudes and phases of each tone is a random variable due to multipath effects. For the noncoherent detector design, the output of each branch can be expressed as a non-central Chi square random variable [Ref. 2]. For the signal branch

$$f_{R_1}(r_1 | a_c, s_1) = \frac{1}{2\sigma^2} \exp\left\{ -\frac{\left(r_1 + 2a_c^2 T_b^2\right)}{2\sigma^2} \right\} I_0\left[\frac{a_c T_b}{\sigma^2} \sqrt{2r_1} \right] u(r_1) \tag{52}$$

and for branch two containing the interference tone

$$f_{R_2}(r_2 | a_J, s_1) = \frac{1}{2\sigma^2} \exp\left\{ -\frac{\left(r_2 + 2a_J^2 T_b^2\right)}{2\sigma^2} \right\} I_0\left[\frac{a_J T_b}{\sigma^2} \sqrt{2r_2} \right] u(r_2) \tag{53}$$

where $\sigma^2 = N_o T_b$. The probability of error (50) is

$$P_r(R_2 > R_1 | a_c, a_J, s_1) = \int_0^\infty \int_{R_1}^\infty f_{R_1 R_2}(r_1, r_2 | a_J, a_c, s_1) dr_2 dr_1 \tag{54}$$

This represents the probability conditioned on the amplitudes of a_c and a_J. The orthogonal receiver structure and independent fading of the interference tone and the signal tone allow the joint probability density function to be separated. Hence, (54) simplifies to

$$P_r(R_2 > R_1 | s_1) = \int_0^\infty f_{R_1}(r_1 | a_c, s_1) \left[\int_{R_1}^\infty f_{R_2}(r_2 | a_J, s_1) dr_2 \right] dr_1 \tag{55}$$

The evaluation of (55) is simplified by applying the quadratic transformation to convert (52) and (53) to Ricean random variables [Ref. 11]. If $r_1 = v_1^2$, then $\frac{dr_1}{dv_1} = 2v_1$. Using this substitution in (52), we obtain

$$f_{V_1}(v_1|a_c, s_1) = \frac{v_1}{2\sigma^2} \exp\left\{-\frac{\left(v_1^2 + 2a_c^2 T_b^2\right)}{2\sigma^2}\right\} I_0\left[\frac{\sqrt{2}\, a_c T_b v_1}{\sigma^2}\right] u(v_1) \qquad (56)$$

Similarly for the branch output containing the interference tone

$$f_{V_2}(v_2|a_J, s_1) = \frac{v_2}{2\sigma^2} \exp\left\{-\frac{\left(v_2^2 + 2a_J^2 T_b^2\right)}{2\sigma^2}\right\} I_0\left[\frac{\sqrt{2}\, a_J T_b v_2}{\sigma^2}\right] u(v_2) \qquad (57)$$

Now (55) can be expressed as

$$P_r(V_2 > V_1|s_1) = \int_0^\infty f_{V_1}(v_1|a_c, s_1)\left[\int_{V_1}^\infty f_{V_2}(v_2|a_J, s_1) dv_2\right] dv_1 \qquad (58)$$

The inner integral equation has no simple solution, but is represented symbolically as Marcum's Q function which is defined as [Ref. 14]

$$Q(\alpha, \beta) = \int_\beta^\infty v \exp\left\{-\frac{1}{2}(v^2 + \alpha^2)\right\} I_0[\alpha v] dv \qquad (59)$$

Hence, (58) is expressed as

$$P_r(v_2 > v_1|s_1) = \int_0^\infty Q\left(\sqrt{2}\, a_J T_b/\sigma, \frac{v_1}{\sigma}\right) \times \frac{v_1}{\sigma^2} \exp\left\{-\frac{v_1^2 + 2a_c^2 T_b^2}{2\sigma^2}\right\} I_0\left[\frac{\sqrt{2}\, a_c T_b v_1}{\sigma^2}\right] dv_1 \qquad (60)$$

which can be evaluated to obtain [Ref. 15]

$$P_r(v_2 > v_1|s_1) = \frac{1}{2}\left[1 - Q\left(\frac{a_c T_b}{\sigma}, \frac{a_J T_b}{\sigma}\right) + Q\left(\frac{a_J T_b}{\sigma}, \frac{a_c T_b}{\sigma}\right)\right] \qquad (61)$$

Equation (58) represents the contribution to the probability of bit error when the signal and jammer occupy different tones within a hop. It remains to determine the contribution due to a collocation of interfering and signal tones. That is

$$P_r(\text{error}\,|s_2) = P_r(R_1 > R_2|s_2) \tag{62}$$

where

$$f_{R_1}(r_1) = \frac{1}{2\sigma^2}\exp\left\{\frac{-r_1}{2\sigma^2}\right\}u(r_1) \tag{63}$$

Since the signal and the interference are in the same tone location, the output of the in-phase and quadrature portions of branch two due to signal and jamming tones is

$$\sqrt{2}\,T_b[a_c\cos(\theta) + a_J\cos(\theta_J) \tag{64}$$

and

$$\sqrt{2}\,T_b[a_c\sin(\theta) + a_J\sin(\theta_J)] \tag{65}$$

respectively. The phase of the jammer is generally different from that of the signal. Squaring and summing to form the branch output produces

$$R_2(\theta - \theta_J) = 2T_b^2\left[a_c^2 + a_J^2 + 2a_c a_J(\cos\theta\cos\theta_J + \sin\theta\sin\theta_J\right] \tag{66}$$

which is simplified to

$$R_2(\delta) = 2T_b^2\left[a_c^2 + a_J^2 + 2a_c a_J\cos\delta\right] \tag{67}$$

where $\delta = \theta - \theta_J$. Now, replacing $2a_J^2T_b^2$ with (67) in (53) we get

$$f_{R_2}(r_2|a_c, a_J, \delta, s_2) = \frac{1}{2\sigma^2}\exp\left\{-\frac{\left(r_2 + 2T_b^2\left(a_c^2 + a_J^2\right)\right)}{2\sigma^2}\right\}I_0\left[\frac{T_b}{\sigma^2}\sqrt{2r_2\left(a_c^2 + a_J^2\right)}\right]u(r_2) \tag{68}$$

Now,

$$P_r(R_1 > R_2 | s_2, \delta) = \int_0^\infty f_{R_2}(r_2 | a_c, a_J, \delta, s_2) \times \left[\int_{R_2}^\infty f_{R_1}(r_1 | s_2) dr_1 \right] dr_2 \qquad (69)$$

Thus, the probability of error arising from collocation of the jammer and the signal is computed from a probability density function conditional on δ. In this case the non-signal branch is unaffected by the jamming tone. Substituting (63) and (68) into (69), we get

$$P_r(R_1 > R_2 | s_2, \delta) = \frac{1}{2} \times \exp\left\{ -\frac{T_b^2}{2\sigma^2}\left(a_c^2 + a_J^2 + 2a_c a_J \cos\delta \right) \right\} \qquad (70)$$

This can be simplified into familiar terms by replacing

$$a_c^2 \frac{T_b^2}{2\sigma^2} \Rightarrow a_c^2 \frac{T_b}{N_o} \Rightarrow \frac{E_b}{N_o} \Rightarrow \gamma_b \qquad (71)$$

and similarly for the jammer power term

$$a_J^2 \frac{T_b^2}{2\sigma^2} \Rightarrow a_J^2 \frac{T_b}{N_o} \Rightarrow \frac{E_J}{N_o} \Rightarrow \gamma_J \qquad (72)$$

Then the conditional expression in (70) then becomes

$$P_r(R_1 > R_2 | s_1, \delta) = \left(\frac{1}{2} \right) \exp\left\{ \frac{-1}{2}\left(\gamma_b + \gamma_J + 2\sqrt{\gamma_b \gamma_J}\, \cos\delta \right) \right\} \qquad (73)$$

The nuisance parameter δ may be removed by multiplying by its probability density function and integrating the conditional density. That is

$$P_r(R_1 > R_2 | s_1) = \frac{1}{4\pi} \int_0^{2\pi} \exp\left\{ \frac{-1}{2}\left(\gamma_b + \gamma_J + 2\sqrt{\gamma_b \gamma_J}\, \cos\delta \right) \right\} d\delta \qquad (74)$$

where δ is modeled as a uniform random variable. Since the integral is only over δ, then [Ref. 10]

$$P_r(R_1 > R_2|s_1) = \exp\left\{\frac{-1}{2}(\gamma_b + \gamma_J)\right\} \times \frac{1}{4\pi}\int_0^{2\pi} \exp\left\{\sqrt{\gamma_b\gamma_J}\cos\delta\right\}d\delta \tag{75}$$

which can be evaluated to obtain

$$P_r(R_1 > R_2|s_1) = \left(\frac{1}{2}\right) \times \exp\left\{-\frac{1}{2}(\gamma_b + \gamma_J)\right\} \times I_0\left[\sqrt{\gamma_b\gamma_J}\right] \tag{76}$$

Therefore, the phase relationship between the signal and the jammer plays a significant role as evidenced by the modified Bessel function term. This makes physical sense. When the phase is the same or nearly so there is reinforcement of the signal tone by the interfering tone, but when the phase difference approaches 180 degrees there is destructive interference.

This allows us to compute the probability of bit error in the absence of fading by substituting (61) and (76) into (48).

$$P_b(a_c, a_J) = \frac{1}{4}\left[1 - Q\left(\sqrt{\frac{a_c T_b}{\sigma}}, \sqrt{\frac{a_J T_b}{\sigma}}\right) + Q\left(\sqrt{\frac{a_J T_b}{\sigma}}, \sqrt{\frac{a_c T_b}{\sigma}}\right)\right.$$

$$\left. + \exp\left\{\frac{-T_b^2}{2\sigma^2}\left(a_c^2 + a_J^2\right)\right\} I_0\left[\frac{a_c a_J T_b^2}{\sigma^2}\right]\right] \tag{77}$$

An equivalent expression using (71) and (72) is

$$P_b(\gamma_b, \gamma_J) = \frac{1}{4}\left[1 - Q\left(\sqrt{\gamma_b}, \sqrt{\gamma_J}\right) + Q\left(\sqrt{\gamma_J}, \sqrt{\gamma_b}\right) + \exp\left\{\frac{-1}{2}(\gamma_b + \gamma_J)\right\} I_0\left[\sqrt{\gamma_b\gamma_J}\right]\right] \tag{78}$$

Using a Q function property [Ref. 15, pp. 396], we can reduce this to an expression containing just one Q function as

$$P_b(a_c, a_J) = \left(\frac{1}{2}\right) \times Q\left(\sqrt{\frac{a_J T_b}{\sigma}}, \sqrt{\frac{a_c T_b}{\sigma}}\right)$$

$$-\left[I_0\left[\frac{a_c a_J T_b^2}{\sigma^2}\right] - 1\right] \times \exp\left\{\frac{-T_b^2}{2\sigma^2}\left(a_c^2 + a_J^2\right)\right\} \tag{79}$$

Now, the amplitudes of the received interference tone and signal tone are Ricean random variables where

$$f_{A_J}(a_J) = \frac{a_J}{\sigma_J^2} \exp\left\{-\left(\frac{a_J^2 + \alpha_J^2}{2\sigma_J^2}\right)\right\} \times I_0\left[\frac{a_J \alpha_J}{\sigma_J^2}\right] u(a_J) \tag{80}$$

$$f_{A_c}(a_c) = \frac{a_c}{\sigma_c^2} \exp\left\{-\left(\frac{a_c^2 + \alpha_c^2}{2\sigma_c^2}\right)\right\} \times I_0\left[\frac{a_c \alpha_c}{\sigma_c^2}\right] u(a_c) \tag{81}$$

Where in each case the second moment can be expressed as

$$\overline{a_i^2} = \alpha_i^2 + 2\sigma_i^2 \text{ for i= } J, c. \tag{82}$$

We first remove the conditioning on a_c in (79). The technique is to take each piece of (79), multiply by (81), and integrate over all possible values of a_c. Hence, for the first piece

$$\int_0^\infty Q\left(\sqrt{\frac{a_J T_b}{\sigma}}, \sqrt{\frac{a_c T_b}{\sigma}}\right) f_{A_c}(a_c) da_c =$$

$$\int_0^\infty Q\left(\sqrt{\frac{a_J T_b}{\sigma}}, \sqrt{\frac{a_c T_b}{\sigma}}\right) \frac{a_c}{\sigma_c^2} \exp\left\{-\left(\frac{a_c^2 + \alpha_c^2}{2\sigma_c^2}\right)\right\} \times I_0\left[\frac{a_c \alpha_c}{\sigma_c^2}\right] da_c \tag{83}$$

$$= \frac{\sigma_c^2 T_b^2}{\sigma_c^2 T_b^2 + \sigma^2}\left[1 - Q\left(\sqrt{\frac{\alpha_c^2 T_b^2}{\sigma_c^2 T_b^2 + \sigma^2}}, \sqrt{\frac{a_J^2 T_b^2}{\sigma_c^2 T_b^2 + \sigma^2}}\right)\right]$$

$$+ \frac{\sigma^2}{\sigma_c^2 T_b^2 + \sigma^2} Q\left(\sqrt{\frac{a_J^2 T_b^2}{\sigma_c^2 T_b^2 + \sigma^2}}, \sqrt{\frac{\alpha_c^2 T_b^2}{\sigma_c^2 T_b^2 + \sigma^2}}\right) \tag{84}$$

The integral of the product of the second piece and (81) is

$$\int_0^\infty \exp\left\{-\frac{T_b^2}{2\sigma^2}\left(a_c^2 + a_J^2\right)\right\} I_0\left[\frac{a_c \alpha_c T_b^2}{2\sigma_c^2}\right] \times \frac{a_c}{\sigma_c^2} \exp\left\{-\left(\frac{a_c^2 + \alpha_c^2}{2\sigma_c^2}\right)\right\} I_0\left[\frac{a_c \alpha_c}{\sigma_c^2}\right] da_c \tag{85}$$

Making the substitutions

$$\hat{\alpha} = \frac{T_b^2}{2\sigma^2} + \frac{1}{2\sigma_c^2},\ B = \frac{a_J T_b^2}{\sigma^2},\ \text{and}\ \Gamma = j\frac{\alpha_c}{\sigma_c^2},\ \text{then}$$

$$\frac{B^2 - \Gamma^2}{4\hat{\alpha}} = \frac{a_J^2 T_b^4 \sigma_c^4 + \alpha_c^2 \sigma^4}{4\sigma^4 \sigma_c^4} \times \frac{2\sigma^4 \sigma_c^4}{T_b^2 \sigma_c^2 + \sigma^2} \tag{86}$$

$$\frac{B\Gamma}{2\hat{\alpha}} = \frac{j\alpha_c a_J T_b^2}{T_b^2 \sigma_c^2 + \sigma^2} \tag{87}$$

in (85), we can use [Ref. 10, equation 6.633.4] to obtain

$$\frac{\sigma^2}{T_b^2 \sigma_c^2 + \sigma^2} \exp\left\{\frac{-T_b^2\left(a_J^2 + \alpha_c^2\right)}{2T_b^2 \sigma_c^2 + 2\sigma^2}\right\} \times I_0\left[\frac{T_b^2 a_J \alpha_c}{T_b^2 \sigma_c^2 + \sigma^2}\right] \tag{88}$$

for the second piece of (79). The remaining piece to be determined is

$$\int_0^\infty \exp\left\{-\frac{T_b^2}{2\sigma^2}\left(a_J^2 + a_c^2\right)\right\} \frac{a_c}{\sigma_c^2} \exp\left\{-\left(\frac{a_c^2 + \alpha_c^2}{2\sigma_c^2}\right)\right\} \bullet I_0\left[\frac{a_c \alpha_c}{\sigma_c^2}\right] da \tag{89}$$

Using [Ref. 10, equation 6.631.4], we evaluate (89) to obtain

$$\frac{\sigma^2}{T_b^2\sigma_c^2+\sigma^2}\exp\left\{-\left[\frac{a_J^2T_b^2}{2\sigma^2}+\frac{\alpha_c^2T_b^2}{2\left(T_b^2\sigma_c^2+\sigma^2\right)}\right]\right\} \tag{90}$$

Finally, combining (84), (88), and (90) with (79), we get the probability of bit error when the signal experiences Ricean fading as

$$P_b(a_J)=\frac{\sigma_c^2T_b^2}{2\left(\sigma_c^2T_b^2+\sigma^2\right)}\left[1-Q\left(\sqrt{\frac{\alpha_c^2T_b^2}{\sigma_c^2T_b^2+\sigma^2}},\sqrt{\frac{a_J^2T_b^2}{\sigma_c^2T_b^2+\sigma^2}}\right)\right]+$$

$$\frac{\sigma^2}{2\left(\sigma_c^2T_b^2+\sigma^2\right)}Q\left(\sqrt{\frac{a_J^2T_b^2}{\sigma_c^2T_b^2+\sigma^2}},\sqrt{\frac{\alpha_c^2T_b^2}{\sigma_c^2T_b^2+\sigma^2}}\right)+$$

$$\frac{\sigma^2}{4\left(T_b^2\sigma_c^2+\sigma^2\right)}\exp\left\{-\frac{\alpha_c^2T_b^2}{2\left(T_b^2\sigma_c^2+\sigma^2\right)}\right\}\times$$

$$\left[\exp\left\{\frac{-a_J^2T_b^2}{2\sigma^2}\right\}-\exp\left\{-\frac{\alpha_J^2T_b^2}{2\left(T_b^2\sigma_c^2+\sigma^2\right)}\right\}\times I_0\left[\frac{a_J\alpha_cT_b^2}{T_b^2\sigma_c^2+\sigma^2}\right]\right] \tag{91}$$

which is now conditional on a_J. Expressing (86) in terms of

$$\zeta_b=\frac{\alpha_c^2T_b^2}{\sigma^2}=\frac{\alpha_c^2T_b}{N_o} \tag{92}$$

$$\xi_b=\frac{2\sigma_c^2T_b^2}{\sigma^2}=\frac{2\sigma_c^2T_b}{N_o} \tag{93}$$

and the direct-to-diffuse power ratio

$$R_b = \frac{\zeta_b}{\xi_b} = \frac{\alpha_c^2}{2\sigma^2} \tag{94}$$

we get

$$P_b(a_J) = \frac{\xi_b/2}{(\xi_b+2)}\left[1 - Q\left(\sqrt{\frac{2\zeta_b}{\xi_b+2}}, \sqrt{\frac{2a_J^2T_b^2/\sigma^2}{\xi_b+2}}\right)\right] +$$

$$\frac{1}{2(\xi_b+2)}Q\left(\sqrt{\frac{2a_J^2T_b^2/\sigma^2}{\xi_b+2}}, \sqrt{\frac{2\zeta_b}{\xi_b+2}}\right) + \frac{1}{2(\xi_b+2)}\exp\left\{-\frac{\zeta_b}{(\xi_b+2)}\right\} \times$$

$$\left[\exp\left\{\frac{-a_J^2T_b^2}{2\sigma^2}\right\} - \exp\left\{-\frac{\alpha_J^2T_b^2/\sigma^2}{\xi_b+2}\right\} \times I_0\left[\frac{a_J\sqrt{\zeta_b}\,T_b/\sigma}{\xi_b+2}\right]\right] \tag{95}$$

Using [Ref. 15]

$$Q\left(\sqrt{\frac{2a_J^2T_b^2/\sigma^2}{\xi_b+2}}, \sqrt{\frac{2\zeta_b}{\xi_b+2}}\right) = 1 - Q\left(\sqrt{\frac{2\zeta_b}{\xi_b+2}}, \sqrt{\frac{2a_J^2T_b^2/\sigma^2}{\xi_b+2}}\right) +$$

$$\exp\left\{\frac{-1}{2}\left(\frac{2\alpha_J^2T_b^2/\sigma^2 + 2\zeta_b}{\xi_b+2}\right)\right\} \times I_0\left[\frac{2\sqrt{\zeta_b}}{\xi_b+2}a_JT_b/\sigma\right] \tag{96}$$

in (95), we obtain

$$P_b(a_J) = \frac{1}{2}\left[1 - Q\left(\sqrt{\frac{2\zeta_b}{\xi_b+2}}, \sqrt{\frac{2a_J^2T_b^2/\sigma^2}{\xi_b+2}}\right)\right] + \frac{1}{2(\xi_b+2)}\exp\left\{\frac{-\zeta_b}{\xi_b+2}\right\} \times$$

$$\left[\exp\left\{-a_J^2T_b^2/2\sigma^2\right\} + \exp\left\{\frac{-a_J^2T_b^2}{\sigma^2(\xi_b+2)}\right\} \times I_0\left[\frac{2a_JT_b\sqrt{\zeta_b}}{\sigma(\xi_b+2)}\right]\right] \tag{97}$$

We now employ a similar approach to remove the conditioning on a_J. Integrating the product of (80) and (97) over all possible receiver jammer amplitudes, a_J, we get

$$P_b = \frac{1}{2}\left[1 - Q\left(\sqrt{\frac{2\zeta_b}{(\xi_b+\xi_J+2)}}, \sqrt{\frac{2\zeta_J}{(\xi_b+\xi_J+2)}}\right)\right] +$$

$$\frac{(\xi_J+2)}{2(\xi_b+\xi_J+2)} \exp\left\{\frac{-(\zeta_b+\zeta_J)}{\xi_b+\xi_J+2}\right\} \times I_0\left[\frac{2\sqrt{\zeta_b\zeta_J}}{\xi_b+\xi_J+2}\right] \tag{98}$$

where

$$\zeta_J = \frac{\alpha_J^2 T_b^2}{\sigma^2} = \frac{\alpha_J^2 T_b}{N_o} \tag{99}$$

$$\xi_J = \frac{2\sigma_J^2 T_b^2}{\sigma^2} = \frac{2\sigma_J^2 T_b}{N_o} \tag{100}$$

$$R_J = \frac{\zeta_J}{\xi_J} = \frac{\alpha_J^2}{2\sigma^2} \tag{101}$$

An alternate expression for the probability of bit error in the case of both signal and jammer fading in terms of weighted Q functions is

$$P_b = \frac{1}{2}\left[1 - Q\left(\sqrt{\frac{\zeta_J}{\xi_b+\xi_J+2}}\sqrt{\frac{2\zeta_b}{\xi_b+2}}, \right)\right] +$$

$$\frac{1}{2}\left[Q\left(\sqrt{\frac{2\zeta_J}{\xi_b+\xi_J+2}}\sqrt{\frac{2\zeta_b}{\xi_b+\xi_J+2}}, \right) - \exp\left\{-\frac{\zeta_b+\zeta_J}{\xi_b+\xi_J+2}\right\} \times I_0\left[\frac{2\sqrt{\zeta_b\zeta_J}}{\xi_b+\xi_J+2}\right]\right] \tag{102}$$

However, since there is no closed form solution for the Q function, in practice it is easier to compute the performance using (98).

a. Special Cases of BFSK with Single Tone Interference

The final aspect of the analysis is to consider how the derived result simplifies for special cases, both as a check on earlier work and to see limiting cases. As check on (98), when there is no signal the probability of bit error reduces to one half as expected.

Next consider the case of no jamming. In this case, $\xi_J = \zeta_J = 0$, and the probability of bit error reduces to

$$P_b = \left(\frac{1}{\xi_b + 2}\right) \times \exp\left\{\frac{-\zeta_b}{\xi_b + 2}\right\} \tag{103}$$

which is the usual BFSK result.

Another limiting case is the performance when both the signal and the jammer experience Rayleigh fading. In this case both ζ_b and ζ_J are zero and all the received energy is in the respective diffuse component. In this case (98) reduces to

$$P_b = \frac{1}{2}\left(\frac{\xi_J + 2}{\xi_b + \xi_J + 2}\right) \tag{104}$$

This displays an inverse linear relationship similar to Rayleigh fading without jamming [Ref. 2]. Performance is improved if we change the case slightly to that where the jammer suffers Rayleigh fading while the signal experiences Ricean fading. Then

$$P_b = \frac{1}{2}\left(\frac{\xi_J + 2}{\xi_b + \xi_J + 2}\right) \times \exp\left\{\frac{-\zeta_b}{\xi_b + \xi_J + 2}\right\} \tag{105}$$

Here any direct signal component that reaches the receiver will serve to drive the probability of bit error lower in an exponential fashion.

Perhaps the most optimistic performance from the communicator's point of view is when the signal has no fading, but the jammer suffers Rayleigh fading. In this case, $\zeta_J = \xi_b = 0$, and (98) reduces to

$$P_b = \left(\frac{1}{2}\right) \exp\left\{\frac{-\zeta_b}{\xi_J + 2}\right\} \tag{106}$$

On the other hand , the most pessimistic performance is likely to occur when the signal suffers Rayleigh fading, but the jammer has no fading. In this case, $\zeta_b = \xi_J = 0$, and (98) reduces to

$$P_b = \frac{1}{2}\left[1 - \frac{1}{(\xi_b + 2)} \exp\left\{\frac{-\zeta_J}{\xi_b + 2}\right\}\right] \tag{107}$$

This performance will be very poor unless there is a relatively large amount of diffuse signal energy received.

3. FFH/BFSK Analysis with Multi-Tone Interference

We now turn our attention to the application of (98) to spread spectrum and the partial band multi-tone jamming scenario. Suppose N is the number of hop slots in the FFH/BFSK system and the jammer transmits q interfering tones. When we credit the jammer with only placing at most one tone per hop slot then

$$\gamma = \left(\frac{q}{N}\right) \tag{108}$$

is the fraction of spread spectrum bandwidth jammed where γ is restricted to

$$\frac{1}{N} \le \gamma \le 1.0 \tag{109}$$

Now,

$$P_b = \left(\frac{q}{N}\right) P_r[error|\text{hop jammed}] + \left(\frac{N-q}{N}\right) P_r[error|\text{hop not jammed}]$$

where

$$P_r[error|\text{hop not jammed}] = P_r[error|BFSK] = \left(\frac{1}{\xi_b + 2}\right) \exp\left\{\frac{-\zeta_b}{\xi_b + 2}\right\} \qquad (110)$$

To apply our earlier result for the BFSK receiver we must define our jammer parameters on a per hop basis. If $\bar{\gamma}_J$ is the average total jammer power, then the average total jammer power per hop is

$$\frac{\overline{\gamma_J}}{\gamma} = \frac{\xi_b}{\gamma} + \frac{\zeta_b}{\gamma}. \qquad (111)$$

which implies ξ_J and ζ_J are replaced by $N\xi_J/q$ and $N\zeta_J/q$, respectively, in (98). Now (110) is given as

$$P_b = \left(\frac{q}{2N}\right)\left[1 - Q\left(\sqrt{\frac{2\zeta_b}{\xi_b + \frac{N}{q}\xi_J + 2}}, \sqrt{\frac{2\frac{N}{q}\zeta_J}{\xi_b + \frac{N}{q}\xi_J + 2}}\right)\right] +$$

$$\left(\frac{q}{2N}\right)\frac{\left(\frac{N}{q}\xi_J + 2\right)}{2\left(\xi_b + \frac{N}{q}\xi_J + 2\right)} \exp\left\{\frac{-\left(\zeta_b + \frac{N}{q}\zeta_J\right)}{\xi_b + \frac{N}{q}\xi_J + 2}\right\} \times I_0\left[\frac{2\sqrt{\zeta_b \frac{N}{q}\zeta_J}}{\xi_b + \frac{N}{q}\xi_J + 2}\right]$$

$$+\left(\frac{N-q}{N}\right)\left(\frac{1}{\xi_b + 2}\right)\exp\left\{-\left(\frac{\zeta_b}{\xi_b + 2}\right)\right\} \qquad (112)$$

In the case of FFH/BFSK with one hop per bit, no fading, and no thermal noise (N_o=0), an analytic expression for the worst case number of jamming tones, q_o, is

$$1 \le \mathrm{INTG}\left(\frac{N\overline{\gamma_J}}{\overline{\gamma_b}}\right) = q_o \le N \tag{113}$$

One aim of this thesis is to determine if this limited analytic result for q_o remains true for FFH/BFSK over Ricean fading channels in the presence of thermal noise. This is accomplished by comparing the performance based on q_o and some offset values of q.

4. FFH/BFSK Analysis Allowing Two Interference Tones

We now extend the previous results to a situation which includes the possibility that both receiver branches contain an interfering tone. This is a relaxation of the intelligent jammer scenario employed thus far. In this situation, the probability of bit error may be expressed as

$$\begin{aligned} P_b = {} & P_r[\text{no hops jammed}] \times P_r[\text{error}|\text{no hops jammed}] \\ & + P_r[\text{one tone jammed}] \times P_r[\text{error}|\text{one tone jammed}] \\ & + P_r[\text{two tones jammed}] \times P_r[\text{error}|\text{two tones jammed}] \end{aligned} \tag{114}$$

The first two conditional probabilities were previously determined in Section 2. However, the probability of those events occurring is a sample without replacement situation. That is

$$P_r[\text{one tone jammed}] = P_r[\text{one tone jammed} \cap \text{ one tone not jammed}]$$

$$P_r[0 \text{ tone jammed} \mid 1 \text{ tone not jammed}] \times P_r[1 \text{ tone jammed} \mid 0 \text{ tone not jammed}]$$

$$= \left(\frac{q}{2N}\right)\left(1 - \frac{q-1}{2N-1}\right) = \left(\frac{q}{2N}\right)\left(\frac{2N-q}{2N-1}\right) \tag{115}$$

Similarly

$$P_r[\text{no tones jammed}] = \left(1 - \frac{q}{2N}\right)\left(1 - \frac{q}{2N-1}\right)$$

$$= \left(\frac{2N-q}{2N}\right)\left(\frac{2N-1-q}{2N-1}\right) \tag{116}$$

And lastly, the probability that both tones are jammed is

$$P_r[\text{ both jammed}] = P_r[1 \text{ jammed } \cap 0 \text{ jammed}]$$

$$= \left(\frac{q}{2N}\right)\left(\frac{q-1}{2N-1}\right) \tag{117}$$

All that remains is to determine the probability of error given that both branches are jammed.

a. Extension of Single Interfering Tone Results

Now that both branches of the BFSK receiver contain jamming tones, symmetry is restored . [Ref. 11] Hence, we can determine the probability of bit error supposing that signal s_1 is sent. An error occurs when the output of branch two is greater than the output of branch one and (54) yields

$$P_r[\text{error}|\text{two tones jammed}] = \left(\frac{1}{2}\right)\times$$

$$\left[1 - Q\left(\frac{T_b\sqrt{a_c^2 + a_J^2 + 2a_c a_J \cos\delta}}{\sigma}, \frac{a_J T_b}{\sigma}\right) + Q\left(\frac{a_J T_b}{\sigma}, \frac{T_b\sqrt{a_c^2 + a_J^2 + 2a_c a_J \cos\delta}}{\sigma}\right)\right] \tag{118}$$

Alternatively, this may be expressed as

$$P_r[\text{error}|\text{two tones jammed}] = Q\left(\frac{a_J T_b}{\sigma}, \frac{T_b\sqrt{a_c^2 + a_J^2 + 2a_c a_J \cos\delta}}{\sigma}\right) -$$

$$\left(\frac{1}{2}\right)\exp\left\{-\frac{T_b^2\left(a_c^2 + 2a_J^2 + 2a_c a_J \cos\delta\right)}{2\sigma^2}\right\} \times I_0\left[\frac{T_b^2 a_J\sqrt{a_c^2 + a_J^2 + 2a_c a_J \cos\delta}}{\sigma^2}\right] \quad (119)$$

The conditioning on the received amplitudes of the signal and the jammer is removed by multiplying (119) with (80) and (81) and integrating over all values of a_J and a_c. In addition, the conditioning on the signal-to-jammer phase difference, δ, must also be removed.

In order to make (119) valid for FFH, we substitute (111) into (119). Now, symbolically the probability of error in the case of both tones jammed, P_{b2}, is

$$P_{b2} = \left(\frac{1}{2\pi}\right)\int_0^{2\pi}\int_0^{\infty} f_{A_J}(a_J)\int_0^{\infty} f_{A_c}(a_c)$$

$$\times\left\{Q\left(\frac{a_J T_b}{\sigma}\sqrt{\frac{2N}{q}}, \left(\frac{T_b}{\sigma}\right)\sqrt{a_c^2 + \frac{2N}{q}a_J^2 + 2a_c a_J\sqrt{\frac{2N}{q}}\cos\delta}\right) -\right.$$

$$\left(\frac{1}{2}\right)\exp\left\{-\frac{T_b^2\left(a_c^2 + \frac{4N}{q}a_J^2 + 2a_c a_J\sqrt{\frac{2N}{q}}\cos\delta\right)}{2\sigma^2}\right\}$$

$$\left.\times I_0\left[\frac{T_b^2 a_J\sqrt{\frac{2N}{q}}}{\sigma^2}\sqrt{a_c^2 + \frac{2N}{q}a_J^2 + 2a_c a_J\sqrt{\frac{2N}{q}}\cos\delta}\right]\right\} da_c da_J d\delta \quad (120)$$

Substituting our previous results for BFSK and (120) into (114), we get the total probability of bit error

$$P_b = \left(\frac{2N-q}{2N}\right)\left(\frac{2N-1-q}{2N-1}\right)\left(\frac{1}{\xi_b+2}\right)\exp\left\{\frac{-\zeta_b}{\xi_b+2}\right\}$$

$$+\left(\frac{1}{2}\right)\left(\frac{q}{2N}\right)\left(\frac{2N-q}{2N-1}\right)\left[1-Q\left(\sqrt{\frac{2\zeta_b}{\xi_b+\frac{2N}{q}\xi_J+2}},\sqrt{\frac{4\frac{N}{q}\zeta_J}{\xi_b+\frac{2N}{q}\xi_J+2}}\right)\right]$$

$$+\frac{\left(\frac{2N}{q}\xi_J+2\right)}{2\left(\xi_b+\frac{2N}{q}\xi_J+2\right)}\exp\left\{\frac{-\left(\zeta_b+\frac{2N}{q}\zeta_J\right)}{\xi_b+\frac{2N}{q}\xi_J+2}\right\}\times I_0\left[\frac{2\sqrt{\zeta_b\frac{2N}{q}\zeta_J}}{\xi_b+\frac{2N}{q}\xi_J+2}\right]$$

$$+\left(\frac{q}{2N}\right)\left(\frac{q-1}{2N-1}\right)P_{b2}\left(\zeta_b,\xi_b,\zeta_J,\xi_J,\left(\frac{q}{2N}\right)\right) \tag{121}$$

Further simplification results by using the substitutions

$$\gamma_b = \frac{a_c^2 T_b}{\mathrm{N_o}} \tag{122}$$

which implies

$$d\gamma_b = \frac{2a_c T_b}{\mathrm{N_o}} da_c \tag{123}$$

and

$$\gamma_J = \frac{a_J^2 T_b}{\mathrm{N_o}} \tag{124}$$

which implies

$$d\gamma_J = \frac{2a_J T_b}{\mathrm{N_o}} da_J \tag{125}$$

Then using (122) through (125) in (80) and (81)

$$f_{\Gamma_c}(\gamma_c) = \left(\frac{1}{\xi_c}\right) \exp\left\{-\frac{\gamma_c + \zeta_c}{\xi_c}\right\} \times I_0\left[2\sqrt{\frac{\gamma_c \zeta_c}{\xi_c}}\right] \tag{126}$$

and

$$f_{\Gamma_J}(\gamma_J) = \left(\frac{1}{\xi_J}\right) \exp\left\{-\frac{\gamma_J + \zeta_J}{\xi_J}\right\} \times I_0\left[2\sqrt{\frac{\gamma_J \zeta_J}{\xi_J}}\right] \tag{127}$$

b. Special Cases when Allowing Two Interference Tones

As a consequence of the triple nested numerical integration required by (120) in order to evaluate (121), obtaining numerical results when two tones can jam a single hop slot is computationally intensive. Based on the results when thermal noise is neglected, we expect the performance will be better than when only a single interfering tone is allowed.

When there is no signal fading

$$\overline{\gamma_b} = \gamma_b = \zeta_b \text{ and } \xi_b = 0 \tag{128}$$

and when there is no jammer fading

$$\overline{\gamma_J} = \gamma_J = \zeta_J \text{ and } \xi_J = 0 \tag{129}$$

In the case of Rayleigh fading of the signal

$$\overline{\gamma_b} = \xi_b \text{ and } \zeta_b = 0 \tag{130}$$

and

$$\overline{\gamma_J} = \xi_J \text{ and } \zeta_J = 0 \tag{131}$$

when the jammer is Rayleigh faded. Two limiting cases allow evaluation of the most pessimistic and most optimistic performance. Optimistically, from the communicator's

point of view, when there is no signal fading and Rayleigh fading of the jammer, the probability of bit error reduces to

$$P_b = \left(\frac{2N-q}{2N}\right)\left(\frac{2N-q-1}{2N-1}\right)\exp\left\{\frac{-\zeta_b}{2}\right\} + \left(\frac{q}{4N}\right)\left(\frac{2N-q}{2N-1}\right)\exp\left\{\frac{-\zeta_b}{\frac{2N\xi_J}{q}+2}\right\} +$$

$$\left(\frac{q}{2N}\right)\left(\frac{2N-q}{2N-1}\right)\left(\frac{1}{2\pi}\right)\int_0^{2\pi}\int_0^{\infty} f_{\Gamma_J}(\gamma_J)\times\left\{Q\left(\sqrt{2N\gamma_J/q}\,,\sqrt{\gamma_b+2N\gamma_J/q+2\sqrt{2N\gamma_b\gamma_J/q}\,\cos\delta}\right)\right.$$

$$-\left(\frac{1}{2}\right)\exp\left\{\frac{-1}{2}\left(\gamma_b+4N\gamma_J/q+2\sqrt{2N\gamma_b\gamma_J/q}\,\cos\delta\right)\right\}$$

$$\left.\times I_0\left[\sqrt{2N\gamma_J/q}\,\sqrt{\gamma_b+2N\gamma_J/q+2\sqrt{2N\gamma_b\gamma_J/q}\,\cos\delta}\,\right]\right\}d\gamma_J d\delta \qquad (132)$$

which requires two numerical integrations rather than three.

The most pessimistic performance result from Rayleigh fading of the signal and no fading of the jammer. In this case,

$$P_b = \left(\frac{2N-q}{2N}\right)\left(\frac{2N-q-1}{2N-1}\right)\exp\left\{\frac{-\zeta_b}{2}\right\} + \left(\frac{q}{4N}\right)\left(\frac{2N-q}{2N-1}\right)\exp\left\{\frac{-\zeta_b}{\frac{2N\xi_J}{q}+2}\right\}$$

$$\left(\frac{q}{2N}\right)\left(\frac{2N-q}{2N-1}\right)\left(\frac{1}{2\pi}\right)\int_0^{2\pi}\int_0^{\infty} f_{\Gamma_b}(\gamma_b)\times\left\{Q\left(\sqrt{2N\gamma_J/q}\,,\sqrt{\gamma_b+2N\gamma_J/q+2\sqrt{2N\gamma_b\gamma_J/q}\,\cos\delta}\right)\right.$$

$$-\left(\frac{1}{2}\right)\exp\left\{\frac{-1}{2}\left(\gamma_b+4N\gamma_J/q+2\sqrt{2N\gamma_b\gamma_J/q}\,\cos\delta\right)\right\}$$

$$\left.\times I_0\left[\sqrt{2N\gamma_J/q}\,\sqrt{\gamma_b+2N\gamma_J/q+2\sqrt{2N\gamma_b\gamma_J/q}\,\cos\delta}\,\right]\right\}d\gamma_b d\delta \qquad (133)$$

Further simplification when neither the signal nor the jammer fade. In this instance (132) reduces to

$$P_b = \left(\frac{2N-q}{4N}\right)\left(\frac{2N-q-1}{2N-1}\right)\exp\left\{-\left(\frac{\zeta_b}{2}\right)\right\}+$$

$$\left(\frac{q}{4N}\right)\left(\frac{2N-q}{2N-1}\right)\left[1-Q\left(\sqrt{\zeta_b}\,,\sqrt{2N\zeta_J/q}\right)\right.$$

$$\left.\exp\left\{-\frac{1}{2}(\zeta_b+2N\zeta_J/q)\right\}\times I_0\left[\sqrt{2N\zeta_b\zeta_J/q}\,\right]\right]$$

$$+\left(\frac{q}{2N}\right)\left(\frac{q-1}{2N-1}\right)\left(\frac{1}{2\pi}\right)\int_0^{2\pi}\left\{Q\left(\sqrt{2N\zeta_J/q}\,,\sqrt{\gamma_b+2N\gamma_J/q+2\sqrt{2N\gamma_b\gamma_J/q}\,\cos\delta}\,\right)\right.$$

$$-\left(\frac{1}{2}\right)\exp\left\{\left(\frac{1}{2}\right)\left(\gamma_b+4N\gamma_J/q+2\sqrt{2N\gamma_b\gamma_J/q}\,\cos\delta\right)\right\}$$

$$\left.\times I_0\left[\sqrt{2N\gamma_J/q}\,,\sqrt{\gamma_b+2N\gamma_J/q+2\sqrt{2N\gamma_b\gamma_J/q}\,\cos\delta}\,\right]\right\}d\delta \qquad (134)$$

where a single finite numerical integration over the phase angle is required. In this thesis only (134) is evaluated. Further work in this area could consider the effects of Ricean fading in the both tones jammed case based on (120).

C. MULTI-TONE INTERFERENCE NUMERICAL PROCEDURE

The crux of the numerical computation for this problem is the accurate and efficient computation of Marcum's Q function. Originally the Q function described a shorthand notation for the probability integral representing the output of a correlation detector containing a radar target in the presence of narrowband Gaussian noise [Ref. 14].

The Q function, described by (59), has no closed form solution expressible in a finite number of terms. Frequently cited equivalent expressions containing an infinite series of Bessel functions, while valuable as analysis tools, do not ease the computational burden. The strategy is to test the input arguments for their magnitude, difference, and the presence of zeros. Based on the input arguments the program computes the value of the Q function in an appropriate subroutine and returns to the calling program.

First, the presence of a zero passed as an input argument is tested. If present the following simplification results

$$Q(\alpha, 0) = 1.0 \tag{135}$$

and

$$Q(0, \beta) = \exp\left\{-\left(\tfrac{1}{2}\right)\beta^2\right\} \tag{136}$$

The second consideration is the magnitude and difference of the input arguments. If the product of the arguments is greater than ten and their difference is greater than five, then the Q function is computed using an asymptotic polynomial. If the magnitude of the product is greater than 1000, then the Q function is computed by directly integrating (59) using a large argument approximation for the Bessel function. For the semi-infinite

integration required here, the Romberg technique is very efficient. The Romberg technique is a recursive implementation of Richardson's extrapolation which is continued until a user specified tolerance is reached. In theory and in practice it offers much faster convergence and smaller errors than the standard trapezoidal or Simpson technique. [Ref. 16]

If none of these conditions is satisfied the program defaults to a computation based on a numerical inverse Laplace transform. The integrand of (59) is expressed in the Laplace domain as [Ref. 10, equation 6.643.4]

$$F(s) = 1 - \left(\frac{1}{2s+1}\right) \times \exp\left\{-\left(\frac{\alpha^2}{2}\right)\left(1 - \frac{1}{2s+1}\right)\right\} \tag{137}$$

Then the integration may be determined from the inverse transform of

$$Q(\alpha, \beta) \Leftrightarrow F(s) = \frac{1}{s} \times \left[1 - \left(\frac{1}{2s+1}\right) \times \exp\left\{-\left(\frac{\alpha^2}{2}\right)\left(1 - \frac{1}{2s+1}\right)\right\}\right] \tag{138}$$

This is useful for many intermediate values of the input arguments.

D. MULTI -TONE INTERFERENCE RESULTS

First, the results for the scenario in which at most one tone is jammed per hop slot are presented. The performance for a wide variety of channel conditions is computed for several representative signal to thermal noise ratios. All figures are for one hop per bit (L=1). For each channel case there are two prime questions to be answered. First, "How does performance vary for fixed values of q?" Second, "Is the no fading analytic and no thermal noise worst case q still valid for fading channels?" To answer the second question the proposed worst case value of q, q_o ,is used to compute performance as well as some values of q offset from q_o. To show the trend, the results of q_o+ 4 and q_o -4 are compared with q_o based performance. Table 2 provides an overview of the channel conditions considered.

TABLE 2. MULTI-TONE CHANNEL CONDITIONS

NAME	E_b/N_o dB	R_b / Ricean Fading	R_J / Ricean Fading
Figure 25	13.35	100 / Very Weak	100 / Very Weak
Figure 26	13.35	100 / Very Weak	0.0 / Rayleigh
Figure 27	13.35	0.0 / Rayleigh	100 / Very Weak
Figure 29	13.35	10 / Moderate	10 / Moderate
Figure 29	13.35	0.0 / Rayleigh	0.0 / Rayleigh
Figure 30	13.35	10 / Moderate	1 / Strong
Figure 31	13.35	50 / Weak	50 / Weak
Figure 32	13.35	25 / Low	25 / Low
Figure 33	20	10 / Moderate	10 / Moderate
Figure 34	20	1 / Strong	10 / Moderate
Figure 35	20	10 / Moderate	1 / Strong

Initially, we consider the case where fading has very little influence to compare with a no fading analytic result. Figure 25 is an illustration of the performance obtained with a moderate signal-to-thermal noise ratio that typically provides a 10^{-5} bit error ratio in the absence of fading and interference. Thus, Figure 25 provides a good basis for comparison with the no fading case. The worst case performance is seen as the envelope of the fixed q curves. As the signal-to-jammer power increases, the performance quickly approaches $2x10^{-5}$, which is very close to the no jamming performance. We can also see that the degradation inflicted by multi-tone jamming is strongly influenced the choice of a fixed number of interference tones.

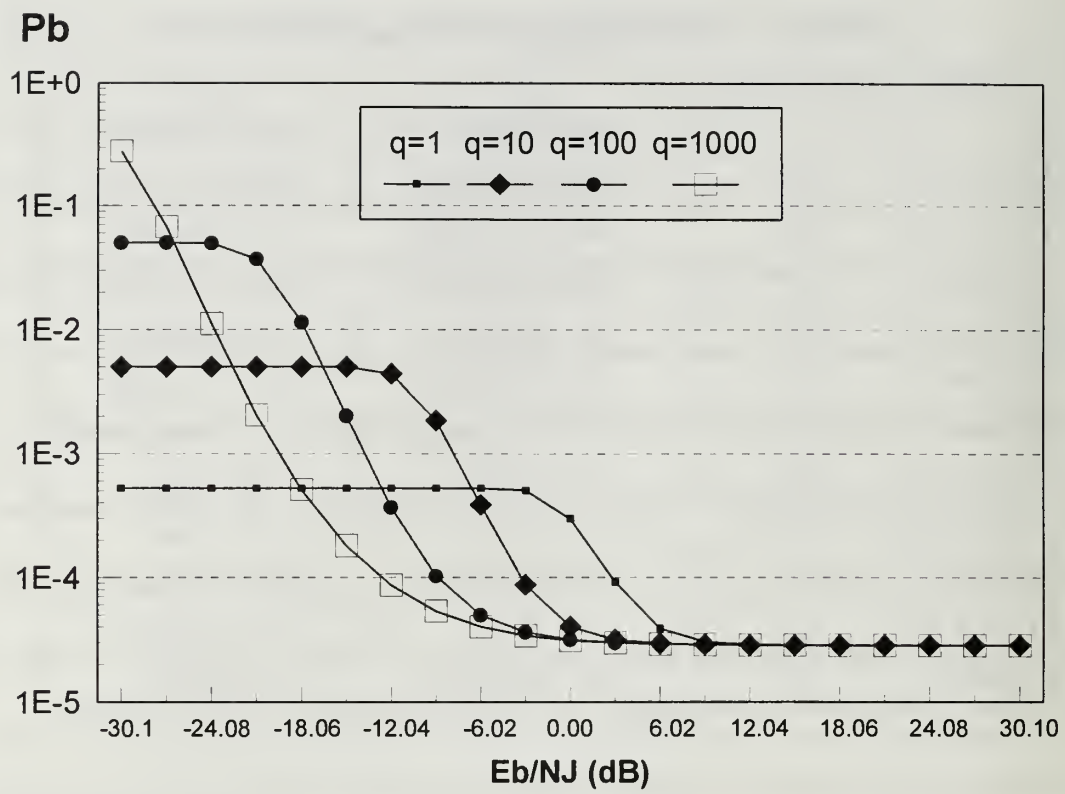

Figure 25. E_b/N_o=13.35dB, R_b =100, R_J=100

To bracket the range of expected performance the case of extreme of Rayleigh jammer fading and very weak signal fading is depicted in Figure 26. Here the performance is slightly improved at lower signal-to-jammer power ratios than is observed in Figure 25. Equivalently, the worst case envelope is slightly inclined more toward the y-axis indicating better performance. However, at low signal-to-jammer power levels, the performance is still relatively poor.

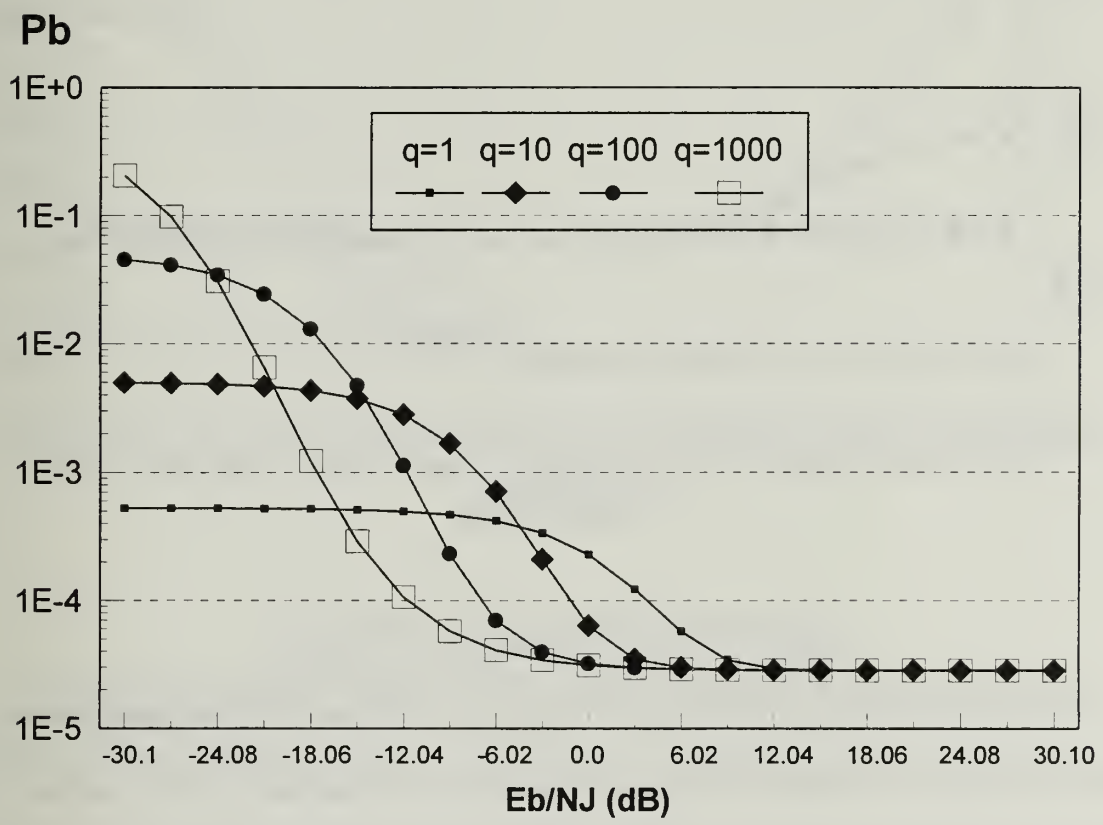

Figure 26. E_b/N_o=13.35dB, R_b=100, R_J=0.0

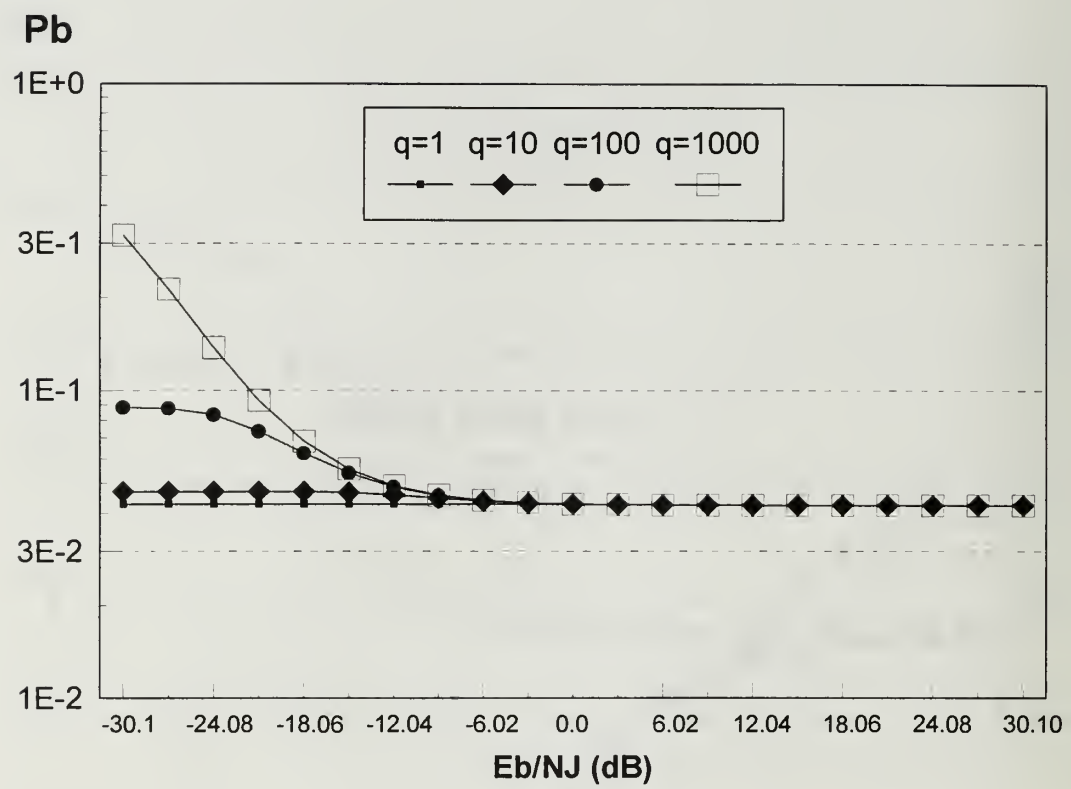

Figure 27. E_b/N_o=13.35dB, R_b= 0, R_J=100

At the other extreme, a pessimistic performance is obtained when the signal suffers Rayleigh fading, but the jammer has very weak fading. The jammer is able to reduce performance overall and maintain a high bit error ratio (BER) for higher signal-to-jammer power ratios. Even at E_b/N_J=30dB, the effects of fading and jamming produce a BER near $4x10^{-2}$.

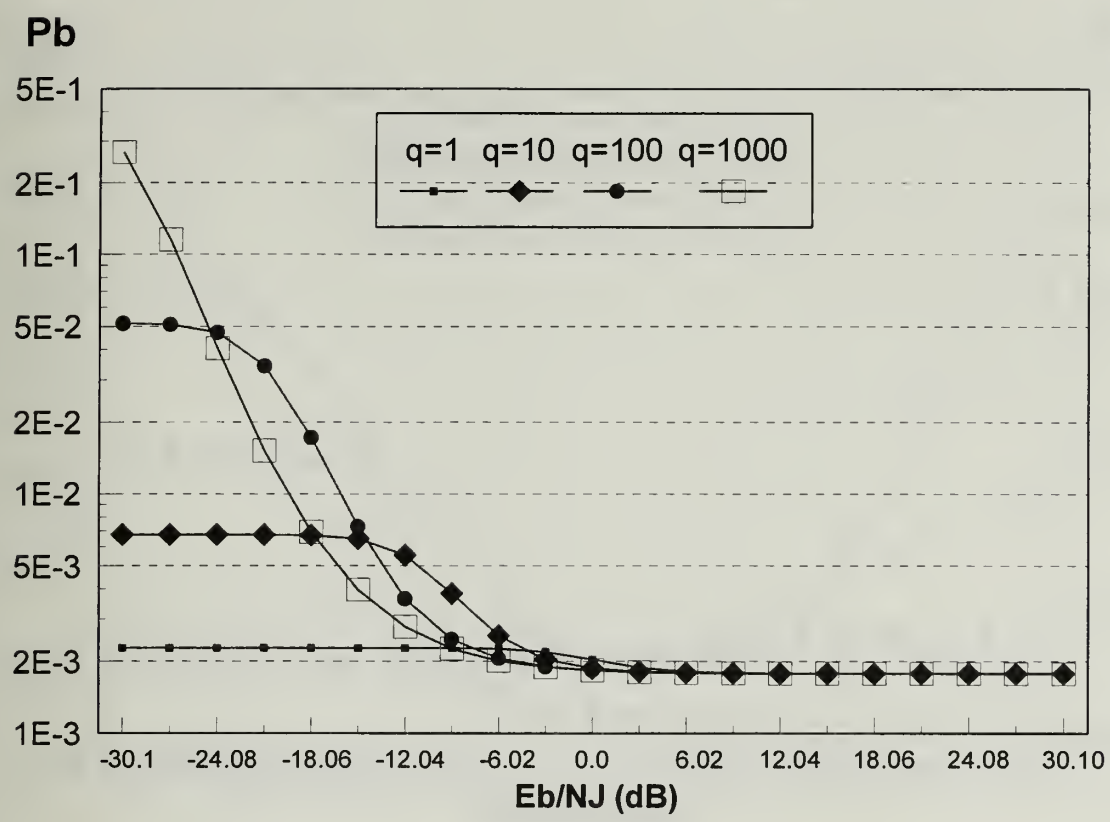

Figure 28. E_b/N_o=13.35dB, R_b=10, R_J=10

In Figure 28 we display the performance when both the signal and the jammer experience moderate Ricean fading. As expected the performance lies between the optimistic case of Figure 26 and the pessimistic case of Figure 27. In this case each tone contains the same direct-to-diffuse power ratio, but as E_b/N_J grows above 0dB, the direct signal power is greater than the direct jammer power and is able to mitigate the influence of multi-tone jamming.

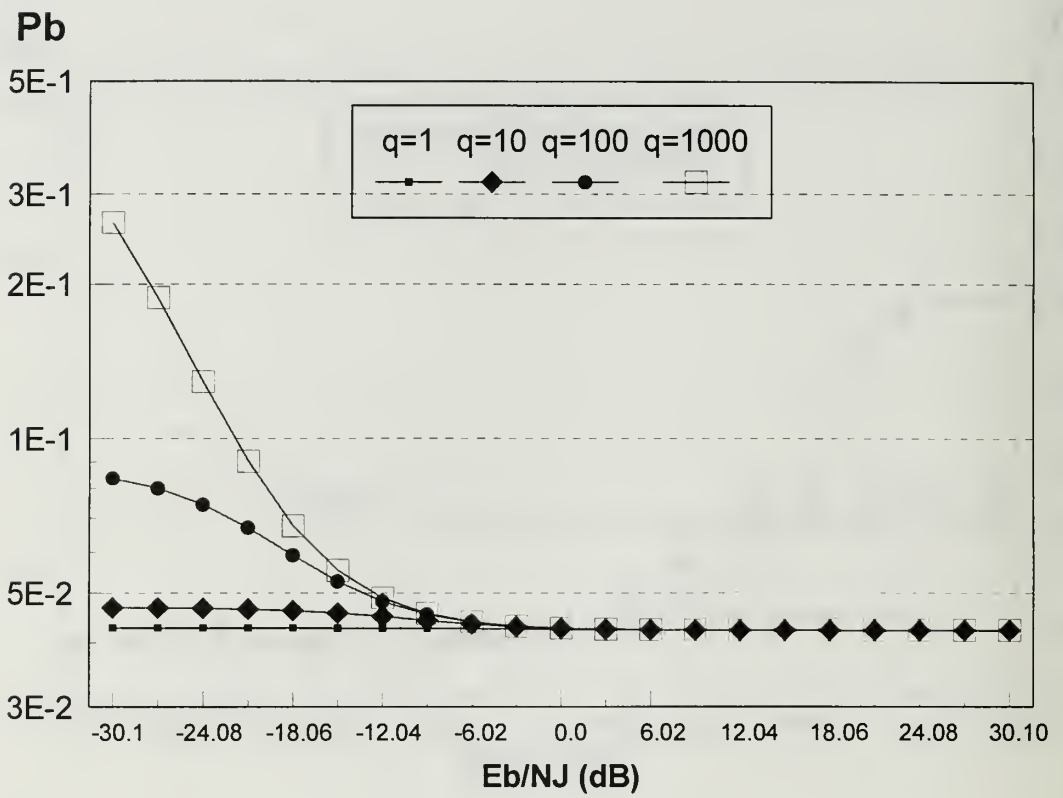

Figure 29. E_b/N_o=13.35dB, R_b=0, R_j=0

In Figure 29, the signal and jammer again share the same direct-to-diffuse power ratio, but now Rayleigh fading is assumed. The performance is worse overall compared with the moderate Ricean case and approximately 3dB worse at higher signal-to-jammer power levels. Also note that the worst case occurs at q=1000. Therefore, the greatest degradation occurs when the jammer is forced into the multi-tone equivalent of broadband jamming.

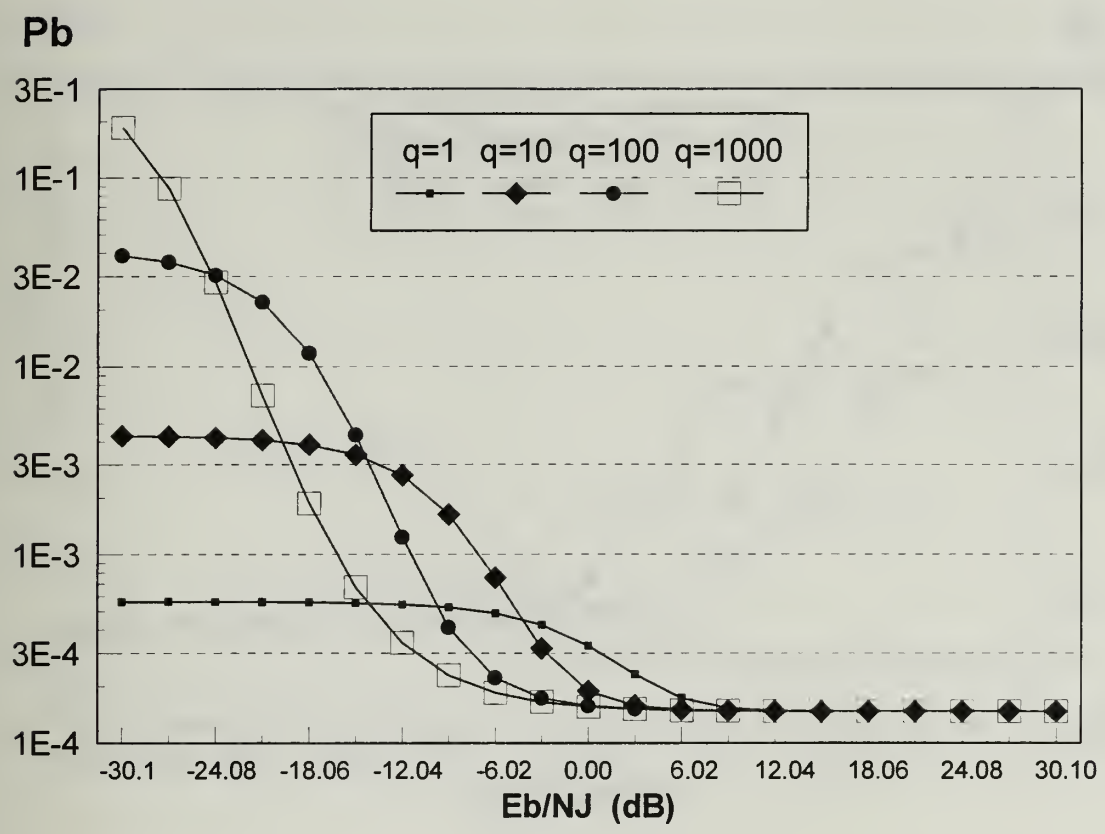

Figure 30. E_b/N_o=13.35dB, R_b=10, R_J=1

In Figure 30, the channel conditions are more favorable to the communicator and represent a ten fold increase in the R_b over the R_J from the performance depicted in Figure 28. At the critical value of 0dB for the signal-to-jammer power ratio (E_b/N_J) the performance in the favorable channel (Figure 30) is $3.3\text{x}10^{-4}$ while in the moderate Ricean channel (Figure 28) the same E_b/N_J produces a BER of $2.1\text{x}10^{-3}$. So the fact that the jammer suffers more fading over the Ricean channel produces a small improvement for the communicator.

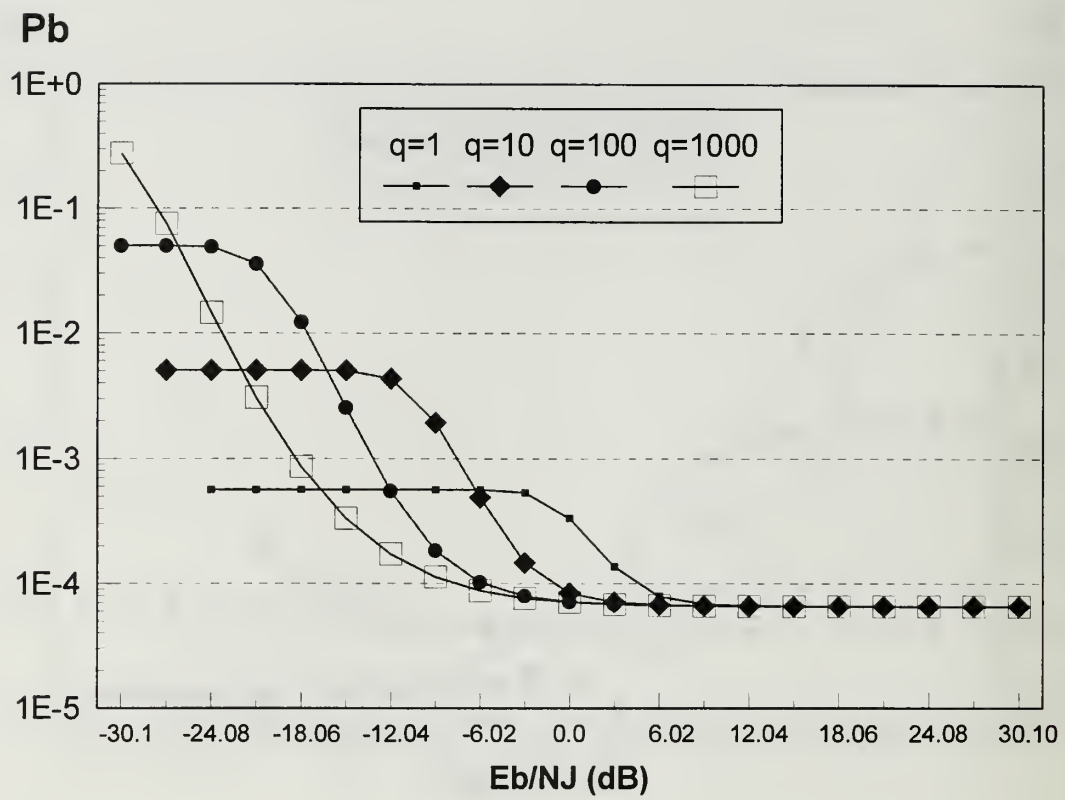

Figure 31. E_b/N_o=13.35dB, R_b=50, R_J=50

Figure 31 is similar to Figure 25, but includes less fading. The performance is essentially the same as the very weak fading performance, but with some slight improvement for E_b/N_J greater than 0dB. As in earlier fading channel cases, the performance varies greatly for fixed values of q when the jammer has a power advantage.

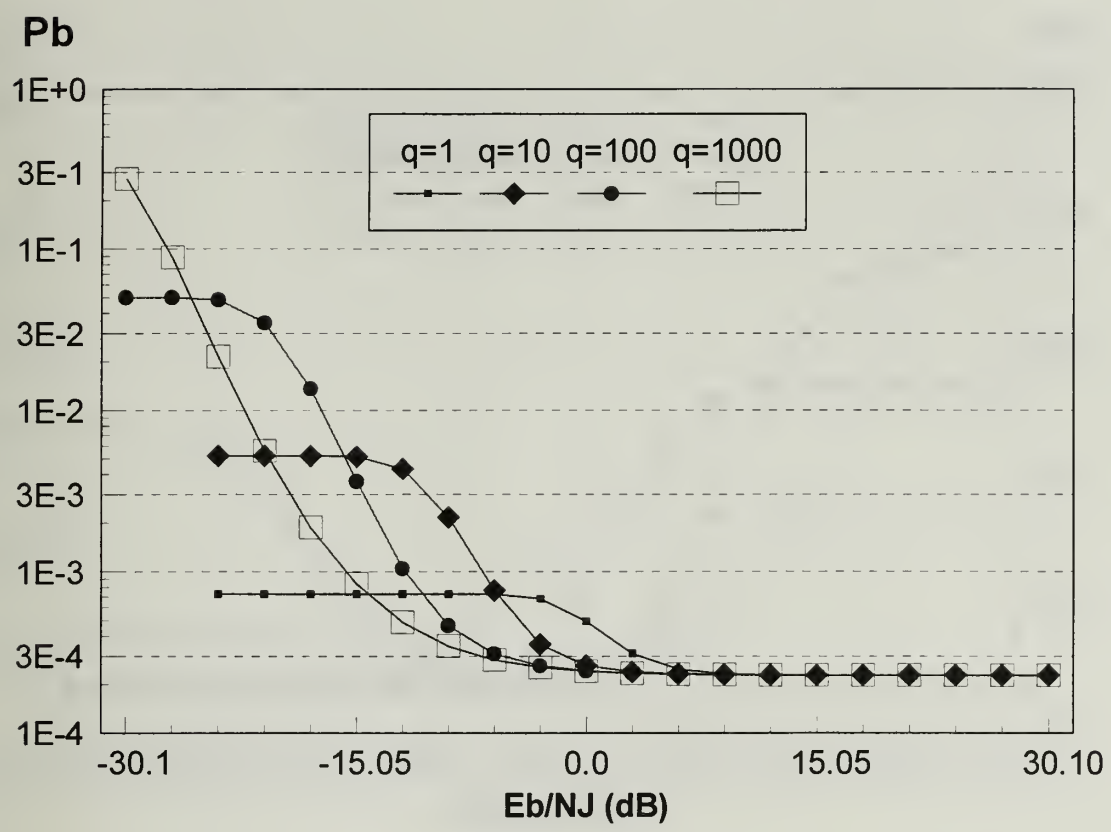

Figure 32. E_b/N_o=13.35dB, R_b=25, R_J=25

Figure 32 depicts another drop in the channel direct-to-diffuse ratio shared by the signal and jammer. At this level the difference in performance below the very weak case where the direct-to-diffuse ratio was 100 is noticeable. When the jammer enjoys a power advantage, the BER is still unacceptably high. The worst case envelope curve is nearly linear above E_b/N_o=0dB and nearly flat for all choices of q above 0dB.

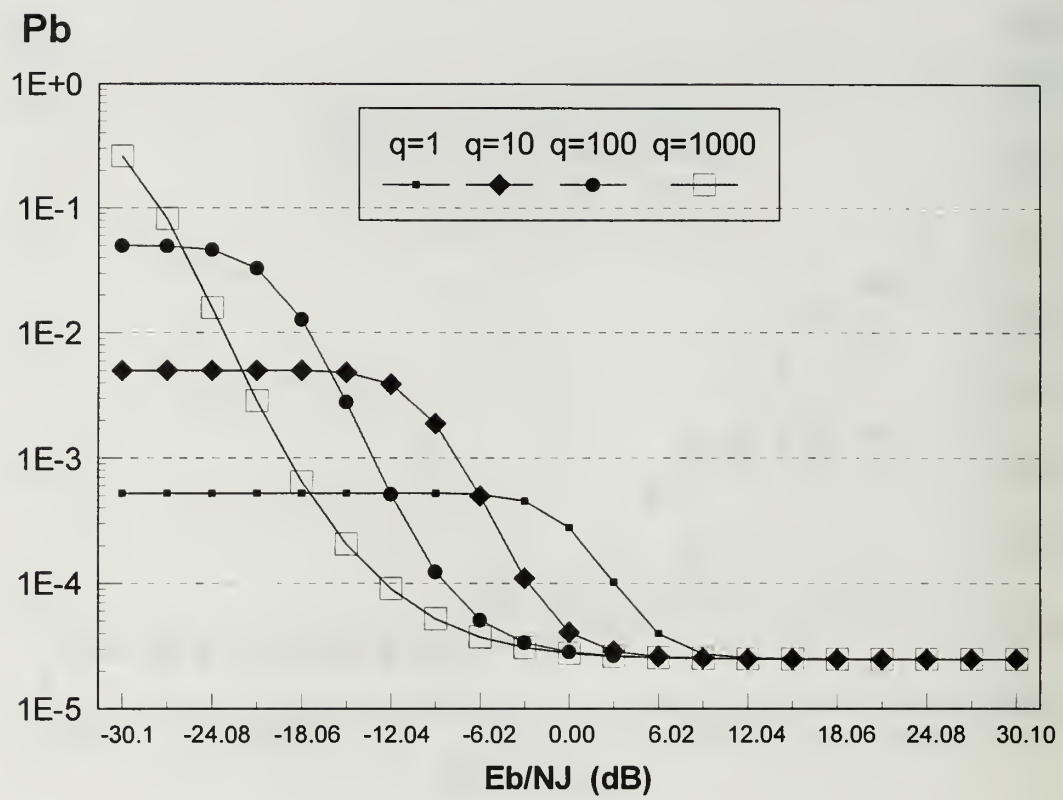

Figure 33. E_b/N_o=20dB, R_b=10, R_J=10

In Figure 33 we begin to look at the performance for larger signal-to-thermal noise ratios. An increase in E_b/N_o from 13.35dB (Figure 28) to 20dB (Figure 33) both in moderate Ricean fading, provides an overall improvement in performance. However, the improvement is significant when E_b/N_J is greater than -12dB and provides nearly a factor of ten at 0dB.

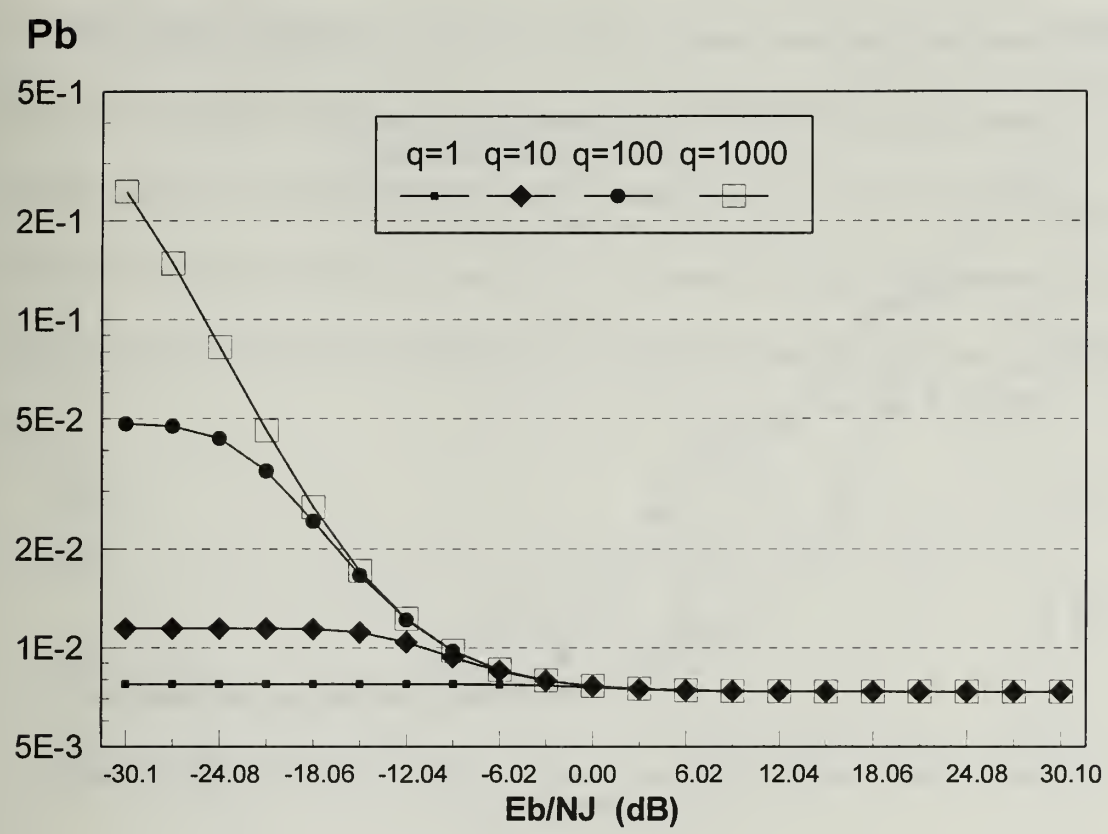

Figure 34. E_b/N_o=20dB, R_b=10, R_J=10

Figure 34 shows how rapidly performance can degrade even for a strong 20dB signal-to-thermal noise power ratio when the signal fading progresses from moderate (Figure 33) to strong Ricean fading. Similar to the situation observed in Figure 27 , the worst case performance is obtained when the jammer places an interfering tone in every hop slot. The jammer therefore, need not be very sophisticated to prevent efficient communications. In Figure 35 the roles are reversed. With the same signal-to-thermal noise ratio, the signal experiences moderate Ricean fading while the jammer experiences strong Ricean fading.

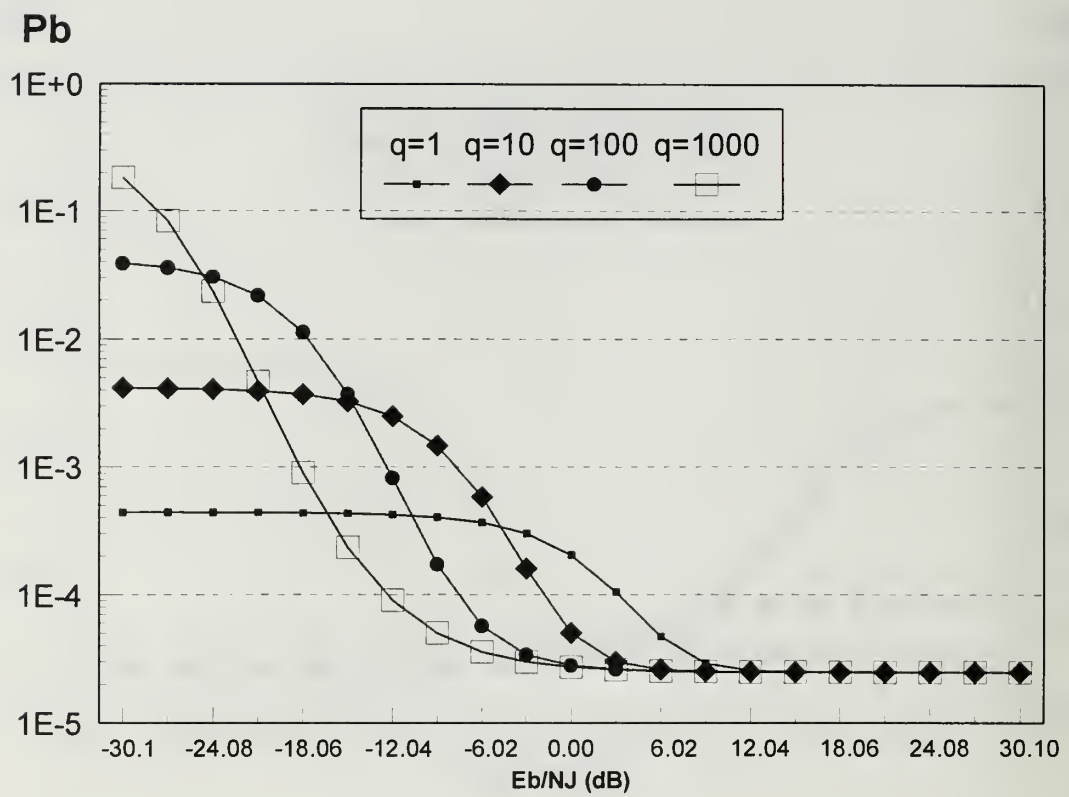

Figure 35. E_b/N_o=20dB, R_b=10, R_J=1

With moderate Ricean signal fading a particular value of q_o is required to cause the worst case performance demanding greater jammer sophistication. The strongly faded jamming tone is much less effective when E_b/N_J is greater than 0dB. Previously we observed an approximate tenfold drop in BER experienced for the E_b/N_o=13.35dB case as the jammer fading grew from moderate (R_J=10) to strong (R_J=1) at E_b/N_J=0dB. This trend is more pronounced at the E_b/N_o=20dB level as we transition from Figure 34 to Figure 35 where the improvement is greater than a factor of 25.

The influence of fading on the selection of q to cause worst case performance in the multi-tone environment remains to be answered. For FFH/BFSK in the absence of fading and thermal noise we expect the worst case to occur when q is chosen as the integer portion of the jammer-to-signal power ratio. A comparison of the following worst case performance curves will show them to be the envelope of the previous fixed q computed curves.

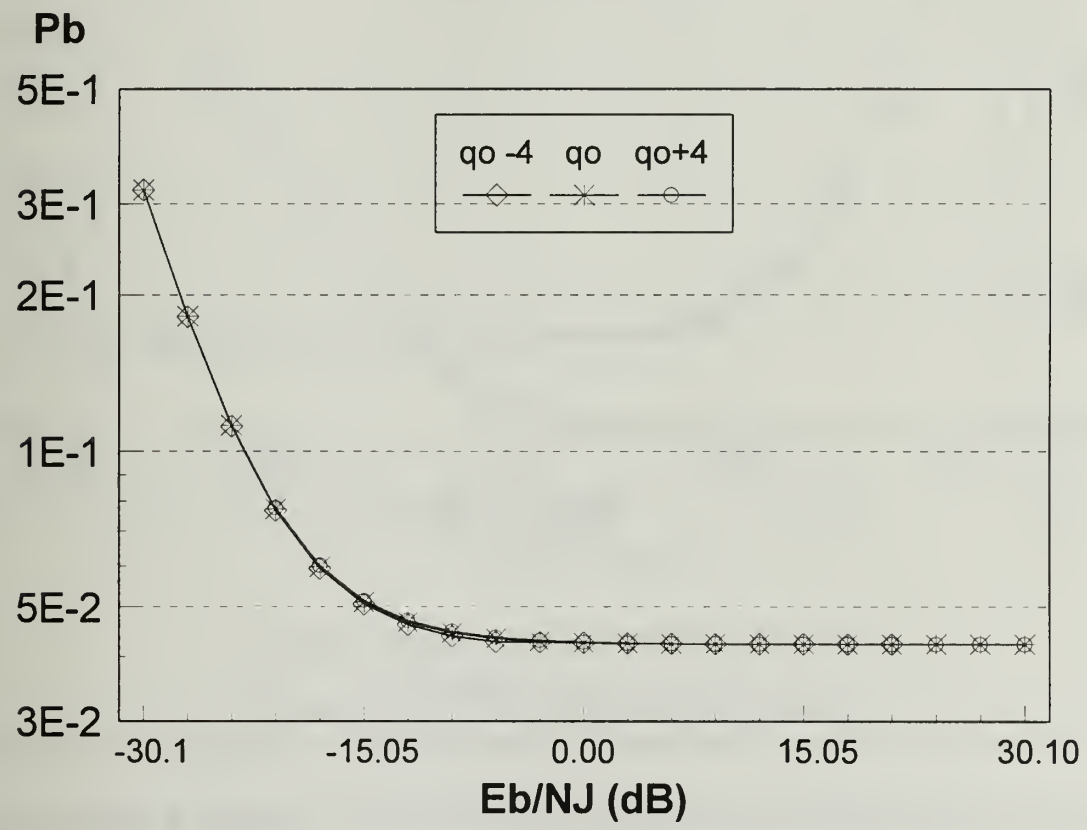

Figure 36. Worst Case Multi-Tone Jamming for
E_b/N_o=13.35dB, R_b=0, R_J=100

The most pessimistic case for the communicator is pictured in Figure 36 where the signal has Rayleigh fading and the jammer enjoys essentially no fading. We see that in this situation the jammer does not need to be very sophisticated to hinder communication.

The results displayed in Figure 36 and in Figure 37 indicate there is essentially no difference in the q_0 performance and the q_0 +4 and q_0 -4 cases.

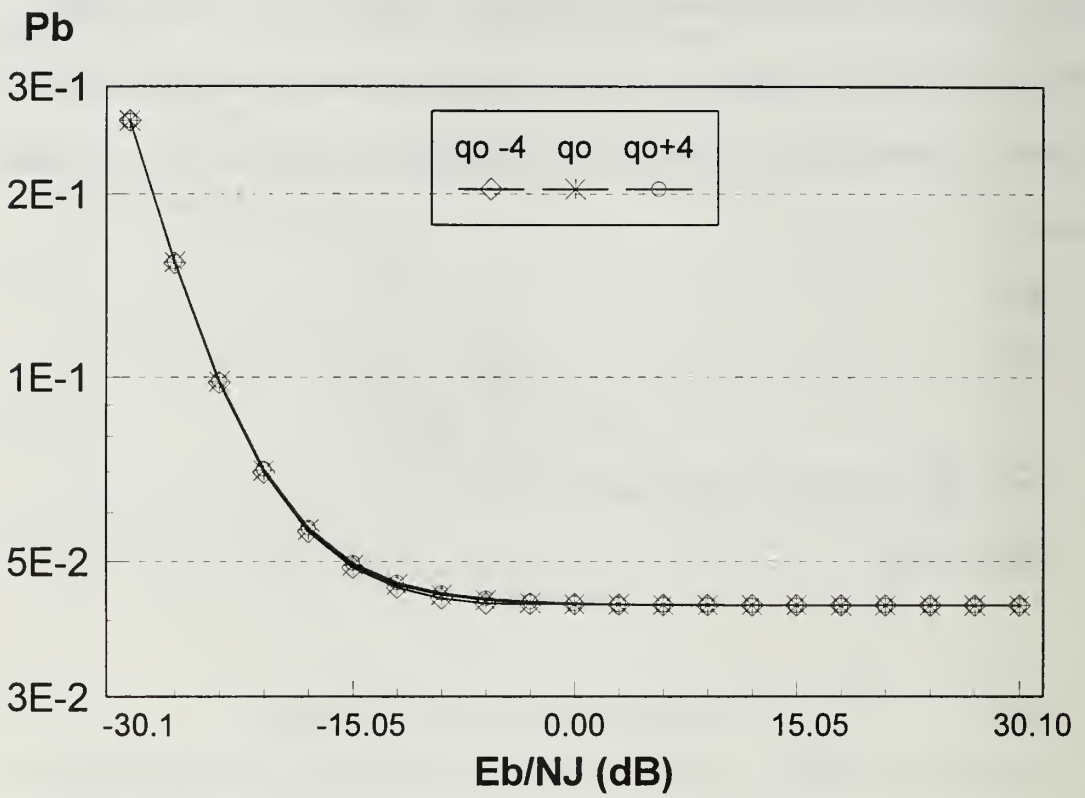

Figure 37. Worst Case Multi-Tone Jamming
E_b/N_o=13.35dB, R_b=0, R_J=0

The conclusion to draw from Figure 37 is the degradation in channel conditions for the jammer does not significantly assist the communicator when both are acting through Rayleigh channels.

For convenience we will denote the q_o+4 and q_o-4 collectively as Δq_o. It is not until there is some appreciable direct signal power reaching the receiver that the q_o and Δq_o begin to show some deviation.

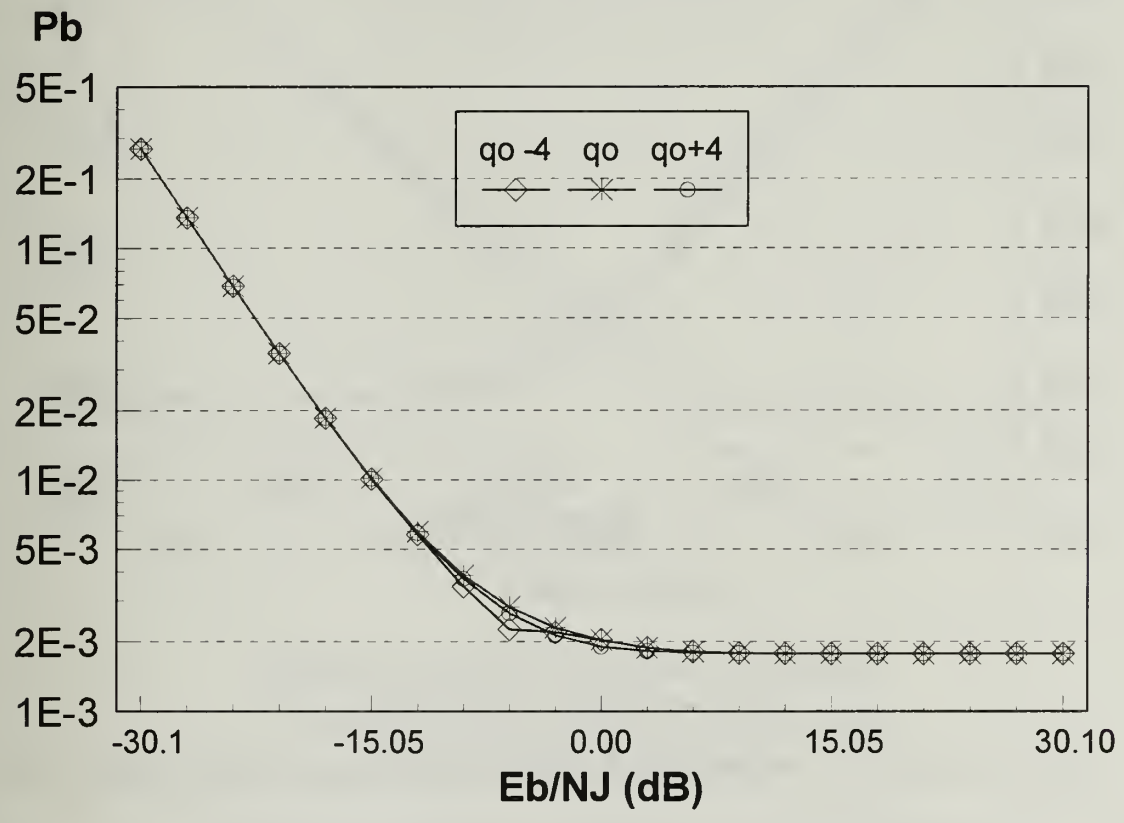

Figure 38. Worst Case Multi-Tone Jamming
E_b/N_o=20dB, R_b=10, R_J=10,

In Figure 38 the Δq_o curves dip below the anticipated worst case curve. The trend progresses as the direct-to-diffuse ratio increases in Figure 39 and Figure 40 respectively.

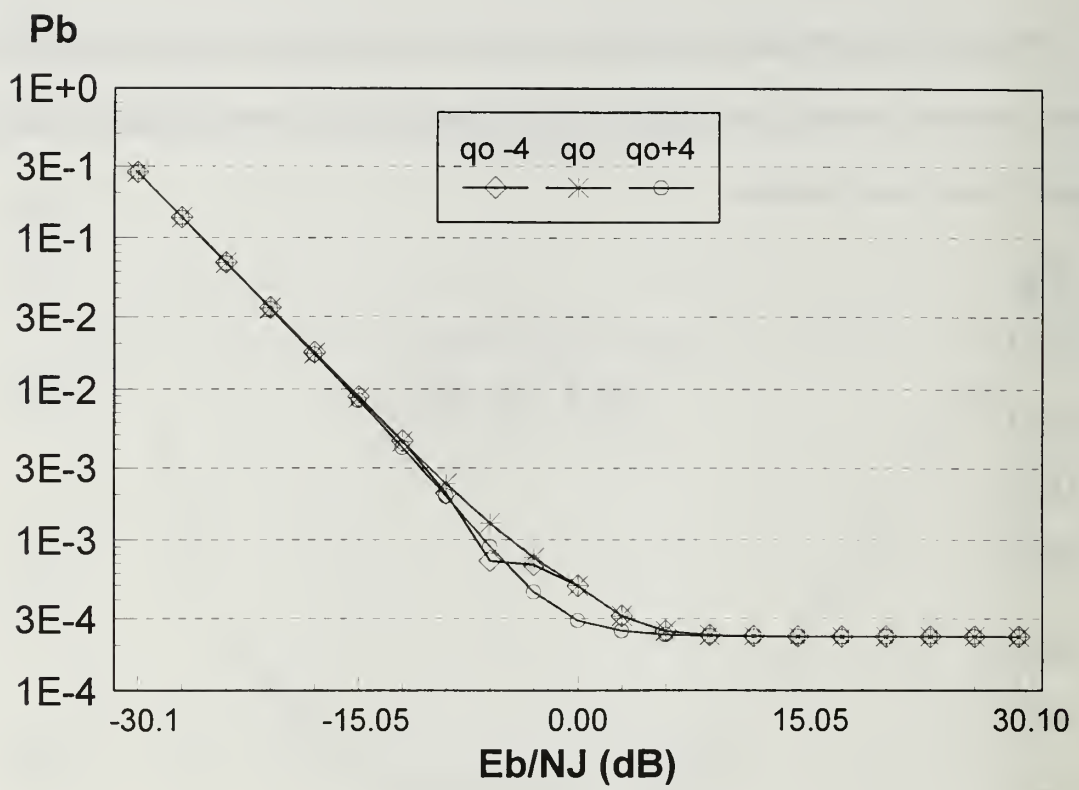

Figure 39. Worst Case Multi-Tone Jamming
E_b/N_o=13.35dB, R_b=25, R_J=25.

Since the value of q is required to be a positive integer greater than or equal to one, there is a small discontinuity in the q_o-4 curve. At those signal-to-jammer power values where the q_0 value would be less than 5, the q_o-4 defaults to q=1 for the computation.

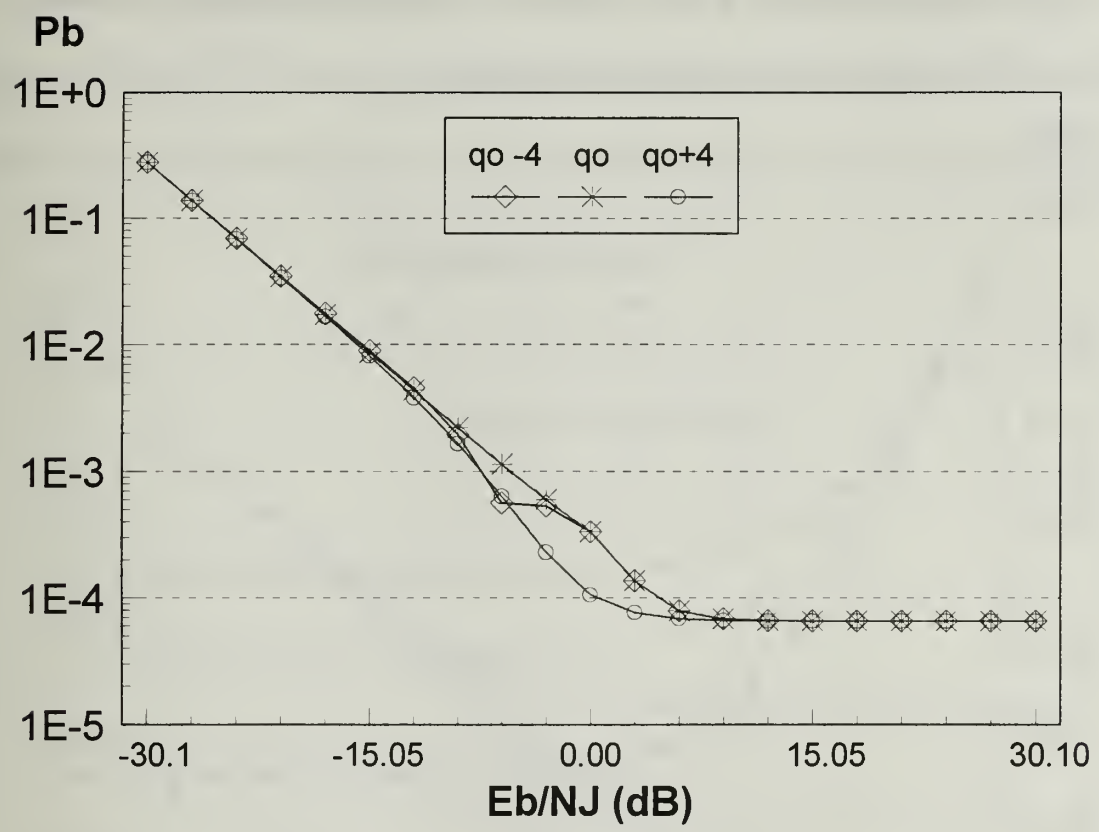

Figure 40. Worst Case Multi-Tone Jamming
E_b/N_o=13.35dB, R_b=50, R_J=50,

The salient observation in Figure 38, Figure 39, and Figure 40 is that the anticipated worst case performance in the no fading and no thermal noise case remains the worst case performance for the weakly and moderately faded channels with moderate thermal noise.

For comparison Figure 41, Figure 42, Figure 43 displays the composite worst case performance for various signal-to-thermal noise ratios.

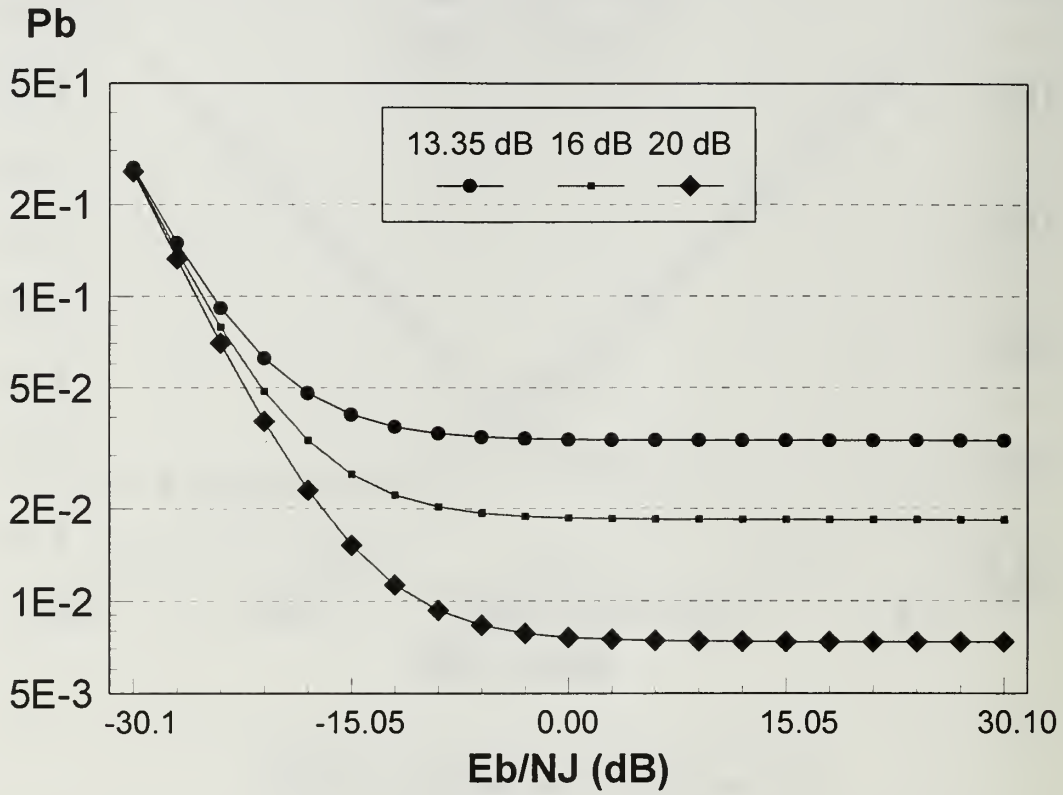

Figure 41. Worst Case Multi-Tone Jamming for Several Values of E_b/N_o, R_b=1, R_J=1

Figure 41 displays the performance when both the signal and the jammer suffer strong fading. The diffuse nature of the channel keeps the probability of bit error relatively high despite high signal-to-jammer power ratios and serves more to the detriment to the communicator than the jammer.

When the channel has moderate vice strong Ricean fading the performance is that shown in Figure 42. Above -6dB E_b/N_J there is a significant improvement in performance over that in Figure 41. The noticeable change in slope for the 20dB curve is

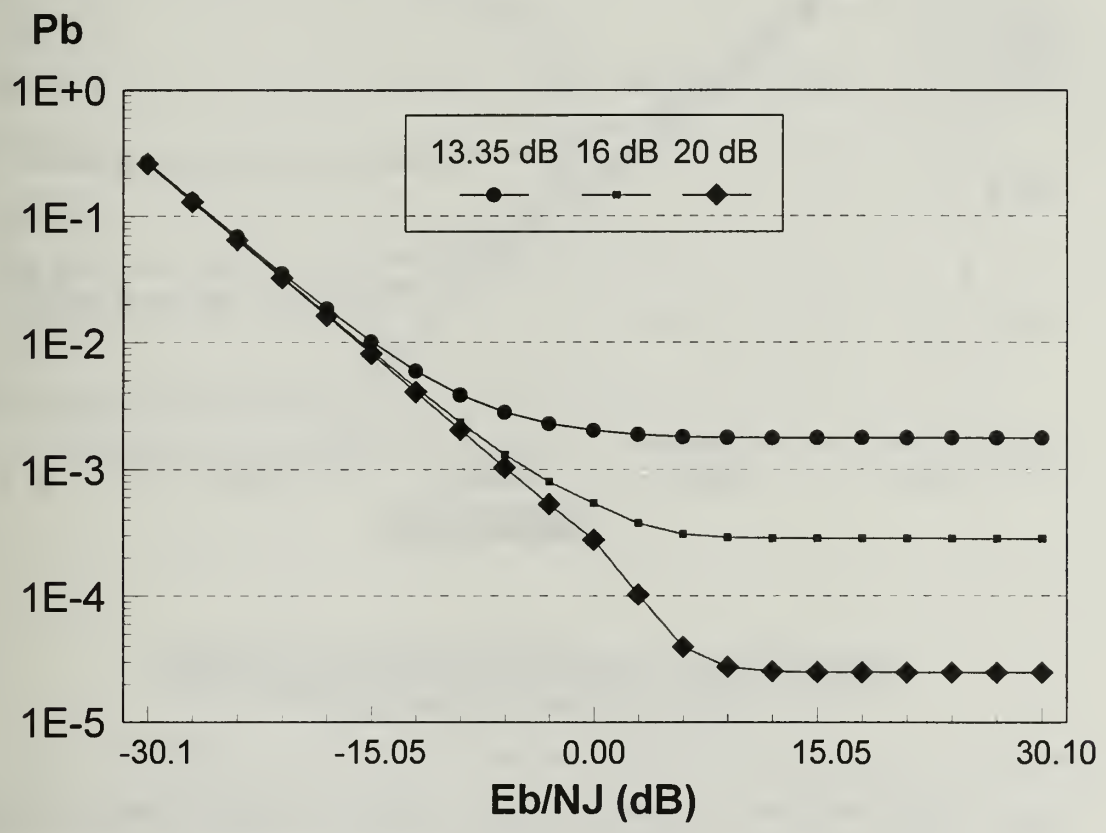

Figure 42. Worst Case Multi-Tone Jamming for Several Values of E_b/N_o, R_b=10, R_J=10

a consequence of the signal-to-jammer phase term in the bit error analysis. When the signal amplitude is consistently greater than the jammer's amplitude, the phase difference has little effect and the rate of improving performance increases. This slope change is also noticeable in Figure 43 for the 20 dB curve.

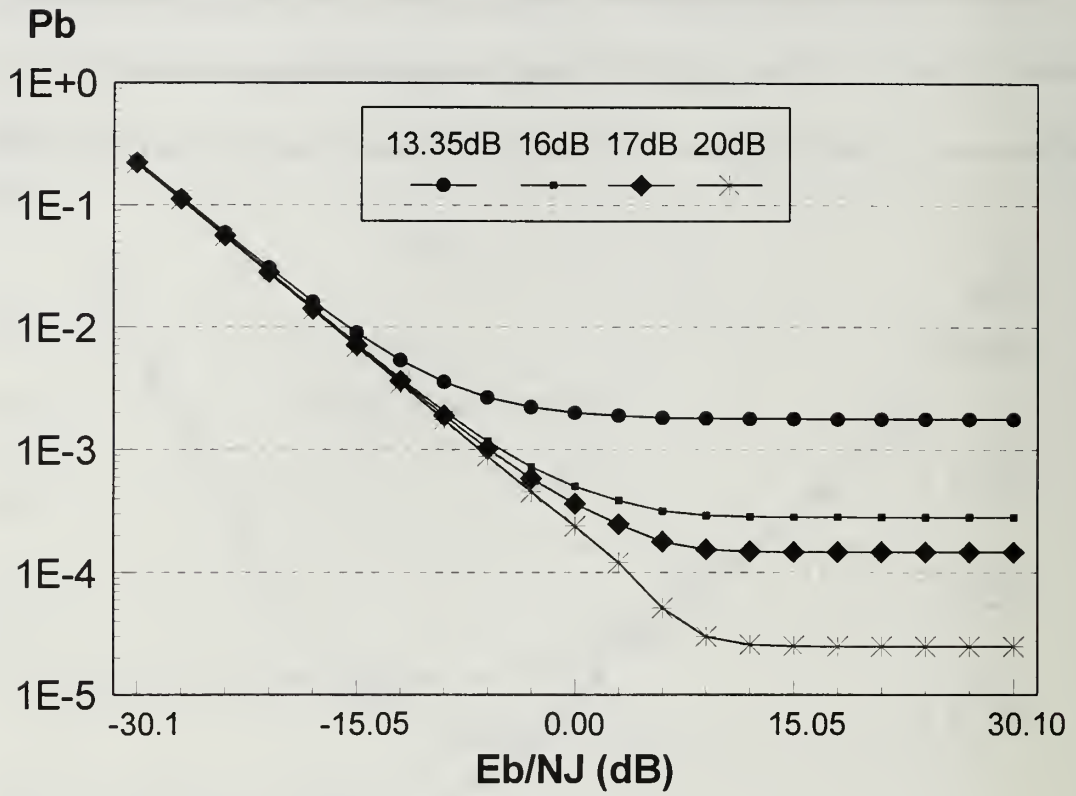

Figure 43. Worst Case Multi-Tone Jamming for Several Values of E_b/N_o, R_b=100, R_J=1

Figure 43 is a composite of performance under channel conditions favorable to the communicator. However, the 10:1 ratio in the signal's direct-to-diffuse over the jammer's direct-to-diffuse ratio provides little relief to the communicator.

Figure 44 displays the performance when the jammer's intelligence is relaxed to allow two interference tones in a hop slot when neither the signal nor the jammer experience fading.

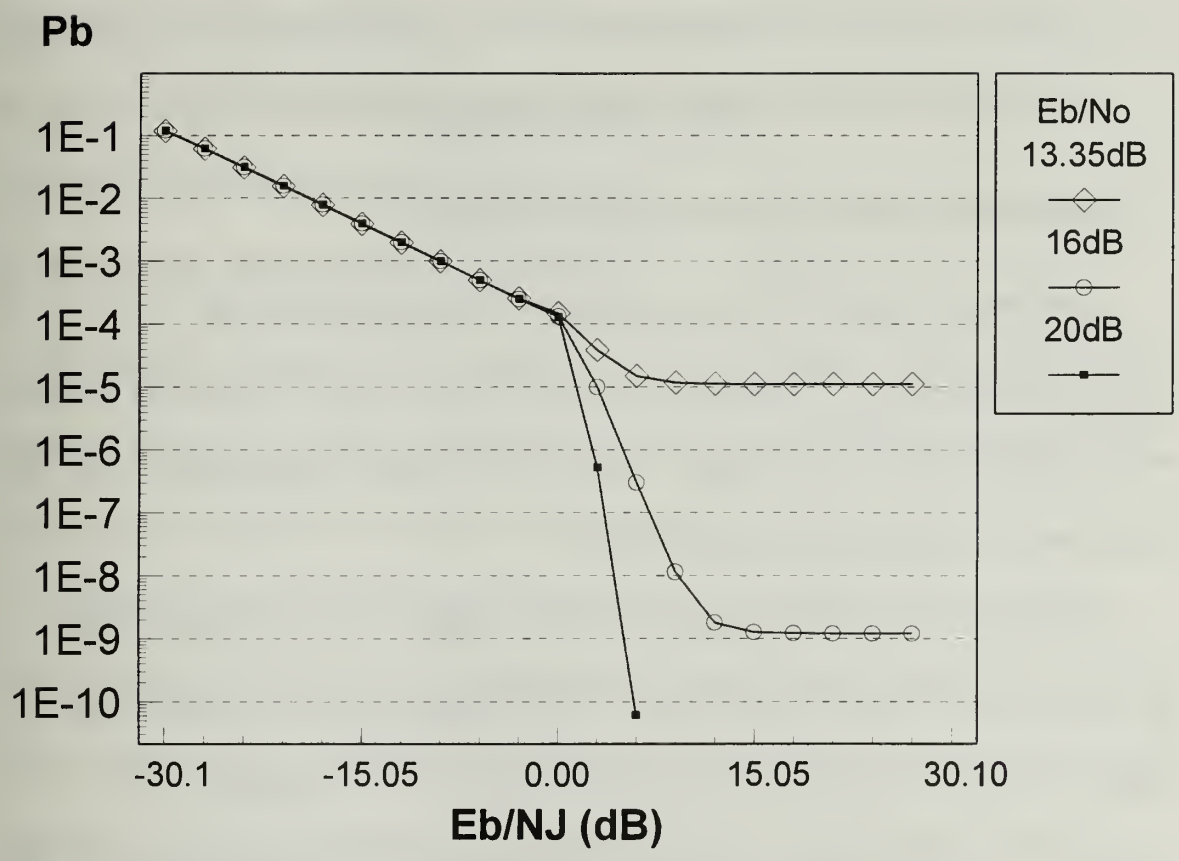

Figure 44. Worst Case Multi-Tone Interference when Allowing Two Jamming Tones per Hop Slot

Figure 44 exhibits the same linear improvement in performance as E_b/N_J decreases for several values of E_b/N_o. There is a marked change in slope at E_b/N_J =0dB. Overall performance is better than the perfromance when at most one tone per hop slot is jammed in a near Gaussian channel as depicted in Figure 40.

IV. CONCLUSIONS

A. FFH/MFSK PARTIAL-BAND NOISE JAMMING

A performance analysis has been completed for the conventional fast frequency-hopped M-ary orthogonal frequency-shift keyed receiver employing diversity with noncoherent reception of signals transmitted over Ricean fading channels. We can draw several conclusions based on the results.

Diversity alone is insufficient to overcome the effects of worst case partial band jamming acting in Ricean fading channels. The intelligent jammer can optimize the fraction of bandwidth jammed to force a worst case bit error ratio (BER). The noncoherent combining losses experienced by noncoherent systems is aggravated by the low signal-to-total noise ratio. These two factors combine to mitigate the advantages of increased diversity in a constant energy per hop system.

Increasing the modulation order provides only modest improvements in performance which decrease as diversity increases. For most channel conditions, the performance for M=4 and M=8 is essentially the same for all L greater than four. The only remaining advantage for increased modulation order is to offset the reduction in data rate that results from increasing diversity, L, in a constant energy per hop system.

When the signal experiences Rayleigh or strong Ricean fading, the jammer need not be very sophisticated to cause marked impairment to the communicator. Additionally, when comparing the partial-band jamming strategy for M=2 and L=1 in which the signal

suffers moderate to strong fading to multi-tone jamming under the same conditions, we see that the partial-band jamming strategy causes a higher BER while requiring less precise knowledge of the receiver by the jammer.

B. FFH/BFSK MULTI-TONE JAMMING

In this thesis, the case of L=1 is considered for the fast frequency-hopped receiver described above. The influence of Ricean fading of both the signal and the jammer is included in the analysis as is the effect of thermal noise.

First, the counter-intuitive result is obtained that Ricean fading of the jammer provides little, if any, relief to the communicator, while, as expected, moderate to strong fading of the signal tone markedly reduces performance. Worst case multi-tone jamming combined with signal fading produces unacceptably high probabilities of bit error, i.e., greater than 10^{-2}. Above this level it is unlikely that forward error correction coding can be successfully implemented.

The intelligent jammer can select the number of tones to jam which produces a worst case performance. The value of q chosen in the fading channel with thermal noise to cause worst case performance is the same value of q arrived at analytically for the noise free case without fading. For all combinations of channel conditions, not until the signal-to-jammer power ratio exceeds 10dB is the performance essentially thermal noise limited. When the jammer has a 3dB or better power advantage, the performance, in even the most optimistic channel conditions, is very poor and is dominated by the jammer power.

Relaxing the jammer intelligence to allow the case of possibly two interference tones in a hop slot is less efficient from the jammer's point of view. Performance is worse when the jammer is intelligent enough to jam not more than one signal tone per hop. Moreover, to be effective, a multi-tone jammer needs to be more intelligent than a partial band jammer since the former needs to know the exact location of the signal frequencies in addition to the bandwidth knowledge required of the latter.

C. RECOMMENDATIONS

The added complexity of a weighted diversity summer (noise normalized receiver) is warranted in most anti-jam systems. Efforts to reduce the uncoded BER below 10^{-3} will likely produce better overall performance when forward error correcting codes are implemented. When available, side information should be used to avoid a jammer or discard jammed hops.

The partial-band noise jammer who is intelligent enough to force the worst case scenario is more threatening to the communication system than multi-tone interference and will require a detailed threat analysis for hostile sources. Though "dumb", non-hostile interference sources also warrant attention in mission planning since even a single signal tone consistently jammed can cause detriment to the communicator.

LIST OF REFERENCES

[1] C. E. Cook, F.W. Ellersick, L. B. Milstein, and D. L. Schilling, *Spread Spectrum Communications,* New York: IEEE Press, 1983.

[2] J. G. Proakis, *Communication Systems Engineering,* New Jersey: Prentice Hall, 1994.

[3] R. C. Robertson and K. Y. Lee, "Performance of fast frequency-hopped MFSK receivers with linear and self-normalization combining in a Rician fading channel with partial-band interference," *IEEE J. Selected Areas Communication*, vol. 10, pp. 731-741, May 1992.

[4] R. C. Robertson and T. T. Ha, "Error probabilities of fast frequency-hopped MFSK with noise-normalization combining in a fading channel with partial-band interference," *IEEE Trans. Communication*, vol. COM-40, no. 2, pp. 404-412, Feb. 1992.

[5] T. A. Gulliver and E. Barry Felsead, "Antijam by fast FH NCFSK myths and realities," *Proceedings of the IEEE Military Communications Conference,* pp. 187-191, 1993.

[6] J. S. Lee, L. E. Miller, and R. H. French, "The analyses of encoded performances for certain ECCM receiver design strategies for multi hops/symbol FH/MFSK waveforms," *IEEE J. Select. Areas Commun.,* vol. SAC-3, pp. 611-620, Sept. 1985.

[7] T. A. Gulliver, R. E. Ezers, E. B. Felstead, and J. S. Wight, "The performance of diversity combining for fast frequency hopped NCMFSK in Rayleigh fading," *Proceedings of the IEEE Military Communications Conference*, pp. 452-457, 1992.

[8] C. M. Keller and M. B. Pursley, "Diversity combining for channels with fading and partial-band interference," *IEEE J. Select. Areas Commun.*, vol. SAC-5, no. 2, pp. 248-260, Feb. 1987.

[9] A. D. Whalen, *Detection of Signals in Noise,* New York: Academic Press, 1971.

[10] I. S. Gradshteyn and I. M. Ryzhik, *Table of Integrals, Series and Products,* San Diego: Academic Press, 1980.

[11] R. C. Robertson, "Communication ECCM," class notes from EC 4560, Naval Postgraduate School, Monterey, CA, Jul. 1993.

[12] R. S. Simon, M. T. Stroot, and G. H. Weiss, "Numerical inversion of Laplace transforms with application to percentage labeled mitoses experiments," *Comput. Biomed. Res.*, vol. 5, pp. 596-607, 1972.

[13] R. E. Ziemer and R. L. Peterson, *Digital Communications And Spread Spectrum Systems,* New York: Macmillan Publishing Company, 1985.

[14] J. Marcum, "A Statistical Theory of Target Detection by Pulsed Radar," Mathematical Appendix, Report RM-753, Rand Corporation, July 1, 1948. Reprinted in *IEEE Trans. Inform. Theory,* vol. IT-6, no. 2, pp. 59-267, Apr. 1960.

[15] H. L. Van Trees, *Detection, Estimation, and Modulation Theory, Part I,* John Wiley & Sons: New York, 1968.

[16] S. C. Chapra, *Numerical Methods for Engineers with Personal Computer Applications*, chapter 14, McGraw-Hill Book Co.: New York, 1985.

INITIAL DISTRIBUTION LIST

1.	Defense Technical Information Center Cameron Station Alexandria, VA 22304-6145	2
2.	Library, Code 52 Naval Postgraduate School Monterey, CA 93943-5101	2
3.	Chairman, Code EC Department of Electrical and Computer Engineering Naval Postgraduate School Monterey, CA 93943-5121	1
4.	Professor R. Clark Robertson, Code EC/Rc Department of Electrical and Computer Engineering Naval Postgraduate School Monterey, CA 93943-5121	2
5.	Professor A. Lam, Code EC/La Department of Electrical and Computer Engineering Naval Postgraduate School Monterey, CA 93943-5121	1
6.	Naval Research Laboratory Code 9120 4555 Overlook Ave. Washington, DC 20375-5320	1
7.	LT Joseph F. Sheltry 11 Whittier St. Winthrop, MA 02152	2